ISTANBUL TECHNICAL UNIVERSITY ★ GRADUATE SCHOOL OF SCIENCE ENGINEERING AND TECHNOLOGY

OVERVIEW OF DEFORMATION MONITORING TECHNIQUES: A CASE STUDY OF STRUCTURAL DISPLACEMENT ANALYSIS

M.Sc. THESIS

RIHAB TAWFEEQ HUSSEIN

Department of Geomatics Engineering

Geomatics Engineering Programme

JUNE 2020

ISTANBUL TECHNICAL UNIVERSITY ★ GRADUATE SCHOOL OF SCIENCE ENGINEERING AND TECHNOLOGY

OVERVIEW OF DEFORMATION MONITORING TECHNIQUES: A CASE STUDY OF STRUCTURAL DISPLACEMENT ANALYSIS

M.Sc. THESIS

RIHAB TAWFEEQ HUSSEIN
(501171660)

Department of Geomatics Engineering

Geomatics Engineering Programme

Thesis Advisor: Assoc. Prof. Dr. BIHTER EROL

JUNE 2020

ISTANBUL TEKNİK ÜNİVERSİTESİ ★ FEN BİLİMLERİ ENSTİTÜSÜ

DEFORMASYON İZLEME TEKNİKLERİNE GENEL BAKIŞ: YAPISAL YER DEĞİŞTİRMELERİN ANALİZİNDE ÖRNEK BİR ÇALIŞMA

YÜKSEK LİSANS TEZİ

RIHAB TAWFEEQ HUSSEIN
(501171660)

Geomatik Mühendisliği Anabilim Dalı

Geomatik Mühendisliği Programı

Tez Danışmanı: Assoc. Prof. Dr. BIHTER EROL

TEMMUZ 2020

Rihab Tawffeq Hussein, a M.Sc. student of ITU Graduate School of Science Engineering and Technology, student ID 501171660, successfully defended the thesis entitled "OVERVIEW OF DEFORMATION MONITORING TECCHNIQUES: CASE STUDY OF STURUCTURAL DISPLACEMENT ANALYSIS", which she prepared after fulfilling the requirements specified in the associated legislations, before the jury whose signatures are below.

Thesis Advisor:	**Assoc. Prof. Dr. Bihter EROL** Istanbul Technical University	.....
Jury Members:	**Prof. Dr. Hayri Hakan DENLİ** Istanbul Technical University	.....
	Prof. Dr. Atınç PIRTI Yıldız Technical University	.....

Date of Submission : 15 June 2020
Date of Defense : 22 July 2020

To my beloved parents and husband,

FOREWORD

First of all, I would like to express my gratitude to all of the engineering department academies of Istanbul Technical University, whose expertise, understanding, and patience, added considerably to my graduate experience. I would like to thank the other members of my committee for the assistance they provided at all the levels of the research project and I would like to thank people who helped me and motivated me during my thesis journey.

Again, very special thanks go out to my supervisor Assoc. Prof. Dr. Bihter EROL who's motivated, encouraged me and giving me the opportunity to work on such an interesting subject and supporting me during the process.

I must also acknowledge and express my appreciation to jury member, Prof. Dr. Hayri Hakan DENLI and Prof. Dr. Atinc PIRTI for the contribution they gave me during my M.Sc. Period.

I give my deep thanks and appreciation to my husband Harith YOUNUS for being with me, encouraged me to study masters and supporting me during thesis journey.

My first journey was the one I had with my family and especially with my parents. I am so lucky that I was born into such amazing family. Thanks for the soul of my Father Taweeq HUSSEIN, my mother Asia MUHMOOD, my sisters HANEEN and ANGHAM and my brother Mohammed TAWFEEQ.

The data for this thesis are provided by Los Alamos National Laboratory Elói Figueiredo, Engineering Institute in US.

June 2020

RIHAB TAWFEQ
Geomatics Engineering

TABLE OF CONTENTS

ABBREVIATIONS

SHM : Structural Health Monitoring
GPS **:** Global Positioning System
DGPS **:** Digital Global Positioning System
Hz **:** Frequency Hertz
2D **:** Two Dimension
3D **:** Three Dimension
RTK **:** Real Time Kinematic
DSMM **:** Design Structure Matrix Management
VRS **:** Virtual Reference Station
CRP **:** Close Range Photogrammetry
CCD **:** Charge Couple Device
INCA **:** INtelligent CAmera
GSI **:** Geodetic Service Inc
SLR **:** Single Lens Reflex
EDM **:** Electronic Distance Measurement
TLS **:** Terrestrial Laser Scanner
LSSA **:** Least Squair Spectral Analysis
PSD **:** Power Spectral Density
DB **:** Decibels (Decibels)
DFFT **:** Discrete Fast Fourier Transform
FFT **:** Fast Fourier Transformation
DOF **:** Degree Of Freedom

SYMBOLS

h(t)	**:** Time Domain
H(t)	**:** Frequency Domain
W	**:** Wavelets
m, n	**:** Real and Positive number
φ	**:** Arbitrary phase angle in the harmonic loading function.
ω	**:** Loading frequency
ω	**:** Natural frequency
G	**:** Complex constant
H2(ω)	**:** Correction filter in the frequency domain
d(t)	**:** Displacement in time domain
$A_c(\omega)$	**:** Corrected Fourier transformed function
$A_f(\omega)$	**:** Acceleration in frequency domain
$V(\omega)$	**:** Velocity in Frequency Domain
$D(\omega)$	**:** Displacement in Frequency Domain
v(t)	**:** Velocity in Time Domain
d(t)	**:** Displacement in Time Domain
a_0	**:** Acceleration in Time Domain
v_0	**:** Velocity in Time Domain
d_0	**:** Displacement in Time Domain
c_0, c_1	**:** Coefficients of the first-order linear equation, baseline correction
ω_c	**:** Cut-off frequency
G_0	**:** Frequency response at zero frequency
a(t)	**:** Corrected Acceleration
v(t)	**:** Corrected Velocity
d(t)	**:** Corrected Displacement
$a_0(t)$	**:** Initial Acceleration
Δt	**:** Time interval
T_0	**:** Analysis Time
F(*f*)	**:** Discreet Fourier Transform

f_s : Sampling Frequency

f_{max} : Maximum Frequency

Δf : Interval Frequency

$\mathbf{H}(f)$: Complex Frequency response function

U_d : Displacement in Frequency Domain

U_v : Velocity in Frequency Domain

U_a : Acceleration in Frequency Domain

$\mathbf{U_d}$: Displacement response in Frequency Domain

$\mathbf{U_v}$: Velocity response in Frequency Domain

$\mathbf{U_a}$: Acceleration response in Frequency Domain

u : Displacement in Time Domain

$\dot{u}$: Velocity in Time Domain

$\ddot{u}$: Acceleration in Time Domain

LIST OF TABLES

Page

LIST OF FIGURES

Page

OVERVIEW OF DEFORMATION MONITORING TECHNIQUES: A CASE STUDY OF STRUCTURAL DISPLACEMENT ANALYSIS

SUMMARY

The study aims to monitor the health and safety of structures that subject to changes in operational and environmental conditions, which make it difficult to detect and assess damage of structure. The objective of study is to preceive damages by applying structural health monitoring (SHM) to existence of these progressions in operational and environmental conditions. A case study is a simulation experiment of test-bed structure in a laboratory consists of three-story building subject to lateral excitation by electromagnetic shaker.

The data has been collected, recorded by Los Alamos National Laboratory Elói Figueiredo, Engineering Institute in US and shared to scientific community for research purposes. The mentioned data were analysed in the content of this study by using Fast Fourier Transform method to measure the displacement of each story. The displacement of the three-story structure under excitation load was measured in different states condition to convert time domain into the frequency domain. The testing was repeated for different structural state conditions and measurement were recorded for each state to perceive deformation when the structure has experienced basic change caused by operations and environment impacts for this purpose seventeen state condition were set up. The results were interpreted in the conclusion section.

DEFORMASYON İZLEME TEKNİKLERİNE GENEL BAKIŞ: YAPISAL YER DEĞİŞTİRMELERIN ANALİZİNDE ÖRNEK BİR ÇALIŞMA

ÖZET

Deprem sarsıntısı, binanın temelindeki zorla yerinden edilme nedeniyle bina içindeki bu tür göreceli yerinden edilmeye dayanabilmesini sağlar. Binanın altında oluşan gerçek yer değiştirme tam olarak anlaşılmış değildir. Deprem titreşimi en uç olan durumdur, çünkü zamanla evin altında yer değiştirmeye neden olur. Bu durum da binanın tabanı ile üst kotlar arasındaki yanal deformasyonu gerektirir. Sismik bölge ne kadar yüksekse, buna dayatılan göreli deformasyonun şiddeti de o kadar büyüktür. Bu nedenle temel zorluk, ikili talebi karşılamaktır. Bina, düşük yoğunluklu sallanma altında hasarla ve yüksek yoğunluklu sallanma altında çökmeden bu zorlanmış deformasyona dayanabilmelidir. Bina, esnek olmayan deformasyon için geniş bir kapasiteye sahip olmalı ve tüm parçalarında kendilerinin neden olduğu güçlere ve momentlere dayanacak enerjiye sahip olmalıdır.

Bu çalışmanın temel amacı, bir yapının operasyonel ve çevresel etkilerin neden olduğu yapısal değişikliklere uğradığındaki hasarını tespit etmektir. Bu amaçla, Hızlı Fourier Dönüşümü (FFT) yöntemi kullanılarak bir sallanma tablosunda gerçekleştirilen deneyin üç katlı laboratuar yapısından elde edilen çıktı verileri kullanılarak 17 durum koşulu oluşturuldu.

1. bölümde sunulan tezin tanıtımı, referansların motivasyonunu ve kapsamlı bir şekilde gözden geçirilmesi sağlanmıştır.

2. bölümde yapısal sağlık ve deformasyonun izlenmesi için yürütülen tekniklere genel bir bakış sunulmaktadır. Bu genel bakış, yapısal deformasyonların izlenmesinde kullanılan jeodezikler ve jeoteknik yöntemlerini içermektedir.

3. bölümde yapısal izleme veri analizinde, Fourier Dönüşümü Yöntemi ile Hızlandırmayı Filtreleme ve Dönüştürmede uygulanabilecek farklı yöntemler anlatılmaktadır.

4. bölümde kullanılan vaka çalışmasının açıklaması ve yapı, operasyonel ve çevresel etkiye göre yapısal değişikliklere uğradığında hasarı tespit etmek için test plakasının yapısal yer değiştirme verilerini analiz edilmektedir.

Son olarak, 5. bölümde FFT analizinin test yapısı ve tezin kazanımları özetlenmiştir.

Simülasyon denememizde, hasarlı bir tespit test alanı olarak üç katlı bir bina yapısı ve yapının bodrum katında bir uyarım sağlayan elektromanyetik çalkalayıcı (yapı ve çalkalayıcı, taban plakası üzerine yerleştirildi) kullanıldı. Çalkalayıcıdan giriş kuvvetini ölçmek için kullanılan Kanal 1 (kuvvet dönüştürücü) ve Kanal 2-5 (4 ivmeölçer), her bir kattan gelen yanıtı ölçmek için kullanılan uyarma kaynağının karşı tarafındaki her bir katın merkezine bağlandı.

Yapı durumu koşulu dört gruba ayrılır:

1. Mevcut durum.

2. Yapının operasyonel ve çevresel etkilerin neden olduğu kütle ve sertlikte değişiklikler geçirdiği mevcut durum.

3. Bir tamponun uyguladığı doğrusal olmayan durum.

4. Doğrusal olmayan durumların, çevresel ve operasyonel etkilerin olduğu durum.

FFT, sinyal segmentlerinin zaman içindeki frekans kalitesini belirlemek için kullanılmaktadır. FFT, frekans içeriği ve ayrıca frekans içeriğinin zaman içindeki gelişimi hakkında bilgi sunmaktadır. Belirli bir örnekleme oranı için, FFT'nin frekans çözünürlüğü pencerenin uzunluğuna veya süresine göre hesaplanmaktadır. Sabit cihazdan gelen sinyalin frekans kalitesinin zamanla değişmemektedir. Excel'deki Fourier Analizi komutu, FFT'yi ölçmek ve frekans bileşenlerinin zaman içinde nasıl değiştiğini tahmin etmek için kullanılmıştır.

Bu çalışmada, her 8192 veri noktası hızlanma süresi serisi, FFT'yi hesaplamak için 1024 noktaya bölünmüştür. Her bölüm için, ayrık-Hızlı Fourier Dönüşümü, sinyalin zamanla değişen frekans içeriğini tahmin etmek üzere hesaplanır. FFT'yi hesaplamak için kullanılan zaman geçmişinin sabit bir sistemi temsil etmesi durumunda, zamanın bir fonksiyonu olarak frekans içeriğinde hiçbir değişiklik gözlemlememesi beklenir.

Hızlı Fourier Dönüşümü (FFT), veri toplama cihazlarından gelen sinyalleri analiz etmek ve ölçmek için güçlü araçlardır. Hızlı Fourier Dönüşümü (FFT), verilerin zaman alanından frekans alanına dönüştürülmesi için bir algoritmadır. İlk olarak, alanların dönüştürülmesine ilişkin birçok hesaplama nedeniyle, sonuçların yeterince doğru olması durumunda dönüşümün dijital bir bilgisayarda yapılması

gerekmektedir. Mevcut durumda frekans alanına sürekli bir şekilde dönüştürülememektedir, ancak daha sonra zaman alanı verilerini analiz etmek ve dijitalleştirmek gerekmektedir. Bu, algoritmamızın sayısallaştırılmış örnekleri zaman alanından frekans alanındaki örneklere çevirdiğini ima etmektedir.

Hızlı Fourier Dönüşümü (FFT) sadece sinüs dalgası simetrisinden yararlanan daha verimli bir algoritma kullanan bir DFT'dir. FFT, bu simetrilerden faydalanmak için çevrimi iki basamaklı gruplara dönüştürmek ve bölmek adına bir miktar gücün iki sinyal uzunluğunu gerektirmektedir. Bu işlem hızını önemli ölçüde artırır; N, sinyalin uzunluğu ise, bir DFT N2 işlemlerine ihtiyaç duyarken, bir FFT'nin N * log2 (N) 'ye ihtiyacı vardır.

Fourier Dönüşümünün bir parçası olarak test edilen ayrık frekansların sayısı, orijinal dalga formundaki örnek sayısı ile doğru orantılıdır. N, sinyallerin uzunluğu olduğu için, frekans hattı sayısı N / 2'ye eşittir.

Bu çalışmada ölçülen zaman aralığı (Δt) 0.0031 s idi. 1024 veri noktası kullanılmıştır. Sonuç olarak, FFT çalışması, etkilenen en düşük durum için frekans bileşenlerinde önemli bir gelişme olmadığını göstermektedir (Durum 12). Bununla birlikte, sinyalin frekans kalitesinin zaman-değişken mevcudiyetine ilişkin bazı küçük işaretler, en çok etkiye karşılık gelen (Durum 10) etkilenen durum için görülebilir, ancak bu ince ayarlara bir hasar tahmininin dayandırılması zor olacaktır. Fourier dönüşümünün, belirli bir aralıktaki sinyalin ortalama özelliklerini yansıtmaktadır. Bu ortalama özellikler süre boyunca sabit kalmıştır.

1. INTRODUCTION

Structural Health Monitoring (SHM) is that the structural damage detection method. SHM's goal is to enhance the protection and dependability of the engineering structures by detection deformations before a crucial state is reached. To the present finished, technology engineered to switch the qualitative visual examination and maintenance procedures based on the quantity and time with automatic additional operations to assess the damage. These system's application exploitation each device and computer code in order to achieve more cost-effective maintenance depending on condition. You may realize additional information regarding SHM in (Farrar and Worden ,2007).

The first step in increasing the capacity of the SHM is to perform a related operational analysis as a section of SHM response method aims to address four regarding the application of the SHM program (Farrar et al, 2001):

(1) Finding the principle for the protection of life and / or observance the economic science methodology

(2) How is the description of the damage to the monitoring system?

(3) Identifying the operating and the surrounding settings for the system of the interest to work?

(4) locating the boundaries that regarding knowledge acquisition within the operational environments?

The operational analysis shall determine damage to be identified to the greatest extent possible. It also points out the advantages to be achieved from SHM program implementation. The method also starts to set limits on what quantity of movements are monitored and the way the observing is done, Likewise, to monitor specific aspects of system and the distinct options for damage to be discovered.

Data acquisition element of SHM method includes choosing the excitation methods; sorting, variety and position of the sensor; and also, the knowledge acquisition /

storage / process / transmission. With regard to access to data and sensing, the basic concept is that such device does not determine the deformation. Alternatively, calculate the performance of the system considering operating and environment loads or contributions from drivers included in the sensor system. Sensor readings may in one way or another be directly related to the occurrence and locality of the damage, depending on the prevailing sensor techniques and the type of damage that will be detected.

A data acquisition system is the required element of the SHM system to convert sensory data into structural state information. Also, acquiring data should be created related to this information cross examination strategies to successfully achieve SHM.

A damage-sensitive characteristic is a certain amount derived from device data in response to the measured, which related to the presence of structural damage. İn a perfect way, with an -level of damage, a damage sensitive function should adjust in some consistent manner. Most SHM technical literature focuses on distinctive options that may exactly distinguish between damage and undamaged structure (Sohn and Farrar, 2004). Basically, the extraction feature method depends on the synthesis of some models, whether based on physics or data, in response to a data device calculated. The alternative process is to define properties that directly compare waveforms and sensors that are measured before and after damage.

SHM technique's part that got the least coverage in scientific literature is that creating applied mathematical models to enhance the method of damage detection. Applied mathematical models for categorizing features include applying algorithms that are evaluate the distribution of derived options in an attempt to see the state of structure's damaged.

Software standardisation, processing and integrating programs are inherent within the information acquisition, extraction feature and applied mathematics modelling parts of the SHM method. For SHM, information standardisation is that the technique of characteristic changes within the reading of sensors happened due to corruption from unmatching operating and environment settings (Worden et al, 2002). Data cleaning is that the method of choosing information to be transmitted to, or excluded from, the method of choosing to perform. Information fusion is that the technique of group action from multiple sensors data in a shot to extend the accuracy

of method of detection damage. Information compression is the way in which information dimensions or attributes extract data in an attempt to enhance the effective storage of data and improve the mathematical measurement of parameters. The four behaviours will be enforced in each hardware and computer code, and a mixture of two solutions is usually used.

Data structure of damage detection consists of four-stage cycle that addresses the subsequent queries (Worden and Farrar, 2007):

i. Do the damages exist within the system?
ii. Wherever is that the location of damages? and
iii. What type of the damage does exist?
iv. What's the severity of the damages?

Answers to above questions can only be provided in a sequence manner, for example responding with the extent of damage is only possible with a prior understanding of the level of corruption. Statistical algorithms are usually used when implemented in an unsupervised mode to answer questions on the character and placement of damage. Can use mathematical algorithms when implemented in the development of learning under the supervision of the association with experimental models to help determine type and extent of damage.

Structures (including bridges, dams, viaducts, high-rise buildings, etc.) are distorted because of factors like changes in rain, tidal fluctuations, tectonic phenomena, etc. A special branch of Geodesy Science is the monitoring and evaluating deformations of structures. There are many deformation measuring techniques. It can primarily be divided into two as techniques of geodetics and non-geodetics.

Each method of measurement has it is own benefits and drawbacks. The geodetic techniques typically provide sufficient observations for statistical analysis of its performance and for the identification of errors through a network of connected nodes to angle, distance calculations or both. Global data provides distorted structure behaviour, while non-geodetic approaches provide local disturbed information lacking testing compared with several other separate measurements. Instruments used in measurements is geodesic, on the other hand, is easier to adapt to the automated and continuous monitoring of the measuring instruments Geodetic traditional. Traditionally, the use of geodetic methods in the first place to assess the

absolute displacement of specific points of an object's surface with respect to certain points of reference is expected in order to prevent movement. Non-geodetic methods are primarily wont to measure the relative deformation in and around deformed body.

The study's main motivation is geodesic techniques in tracking and evaluating deformations of construction structures. In assessing deformations on the basis of geodetic techniques, terrestrial measurement techniques or spatial positioning techniques and/or combination of both techniques are constituted. The deformations in engineering systems had been calculated by traditional measurement methods until the very beginning of the 1980s. Then, after starting to use GPS measurement technology in geodetic and surveying applications, satellite-based positioning technology became very accurate used in deformation measurement. (Erol et al, 2004).

Three-storey structures were used for the damage detection bed. On each floor, four aluminium bars and panels are built using a rigid mounting joint. In addition, the middle column is suspended from the upper level, which induces a non-linear behaviour when connected to bumper installed on second level. The location of the bumper can be changed to modify the degree of nonlinearity. This structure slides on the bars, allowing it to move only in the horizontal direction. The electromagnetic shaker provides excitement to the main floor of the structure. The building and shaker are placed together on the same plate. A power adapter is attached to the end of the stringer in order to find the input strength of the vibrator. Four accelerometers are connected to each floor on the opposite side of the excitation sources to determine the response from each floor. Accelerometers are installed in middle of the floor and are therefore ineffective for measuring torsion positions in the frame. Data from different structural conditions was collected and processes using a Fast Fourier Transform analyser.

1.1 MOTIVATION

The main objective of this study is to identify deformation when structure undergoes structural changes due to operational and environmental impacts. For this purpose, 17 cases were prepared using the output data obtained from the structure of a three-storey building in the laboratory for an experiment performed in a vibration table using the Fourier transform method (FFT).

1.2 Thesis Overview

An introduction of thesis was presented in Chapter 1, the motivation and comprehensive review of the references was provided.

Chapter 2 provides an overview of to the techniques which are carried out for monitoring the structural health and deformation. This overview includes geodetics and geotechnical techniques that used in monitoring structural deformations.

In Chapter 3, discuses different methods that can be implemented in structural monitoring data analysis, Filtering and Converting the Acceleration Using Fourier Transform Method.

Chapter 4, this chapter provides description of the case study used and an attempt to analyse structural displacement data of the test plate to detect damage when exposed to structural changes in the structure through operational and environmental impact.

Finally, the main conclusion of FFT analysing on test structure are summarized in Chapter Five.

2. DEFORMATION MEASUREMENT TECHNIQUES

As mentioned within the introduction chapter, monitoring structural techniques for deformation have principally been divided into two completely different teams as geodetic and geotechnical methods. Sub-techniques can also be classified as well (Erol et al, 2004). Overview of the techniques used in monitoring structural deformations can be found below:

2.1 Geotechnical Methods

2.1.1 Accelerometers

Accelerometers usually used for observance deformations in structural engineering and that classified underneath geotechnical strategies. Structural displacement is measured using frequency conversion techniques that assume deformation by examining the structure's frequency response. one in all the restrictions of instrument is that it needs direct connect with the structure. Accelerometer connected to central recording unit, fixation required, which may lead to higher maintenance cost. Calibration of these devices with regard to temperature is important in order to obtain accurate results, in particular as temperatures differ through its network. Although vibration frequencies can be detected with accuracy of several hundred Hz or higher, the accelerometer faces a major problem for accurate detection of "very low" vibrations (such as slow-moving structural movements) visible to long-range structures (Roberts et al, 2004). Figures 2.1 and 2.2 show the accelerometers for structural health monitoring and working principle of accelerometres.

Figure 2.1: Accelerometers of Structure Health Monitoring (Roberts et al, 2004).

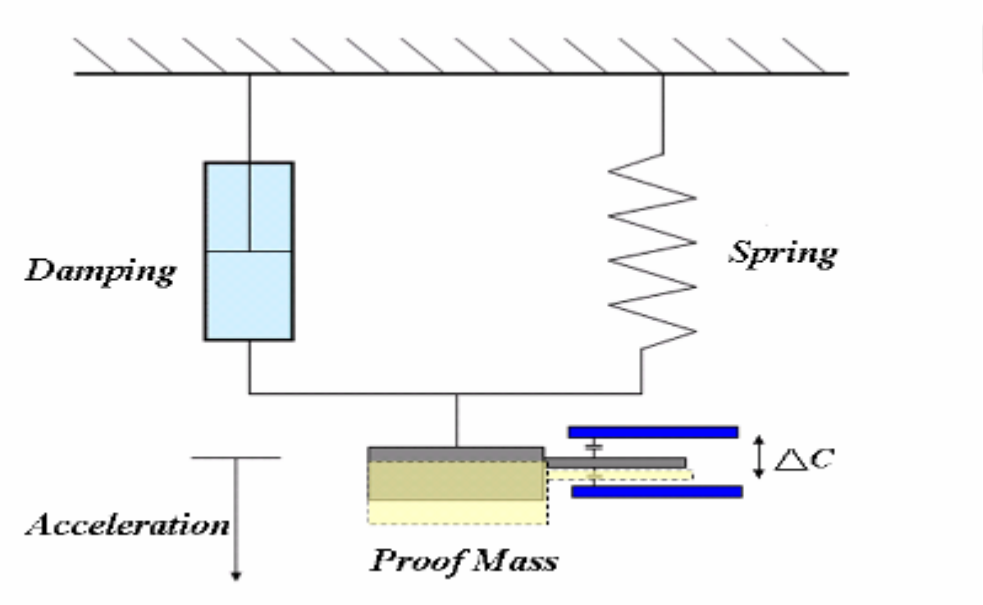

Figure 2.2: Working Principle of Accelerometers (Roberts, 2004).

2.1.2 Inclinometers (Tiltmeters)

Inclinometers and Tilting sensors are also included in this category. Inclinometers are an instrument wont to track the modification in the slope of the ground surface. The unit consists of an electrical device for sensing gravity (measuring servo system, an electric tilt sensor, catalyst wire vibration, MEMS) can make a difference tendency inclination such as low-low second arc. Tiltmeters can be uniaxial or biaxial which allows the measurement of tilt in two perpendicular directions. These are wont to track the slope movements when landslide failure situation is assuming to have the rotational component. The advantages of exploitation tiltmeters it is light-weight, easy operation and comparatively low value. Inclinometers are often read manually or mechanically by attaching them to a drop of knowledge. they'll be combined with inclinometers and extensometers in supposed integrated pit slope observation systems. Tiltmeters could also be wont to track pit-slope movements and subsidence over underground mines, especially long-wall and cave-block operations (Erol, 2010). Figure 2.3 show the functional principle of inclinometers in horizontal and tilt position.

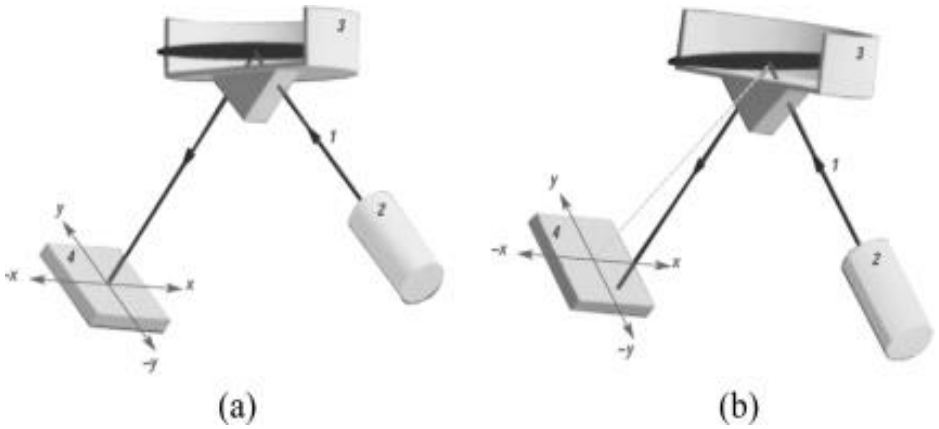

Figure 2.3: Functional Principle of Inclinometers; (a) Horizontal position, (b) Tilt position (Erol, 2010).

2.1.3 Extensometer

This category also includes crack meters, joint meters, strain meters, crack gauges, convergence gauges, distometers and sliding micrometres. Extensometers are instruments wont to the distinction in distance between two points. The measuring points can be placed on the surface to determine ground movements (e.g. spanning a stress crack to trace its gap rate) or could also be placed in an exceedingly borehole to determine differential displacements within the borehole. Extenders differ in nature between those requiring manual measurements and those that are automated using vibrating wired electronics, differential power adapters, or, more recently, optical fibres. The accuracy and frequency of measurements depend on the type of sensor system and the distance between the measurement points. Normal precision ranges from millimetre to millimetre at distances less than one meter when using solid rigid sliding bars between observation points, and normal accuracy ranges from millimetre to centimetre at distances of one or several tens of meters when stretching the elastic tape or wires between observation points.

The extensometers devices that are being presently used have digital readings. Site personnel can take readings or store them in an electronic data recorder and transfer them to a computer later. A limited number of mines created telemetry systems to record readings and verify them in real time or near to that.

The calculation ranges for the expansion gauges available range from a few centimetres (crack gauges) to about 180m (tension bar extension gauges). Most expansion scales within the walls may extend to roughly 30 to 40m. Improved accuracy can be achieved from ± 0.1mm, although wind and temperature effects may cause a negative effect on the precision of an individual result (Ding and Qin, 2000).

2.2 Geodetics Methods

2.2.1 Close range photogrammetry

Photogrammetry enables the employment of images to measure displacement for a long period of time. The system will often not determine, document or monitor almost any displacement within the image. In addition to the camera distance from object, use of the pictogram methodology based on the dimension of the measured object. Near-range tomography (CRP) is a scanning approach that measures the distance from object to camera to just 300 meters or less. when CRP is concerned, the most important device necessary for this methodology could be a digital sensor consisting of a camera entirely of its shapes, prices, accuracy, formats, charger (CCD) and video camera. additionally, to the Smart Camera (INCA) the inherent camera also can be employed in CRP. However, the resolution which will be reached with compact digital cameras is 1: twenty thousand, that is organized by one third (2/3) of these which will be achieved with a digital SLR camera (Ahmed, 2008). Although CRP is often applied in a particular when rapid analysis needed, it is immediate that CRP isn't a good approach once the accuracy of the measurements is higher. Because of the advanced and troublesome conditions that include, CRP cannot be used permanently alone in constructive health monitoring as CRP must integrate with different facilities. Photogrammetric evaluation and principles of photogrammetric techniques used for structural health monitoring are show in figures 2.4 and 2.5.

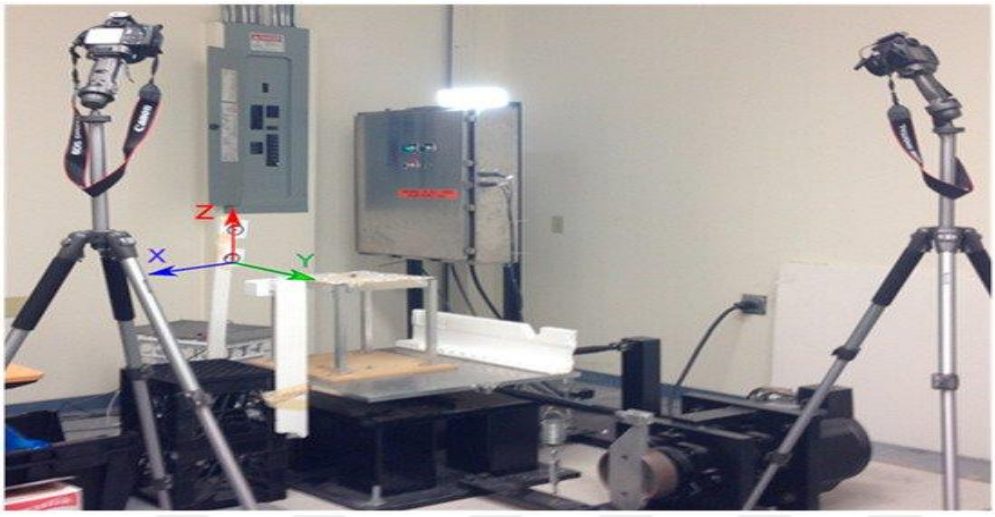

Figure 2.4: Photogrammetric Evaluation of Structural Deformation (Afrouz, 2019).

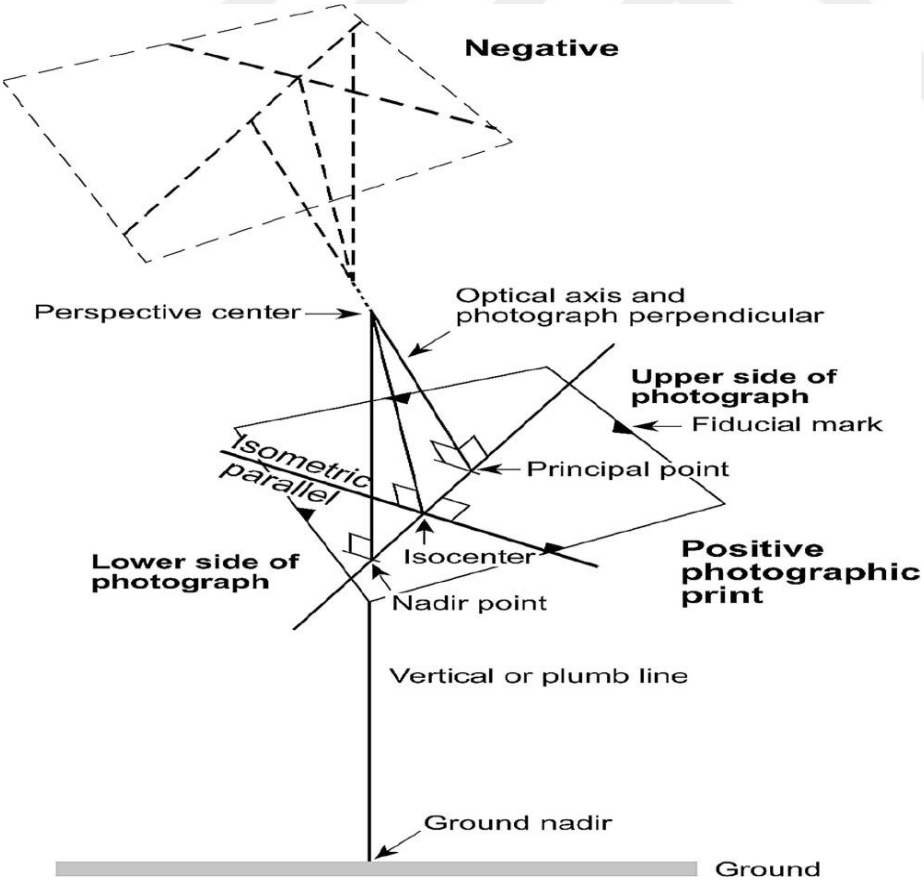

Figure 2.5: Principles of Photogrammetric Techniques (Avsar et al, 2014)

2.2.2 Laser interferometer

The laser interference scale determines difference in space between the point of interest and reference point. To get a distance from point of interest, prism or reflective film must be attached to the frame. Distance change and further analysis can be measured to measure prevailing frequencies and corresponding capacities during observation state. This approach offers an advantage of high precision, but it is not easy to determine point of interest when the vibration of the structure is very large. Moreover, the laser interference meter can also be costly. Aside from being selected to identify 3D displacements, the issue of automation is also a big problem when this method is ever used. The real-time measurements of point of interest is required manually by at least two people because it cannot be started automatically. The climate-dependent laser interferometer is another big drawback to this approach. Due to the difficulty in measuring during rainy conditions due to line-of-sight interference, it's suggested that the laser-based interference scale isn't suitable in most cases for continuous monitoring of man-made structures. Evaluation of structural deformation using laser interferometry is shown if figure 2.6.

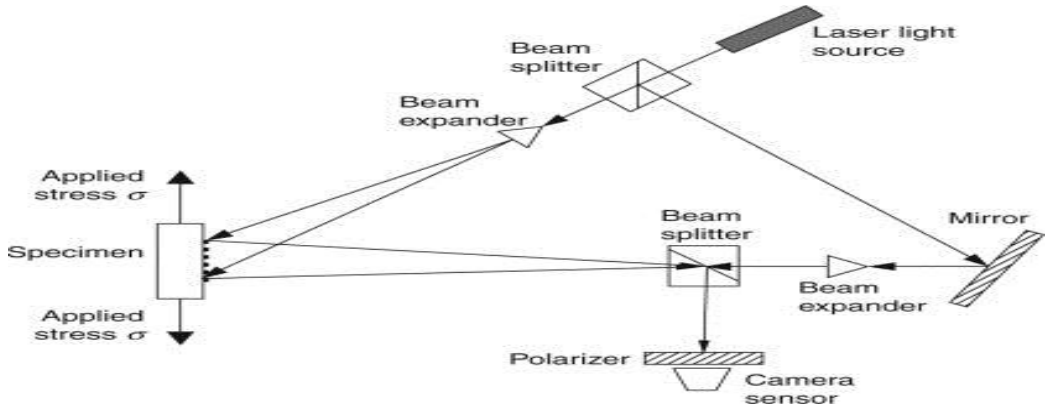

Figure 2.6: Evaluation of Structural Deformation Using Laser Interferometry (Jatmiko and Psimoulis,2017)**.**

2.2.3 Distance and angle measurement using (Total Station)

The total station is originally a mixture of the EDM electronic digital odometer. This device is able to provide vertical angles, directions and horizontal distances. Total Station is currently using the capabilities of a memory storage device and a wireless connection to directly record data using a data recorder or a laptop for additional processing. The integrated robotic station or automatic and reflex recognition and target recognition represents further progress in the field of total station technologies. While usually used for an automated and periodic (recurrent) structural health monitoring system, the most common defects are signal errors and visibility criteria between stations. Total Station also needs a repeated measurement to find the possibility of a human-based error. Also, it requires a clear vision between reference stations and interest structures. Given that a smooth line of sight can be achieved, estimated accuracy of the total station system is five mm horizontal and ten mm vertical (Erol, 2010).

From (Figure 2.7), The X-axis is randomly selected as a line that moves horizontally toward the base of observation structure, while Y-axis is selected as a horizontal line perpendicular to the direction of the building base that is positive in the console's direction, and Z-axis is obviously a vertical line that makes the vertical axis of the system in an occupied station. There is a point that is known to coordinate (A) These are coordinates (XA, YA, ZA).

Based on this point, the coordinates of any given point (B) and its accuracy can be calculated that this state has a unique solution, so that multivariate diffusion technique is used. The geometry of total station techniques used in structural health monitoring is shown in figure 2.6.

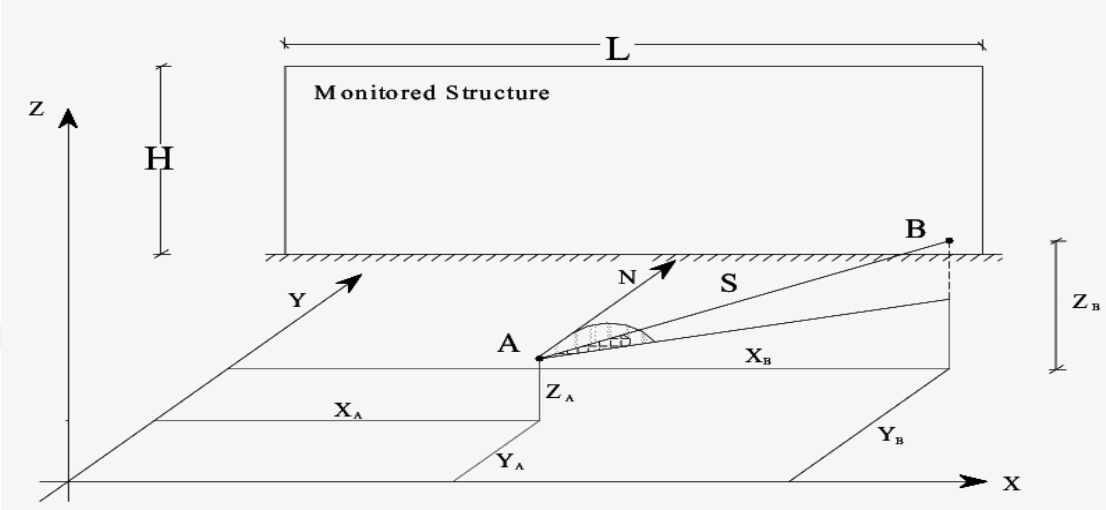

Figure 2.7: The Geometry of Total Station Techniques (Ibanez and Poleszuk, 2018).

2.2.4 GNSS positioning

GNSS techniques is a navigation system based on satellite, which allows a user to obtain a 3D position in X, Y, Z direction or longitude, latitude and elevation and time data in the common reference system and is in service 24 hours every day. GPS can also obtain 3D compensation directly without having to switch to distance or displacement integration. GPS combines high accuracy of results and have ability to continuously scan in all weather conditions and easy installation of equipment. Being able to obtain results in real time, the Global Positioning System (GPS) promises to be a major means of monitoring ongoing and automated structural health, in a particular when rapid results save lives and property. The GPS doesn't need direct line of sight like the EDM laser interferometer. Several experiments have been performed to model the usage of GPS for quantitative health tracking.

GPS receivers with a sampling frequency of 10 Hz to 20 Hz are currently available from a number of manufacturers. İn order to monitored structural health, the GPS must be performed either by mistake (time periods) or continuous measurement. A GPS differential transmission approach is also needed to determine the accuracy in locating only a few millimetres (Anonym, 2002).

2.2.5 LIDAR system

LiDAR was developed in the 1960s as a measurement technique to obtain distance and coordinate target information using a laser pulse. It is also possible to record three-dimensional spatial coordinates with many points and coordinate information on the surface of objects in a relatively short time at a measurement speed of 1,000 to 10,000 points or more per second. Since the 1970s, it has been used to collect 3D information on GIS. In addition, with the continuous development of laser technology, LiDAR system technologies have been developed for various applications. For example, LiDAR systems are currently used in aircraft, satellites, etc. to precisely monitor and analyse the Earth's atmosphere, geography and environment. LiDAR is installed on spacecraft and automatic detection as a way to improve camera performance and measure the shape and distance of subjects. On the ground, simple LiDAR technologies for telemetry and speed violations have been marketed, including a 3D car scanner. Recently, LiDAR is used as the primary technology for structural behaviour monitoring systems in areas such as SHM, and its use and importance are increasing gradually. LiDAR system advantages include the ability to measure hard-to-reach targets remotely such as coastal areas, which are difficult to assess using ground surveys, as well as nuclear reactors, areas with complex geography, and tall buildings.

Unlike contact sensors, the LiDAR system can obtain remote 3D coordinate information for whole objects from one device in a short period of time, allowing engineers to make measurements while maintaining a safe working distance, without requiring direct access to objects. Therefore, LiDAR makes it possible to reduce working time and work resources. In addition, installing a LiDAR device and obtaining raster cloud data makes their use easier than wire-based communication sensors. However, during data acquisition, the LiDAR device must be securely attached to the ground where it is secured, and movement around objects must be reduced to a

minimum so that the emitted laser pulse does not cause interference. (Jo et al, 2020).

2.2.6 Terrestrial laser scanning

Laser Scanning Techniques (TLS) is geodetic technique to monitor the displacement of structures. Many surveying tools and procedure implemented to date to constantly reach to the safety of type of the huge engineering structure. However, the key elements of all techniques are the ability to accurately measure the displacement of a limited amount of points comparison to the amount of the massive building. The number of required points is less if the automatic metering device is used (i.e. by using automated total stations or GPS). But at the other hand, laser scanners can obtain several points, so that the power can be applied to the entire system rather than limited to a few points. This fact is especially important, because in many locations, some grounding points for tools may be very complicated due to the local terrain of the Earth. These imaging systems provide the user with a dense set of 3D vectors to unknown locations of the scanner's location. Point size and high sampling frequency (complete scanning in a few minutes) of Laser scanning provides the users with an incredible density of spatial information For this reason, there is an immense opportunity for these instruments to be used in application monitoring, as these large data sets can provide a great insight into the existence of structural distortions in order to determine risks, discover improvements and validate the structural model. There are, however, two major disadvantages to be faced in this strategy:

1) The accuracy and stability of the geographical references, which is necessary for making comparisons between the various multi-time surveys; And

2) Calculation of distortion based on the withdrawal of the acquired point.

Ground laser scanners (TLS) provide the ability to gain 3D point data on an object or surface of interest (Gordon et al, 2003) and are also used to monitor the deformation of the large concrete dam (Antova, 2015). Table 2.1 provides the accuracy and range of structural health monitoring techniques.

SENSORES	ACCURACY	RANGE
Accelerometer	+/- 0.1mm	+/- 2g
Tiltmeters	0.9 m	Few Km
Extensometer	0.3mm	30 m
GNSS Positioning	2-5 mm	<50 Km
LIDAR	10-20cm	> 100 Km
GPS	5 mm	3 m
Total Station	1.5 mm	>1500 m
Close Range Photogrammetry	20 μm/m	< 100 m
Laser Interferometer	+/-1.5 mm	>80 m
Terrestrial Laser Scanning	+/-2.8 mm	> 600 m

Table 2.1: Accuracy and Range of Structural Health Monitoring Techniques**.**

3. STRUCTURAL MONITORING DATA ANALYSING METHODS

Most of the signal analysis techniques consist of the signal size, moreover as a time and frequency domain with a mixture of time and frequency analyses. The last two are specific details on the signal. Time frequency domain represent two other ways of watching an observance signal. Within the time domain, signals may be analysed within variety of their time history and distinctive signal peaks or other important properties of the signal. Analyses for continuous signals within the frequency domain, the time histories of any digital signal need to be regenerated into the frequency domain using a separate Fast Fourier Transform (DFFT). The Fourier Transform permits North American country to change from one domain to the other; but it doesn't mix the two domains. within the frequency domain, information about time is not easy to access, also, it doesn't give time localization of the spectral components; it solely shows the distribution. exploitation the frequency time domain, it's potential to identify periodicities of an indication which might not be recognized by the other methodology. as an example, if the signalling had constant frequency of vibration at two totally different times, this information would seem as one peak within the DFFT plots (Newland et al 2001).

3.1 Power Spectrum Analyses

Several functions and physical processes, including vibrations of the ground, can be represented in the frequency domain or the time domain. These functions can be stated as the value of h(t) when used in the time domain, or the capacity of H(ω) when used in the frequency domain with - with <∞ <∞. The Fourier transform equations for these are:

$$\mathrm{H}(\omega) = \frac{1}{2\pi} \int_{-\infty}^{\infty} h(t)\ e^{-i\omega \mathrm{t}}\, dt \qquad \textbf{(3.1)}$$

$$\mathrm{h(t)} = \frac{1}{2\pi} \int_{-\infty}^{\infty} H(\omega)\ e^{-i\omega \mathrm{t}}\, d \qquad \textbf{(3.2)}$$

Where ω is in radians.

Thus, you can determine the frequency component of the functions of rotating and non-rotating through this Fourier analysis. In the case of non-periodic jobs, it is believed that the function is repeatable on both sides of the integrated limits given in equation (3.2)

3.1.1 Wavelet analysis

The wavelet analysis was found to produce a decent kind of time- analysis. This can be achieved by a mix of time and spectral domains. In the wavelet analysis, signals are decomposed into a collection of native basic functions referred to as wavelets. The wavelets occupy various periods and have completely different frequency compositions so they fully mirror the signal being analysed along. Wavelet Transform is applied widely in signal process for its advantages that it has solid resolution in both the time-domain and the frequency-domain

3.2 Harmonic Wavelets

The harmonic wavelets determine Fourier transform defined by

$$Wm,n\,(\omega) = 1/(n-m)\,(2\pi) \quad for\ m(2\pi) \leq \omega < n(2\pi) \qquad \textbf{(3.3)}$$

$$0 \qquad \text{elsewhere}$$

where the values of m and n are assumed to be real positive numbers within band from m(2π) to n(2π). The operate contain constant magnitude, that normalized to make ensure that the closed region is unified and that it is zero outside this unit. The function of the corresponding wavelet may be presented as:

$$wm,n(x) = \{exp(in2\pi x) - exp(im2\pi x)\}/\ i2\pi(n-m)x \qquad \textbf{(3.4)}$$

where m and n show the wavelet in the frequency band from m(2π) to n(2π) where n>m. For the purpose of constructing an entire set of wavelets, the neighbouring wave rates should be processed using Fourier transforms, where the frequency bands are touching one another, thus the values of wherever on the axis zero to ∞ are enclosed.

3.3 Fast Fourier Transform

The Fast Fourier Transform (FFT) is a technique for analyzing and measuring signals from data capturing operating systems. Fast Fourier Transform (FFT), the algorithmic rule for transformation the data from the time domain to the frequency domain. First, because of the numerous calculations concerned within the transformation of domains, the transformation should be performed on a computing device if the results be sufficiently correct. currently we will not convert to the frequency domain during a continuous manner, then again, we want to investigate and modify the time domain information. It implies that our algorithmic rule interprets digitized samples from time domain to samples within frequency domain.

The technique of Fast Fourier Transform (FFT) is simply a DFT employing a lot of economical algorithmic rule that takes advantage of wave symmetry. The FFT needs a symbol length of some power of 2 to convert and divide the cycle into cascading teams of 2 to use these symmetries. This dramatically improves process speed; if N is that the length of the signal, a DFT desires N^2 operations whereas FFT desires N*log2(N).

The number of separate frequencies that are tested as a locality of Fourier transform is directly proportional to the number of samples within the original wave. With N being the length of the signals, the amount of frequency line adequate to N/2.

In this study the measured time interval (Δt) was 0.0031 s. The States had 1024 data points.

3.3.1 Time- Series of Fast Fourier Transform

Time series is defined to be N, the data points number in the acquired time-domain signal. Equally spaced samples of the inputs. N is limited to be multiple of 2, for this study 1024 data points used.

The time series is converted the entire time series into a full block of frequency lines. Both samples required record time to measure each line in the frequency domain. Since FFT converts time record block as a whole,

accurate frequency domain results cannot be obtained before a full-time record assembled. However, once finished, you can remove the oldest sample, all samples will be moved to the timeline, and the new sample will be added at the end of the time period. As a result, after filling the record time initially, we have a new record time for each sample time domain, and you'll also get new accurate results for the frequency range for each sample time field.

In case study the duration of the acceleration (*T*) input for the shaking table test 3.17 s for each States. the analysis time (*T*) was then calculated using Equation (3.15), The measured time interval (Δt) was 0.0031 s.

$$T = (1024 - 1) \times 0.00312\, s = 3.17\, s \quad \textbf{(3.15)}$$

3.3.2 Frequency-Series of Fast Fourier Transform

Another function of FFT is that it converts samples of time domain into evenly spaced 1024/2 lines in frequency domain and only get half the number of lines since frequency line really consist of two pieces of information, amplitude and phase. Must adopt a lower frequency spectrum we can be resolved by using the FFT analyzer time record length. The lowest frequency tested equal to zero Hz and highest frequency equal to (f_s/2) = 161.29 Hz which called *fmax.*

Where f_s is the frequency at which the acquired time-domain signal was sampled = 322.58 Hz.

3.3.3 Frequency Range of Fast Fourier Transform

Now, we can easily decide that the highest frequency we can calculate is:

$$fmax = \frac{N}{2} . \frac{1}{dt} \quad \textbf{(3.16)}$$

where, T is the period of time record = 3.17 s.

Because we have spaced N / 2 lines interchangeable with a time record starting at zero Hz. we want to change the frequency spectrum of

measurements, then need to change the *fmax*. data points samples N = 1024 It has been repaired through the implementation of an algorithm FFT. Therefore, we must change the time record period to vary fmax. To do this, we must change the sample rate so that we always have N = 1024 samples in the variable recording time period and these frequencies occur at interval (Δf) equal to the

$$\Delta f = \frac{1}{T} = \frac{F_S}{N} \rightrightarrows 0.315\ Hz \qquad \textbf{(3.17)}$$

Frequency axis equations indicate that the sampling frequency is the factor that rules the frequency band or spectrum bandwidth and that the number of points obtained in time field signal record dictates the resolution of the resolution of the sampling frequency. To increase the frequency accuracy of the frequency range, add a higher number of points obtained at a specific sampling frequency.

3.3.4 Assumptions

- The FFT algorithmic rule is predicated on the principle that now record is recurrent over time. This happens if we have a tendency to measure activity of non-stop signal sort of a wave during this case, the input wave form is alleged to be periodic within the time record.

- The FFT forces one more assumption, that N may be a multiple of two. this permits sure symmetries to occur reducing the quantity of calculations (specifically multiplications) that ought to be done.

- The FFT solely offers samples of the actual Fourier Transform. An additional vital, it's solely a transform of a specific time record for an input.

- The FFT spectrum analyzer desires such a large number of samples per second is to avoid a retardant known as aliasing. Aliasing may be a doable issue with each knowledge device sampled. it's usually unmarked, generally with calamitous results.

3.4 Converting the Acceleration Using Fourier Transform Method

Fourier Transform is widely applied in analysing signal frequency components which can be wont to transmit signal form the time domain to the frequency domain and Inverse Fourier Transform can transmit signals back to time domain. Give a series of discretized acceleration data point (a_r), where r = 0,1,2,3,…,(N-1), the discretized Fourier transform can be defined according to (Han and Chung, 2002) as

$$A_k = \frac{1}{N} \sum_{r=0}^{N-1} a r \, e^{-i(\frac{2\pi k r}{N})} \quad , k=0,1,2,3,....N-1 \qquad \textbf{(3.18)}$$

From properties of Fourier transform, the researcher derives the following expression for the Fourier Transform of displacement

$$D_k = - \frac{1}{(2\pi k)2} A_k , \quad k=0,1,2,3,....N-1 \qquad \textbf{(3.19)}$$

As technology improved over time, many commercial software packages developed algorithms to compute Fast Fourier transform (FFT), which gives terms of discrete Fourier transform with much higher computational efficiency. To obtain the frequency spectrum of an acceleration signal with a sampling rate of 322.58 Hz at 1024 sampled points, (Klingenberg,2005) give a typical FFT algorithm in excel which plots waveform in frequency domain.

Note that time interval = 0.0031s, determining sampling frequency

$$fs = 1/\Delta t = 1/0.0031 = 322.58 \text{ Hz} \qquad \textbf{(3.20)}$$

One limitation of using the available FFT function is that it requires the number of data points that are triggered to be a number with a power of 2, so we decided to use 1024 data points (2^{10}).

Experiments sometimes call the "harmonic content" of the repeated waveform. The harmonic content is a view of the waveform magnitudes (Y axis) versus the frequency (X axis). İt’s often called the frequency spectrum which helps you to picture the waveform according to its frequency content

which enables you to convert the waveform from the time domain to the frequency field using Excel.

The sampled data from this experiement into time domain and frequency domain, the number of data row 1024 data point and the difference in time interval 0.0031ms and the sampled frequency 322.58Hz.

Calculating FFT magnitude by finding the absolute value of FFT complex (This contains an FFT complex number) by selecting it's the output range that is created by Fourier Analysis.

And then multiplying FFT complex function by the following Equation (3.21) to obtains FFT magnitude function.

$$\text{FFT magnitude} = 2/1024 * \text{IMABS (FFT complex).} \qquad \textbf{(3.21)}$$

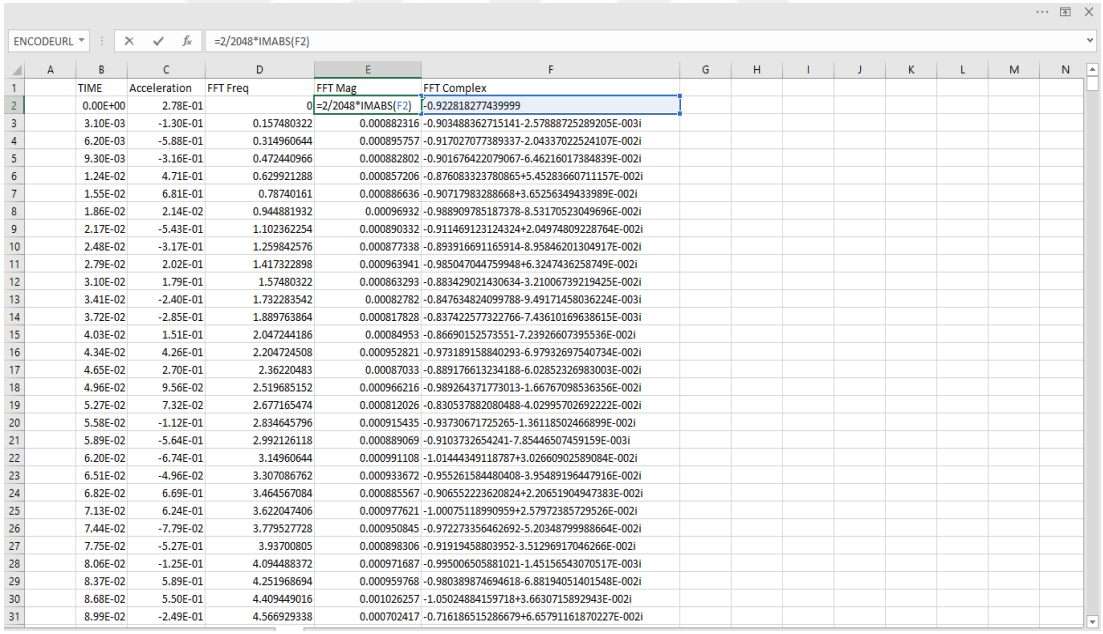

	A	B	C	D	E	F	G	H	I	J	K	L	M	N
1		TIME	Acceleration	FFT Freq	FFT Mag	FFT Complex								
2		0.00E+00	2.78E-01	0	=2/2048*IMABS(F2)	-0.922818277439999								
3		3.10E-03	-1.30E-01	0.157480322	0.000882316	-0.903488362715141-2.57888725289205E-003i								
4		6.20E-03	-5.88E-01	0.314960644	0.000895757	-0.917027077389337-2.04337022524107E-002i								
5		9.30E-03	-3.16E-01	0.472440966	0.000882802	-0.901676422079067-6.46216017384839E-002i								
6		1.24E-02	4.71E-01	0.629921288	0.000857206	-0.876083323780865+5.45283660711157E-002i								
7		1.55E-02	6.81E-01	0.78740161	0.000886636	-0.907179832886681+3.65256349433989E-002i								
8		1.86E-02	2.14E-02	0.944881932	0.00096932	-0.988909785187378-8.53170523049696E-002i								
9		2.17E-02	-5.43E-01	1.102362254	0.000890332	-0.911469123124324+2.04974809228764E-002i								
10		2.48E-02	-3.17E-01	1.259842576	0.000877338	-0.893916691165914-8.95846201304917E-002i								
11		2.79E-02	2.02E-01	1.417322898	0.000963941	-0.9850470447599481+6.3247436258749E-002i								
12		3.10E-02	1.79E-01	1.57480322	0.000863293	-0.883429021430634-3.21006739219425E-002i								
13		3.41E-02	-2.40E-01	1.732283542	0.00082782	-0.847634824099788-9.49171458036224E-003i								
14		3.72E-02	-2.85E-01	1.889763864	0.000817828	-0.837422577322766-7.43610169638615E-003i								
15		4.03E-02	1.51E-01	2.047244186	0.00084953	-0.866901525735551-7.23926607395536E-002i								
16		4.34E-02	4.26E-01	2.204724508	0.000952821	-0.973189158840293-6.97932697540734E-002i								
17		4.65E-02	2.70E-01	2.36220483	0.00087033	-0.889176613234188-6.02852326983003E-002i								
18		4.96E-02	9.56E-02	2.519685152	0.000966216	-0.989264371773013-1.66767098536356E-002i								
19		5.27E-02	7.32E-02	2.677165474	0.000812026	-0.830537882080488-4.02995702692222E-002i								
20		5.58E-02	-1.12E-01	2.834645796	0.000915435	-0.937306717252651-1.36118502466899E-002i								
21		5.89E-02	-5.64E-01	2.992126118	0.000889069	-0.910373265424 1-7.85446507459159E-003i								
22		6.20E-02	-6.74E-01	3.14960644	0.000991108	-1.014443491187873+3.026609025890 84E-002i								
23		6.51E-02	-4.96E-02	3.307086762	0.000933672	-0.955261584480408-3.95489196447916E-002i								
24		6.82E-02	6.69E-01	3.464567084	0.000885567	-0.906552223620824+2.20651904947383E-002i								
25		7.13E-02	6.24E-01	3.622047406	0.000977621	-1.000751189909 59+2.579723857295 26E-002i								
26		7.44E-02	-7.79E-02	3.779527728	0.000950845	-0.972273356462692-5.20348799988664E-002i								
27		7.75E-02	-5.27E-01	3.93700805	0.000898306	-0.919194588039 52-3.51296917046266E-002i								
28		8.06E-02	-1.25E-01	4.094488372	0.000971687	-0.995006505881021-1.45156543070517E-003i								
29		8.37E-02	5.89E-01	4.251968694	0.000959768	-0.980389874694618-6.88194051401548E-002i								
30		8.68E-02	5.50E-01	4.409449016	0.001026257	-1.050248841597 18+3.66307158929 43E-002i								
31		8.99E-02	-2.49E-01	4.566929338	0.000702417	-0.716186515286679+6.65791161870227E-002i								

Figure 3.1: FFT Complex Function in Excel

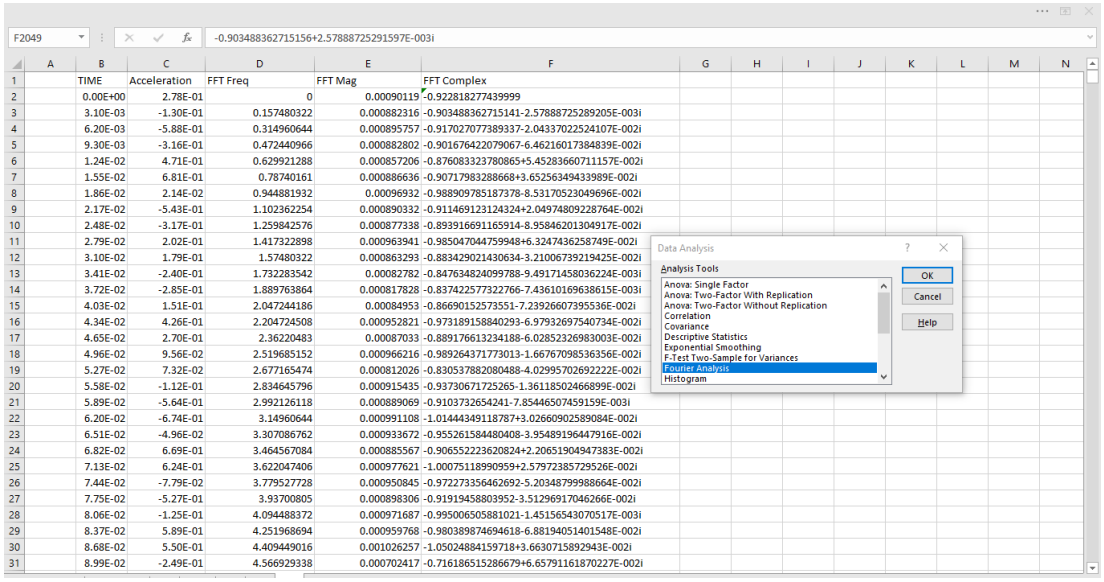

	A	B	C	D	E	F	G	H	I	J	K	L	M	N
1		TIME	Acceleration	FFT Freq	FFT Mag	FFT Complex								
2		0.00E+00	2.78E-01	0	0.00090119	-0.922818277439999								
3		3.10E-03	-1.30E-01	0.157480322	0.000882316	-0.903488362715141-2.57888725289205E-003i								
4		6.20E-03	-5.88E-01	0.314960644	0.000895757	-0.917027077389337-2.04337022524107E-002i								
5		9.30E-03	-3.16E-01	0.472440966	0.000882802	-0.901676422079067-6.46216017384839E-002i								
6		1.24E-02	4.71E-01	0.629921288	0.000857206	-0.876083323780865+5.45283660711157E-002i								
7		1.55E-02	6.81E-01	0.78740161	0.000886636	-0.907179832288668+3.65256349433989E-002i								
8		1.86E-02	2.14E-02	0.944881932	0.00096932	-0.988909785187378-8.53170523049696E-002i								
9		2.17E-02	-5.43E-01	1.102362254	0.000890332	-0.911469123124324+2.04974809228764E-002i								
10		2.48E-02	-3.17E-01	1.259842576	0.000877338	-0.893916691165914-8.95846201304917E-002i								
11		2.79E-02	2.02E-01	1.417322898	0.000963941	-0.985047044759948+6.32474362587495E-002i								
12		3.10E-02	1.79E-01	1.57480322	0.000863293	-0.883429021430634-3.21006739219425E-002i								
13		3.41E-02	-2.40E-01	1.732283542	0.00082782	-0.847634824099788-9.49171458036224E-003i								
14		3.72E-02	-2.85E-01	1.889763864	0.000817828	-0.837422577322766-7.43610169638615E-003i								
15		4.03E-02	1.51E-01	2.047244186	0.00084953	-0.866901525735 51-7.23926607395536E-002i								
16		4.34E-02	4.26E-01	2.204724508	0.000952821	-0.973189158840293-6.97932697540734E-002i								
17		4.65E-02	2.70E-01	2.36220483	0.00087033	-0.889176613234188-6.02852326983003E-002i								
18		4.96E-02	9.56E-02	2.519685152	0.000966216	-0.989264371773013-1.66767098536356E-002i								
19		5.27E-02	7.32E-02	2.677165474	0.000812026	-0.830537882080488-4.02995702692222E-002i								
20		5.58E-02	-1.12E-01	2.834645796	0.000915435	-0.937306717 25265-1.36118502466899E-002i								
21		5.89E-02	-5.64E-01	2.992126118	0.000889069	-0.9103732654241-7.85446507459159E-003i								
22		6.20E-02	-6.74E-01	3.14960644	0.000991108	-1.014443491187 87+3.02660902589084E-002i								
23		6.51E-02	-4.96E-02	3.307086762	0.000933672	-0.955261584480408-3.95489196447916E-002i								
24		6.82E-02	6.69E-01	3.464567084	0.000885567	-0.906552223620824+2.20651904947383E-002i								
25		7.13E-02	6.24E-01	3.622047406	0.000977621	-1.000751189905 59+2.57972385729526E-002i								
26		7.44E-02	-7.79E-02	3.779527728	0.000950845	-0.972273356462692-5.20348799988664E-002i								
27		7.75E-02	-5.27E-01	3.93700805	0.000898306	-0.919194588039 52-3.51296917046266E-002i								
28		8.06E-02	-1.25E-01	4.094488372	0.000971687	-0.995006505881021-1.45156543070517E-003i								
29		8.37E-02	5.89E-01	4.251968694	0.000959768	-0.980389874694618-6.88194051401548E-002i								
30		8.68E-02	5.50E-01	4.409449016	0.001026257	-1.050248841597 18+3.66307158929 43E-002i								
31		8.99E-02	-2.49E-01	4.566929338	0.000702417	-0.716186515286679+6.65791161870227E-002i								

Figure 3.2: FFT Magnitude Function in Excel.

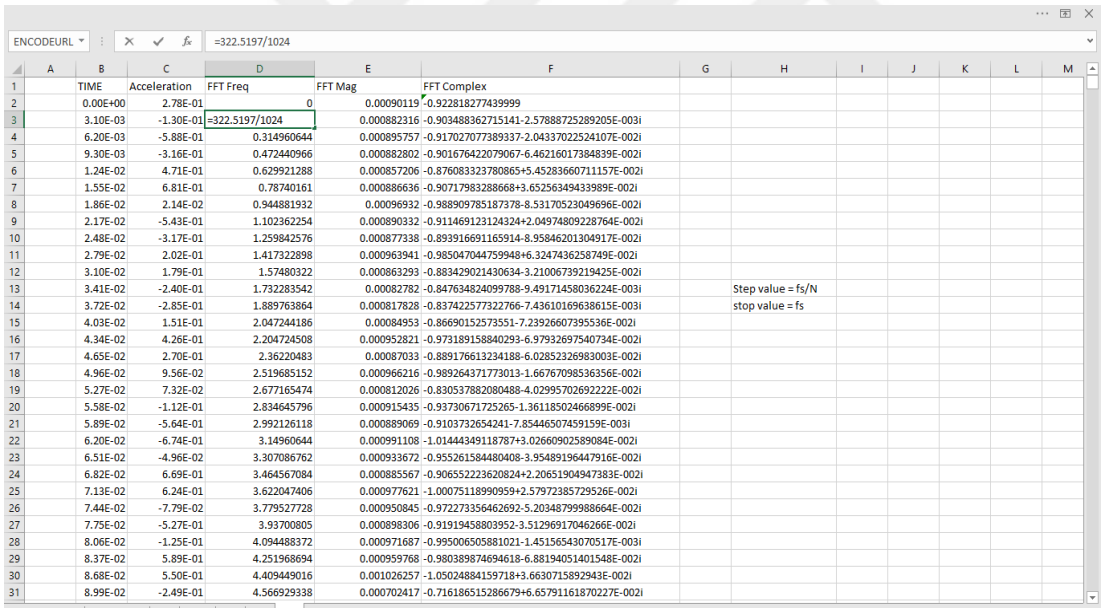

	A	B	C	D	E	F	G	H	I	J	K	L	M
1		TIME	Acceleration	FFT Freq	FFT Mag	FFT Complex							
2		0.00E+00	2.78E-01	0	0.00090119	-0.922818277439999							
3		3.10E-03	-1.30E-01	=322.5197/1024	0.000882316	-0.903488362715141-2.57888725289205E-003i							
4		6.20E-03	-5.88E-01	0.314960644	0.000895757	-0.917027077389337-2.04337022524107E-002i							
5		9.30E-03	-3.16E-01	0.472440966	0.000882802	-0.901676422079067-6.46216017384839E-002i							
6		1.24E-02	4.71E-01	0.629921288	0.000857206	-0.876083323780865+5.45283660711157E-002i							
7		1.55E-02	6.81E-01	0.78740161	0.000886636	-0.907179832288668+3.65256349433989E-002i							
8		1.86E-02	2.14E-02	0.944881932	0.00096932	-0.988909785187378-8.53170523049696E-002i							
9		2.17E-02	-5.43E-01	1.102362254	0.000890332	-0.911469123124324+2.04974809228764E-002i							
10		2.48E-02	-3.17E-01	1.259842576	0.000877338	-0.893916691165914-8.95846201304917E-002i							
11		2.79E-02	2.02E-01	1.417322898	0.000963941	-0.985047044759948+6.32474362587495E-002i							
12		3.10E-02	1.79E-01	1.57480322	0.000863293	-0.883429021430634-3.21006739219425E-002i							
13		3.41E-02	-2.40E-01	1.732283542	0.00082782	-0.847634824099788-9.49171458036224E-003i		Step value = fs/N					
14		3.72E-02	-2.85E-01	1.889763864	0.000817828	-0.837422577322766-7.43610169638615E-003i		stop value = fs					
15		4.03E-02	1.51E-01	2.047244186	0.00084953	-0.866901525735 51-7.23926607395536E-002i							
16		4.34E-02	4.26E-01	2.204724508	0.000952821	-0.973189158840293-6.97932697540734E-002i							
17		4.65E-02	2.70E-01	2.36220483	0.00087033	-0.889176613234188-6.02852326983003E-002i							
18		4.96E-02	9.56E-02	2.519685152	0.000966216	-0.989264371773013-1.66767098536356E-002i							
19		5.27E-02	7.32E-02	2.677165474	0.000812026	-0.830537882080488-4.02995702692222E-002i							
20		5.58E-02	-1.12E-01	2.834645796	0.000915435	-0.937306717 25265-1.36118502466899E-002i							
21		5.89E-02	-5.64E-01	2.992126118	0.000889069	-0.9103732654241-7.85446507459159E-003i							
22		6.20E-02	-6.74E-01	3.14960644	0.000991108	-1.014443491187 87+3.02660902589084E-002i							
23		6.51E-02	-4.96E-02	3.307086762	0.000933672	-0.955261584480408-3.95489196447916E-002i							
24		6.82E-02	6.69E-01	3.464567084	0.000885567	-0.906552223620824+2.20651904947383E-002i							
25		7.13E-02	6.24E-01	3.622047406	0.000977621	-1.000751189905 59+2.57972385729526E-002i							
26		7.44E-02	-7.79E-02	3.779527728	0.000950845	-0.972273356462692-5.20348799988664E-002i							
27		7.75E-02	-5.27E-01	3.93700805	0.000898306	-0.919194588039 52-3.51296917046266E-002i							
28		8.06E-02	-1.25E-01	4.094488372	0.000971687	-0.995006505881021-1.45156543070517E-003i							
29		8.37E-02	5.89E-01	4.251968694	0.000959768	-0.980389874694618-6.88194051401548E-002i							
30		8.68E-02	5.50E-01	4.409449016	0.001026257	-1.050248841597 18+3.66307158929 43E-002i							
31		8.99E-02	-2.49E-01	4.566929338	0.000702417	-0.716186515286679+6.65791161870227E-002i							

Figure3.3: FFT Frequency Function in Excel.

Then find FFT frequency is equal to

$$\text{FFT frequency} = 1 * fs/N \quad \textbf{(3.22)}$$

To convert from acceleration to displacement in the manner of Equation (3.23)

$$Displacement = 0.5 * acceleration * t2 \quad \textbf{(3.23)}$$

During this method, the content of the original signal is modulated on the basis of the transformation function, representing the characteristics of the device. Upon going through the high-pass filter used at this juncture, the low-frequency components are extracted.

4. CASE STUDY: ANALYSING STRUCTURAL DISPLACEMENT OF TEST PLATE

The structure that can be tested in a well-controlled laboratory environment is used to demonstrate extraction process and the subsequent testing and calibration of the model. In this model validation analysis, both linear and nonlinear system modelling are treated; thus, the test bed structure may also incorporate and regulate nonlinear behaviour. The description of the structure and the data acquisition are explained in this chapter.

In this section an attempt is to analyse these test data to measure the damage of structure when it's undergone structural changes by the operation and environment effect. Environmental and operational condition changes, which is difficulties in detecting structural damage and identified. Such variation usually causes change stiffness or mass in linear manner. In order to replicate these operational and environmental changes, specific stiffness and mass condition tests were conducted. The stiffness of some selected column was reduced by 50% and 1.2kg mass added to the first floor and base. In addition, damage detection was simulated by introducing nonlinearities into a specific building or structure when the distance between the suspended column and the bumper varied.

The three-story building test data will be provided by Los Alamos National Laboratory Elói Figueiredo, Engineering Institute - institute information of technology.

4.1 Test- Bed Structure Description

A Three-level structure shown in (Figure 4.1a) is the test-bed system used in study. This structure involves aluminium columns and plates assembled using bolted joints. Size of each floor plate is (0.305×0.305×0.025) m, and each of them is connected to the level above and/or the level below using four aluminium columns (0.177×0.025×0.006) m each. The structure can slide on the rails that allow its movement in only the x-direction; therefore, it can accurately be represented like four degree of freedom (DOF) system.

(Figure 4.2) shows a schematic of the basic dimensions of the test-bed structure.

Additionally, a centre column (0.150×0.025×0.025) m is suspended from the third floor, and a bumper mechanism is attached to the second floor as shown in (Figure 4.1b) and (Figure 4.3) respectively. Depending on the oscillation's amplitude and the size of the gap between the column and the bumper, a level of nonlinearity is introduced into the system as a result of the impacting between the column and the bumper mechanism. The bumper's position can be manipulated to change the size of the impact that happens during a specific action. This design was driven by many realistic examples where the cracks open, cut and close under dynamic loads. Note that the stiffness between the 2nd and 3rd floors (Figure 4.1a) becomes higher when the bumper contacts the column; additionally, the impact causes energy dissipation.

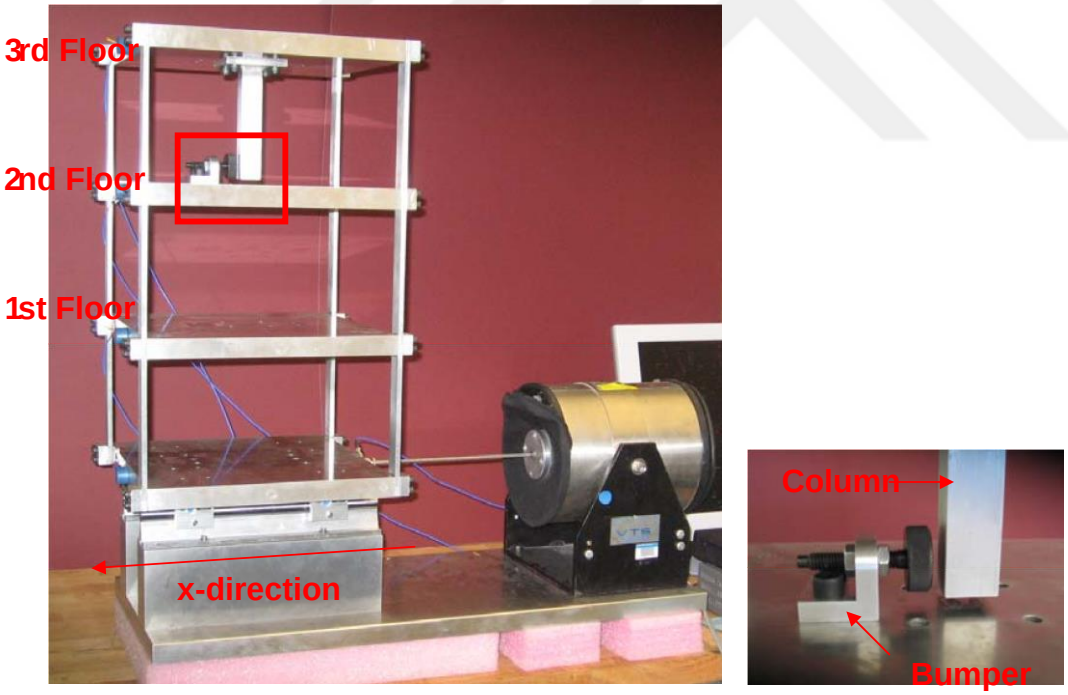

(a) Three-story frame structure

b) An adjustable bumper and the suspended column

Figure 4.1: Set-up of the Three-Story Structure.

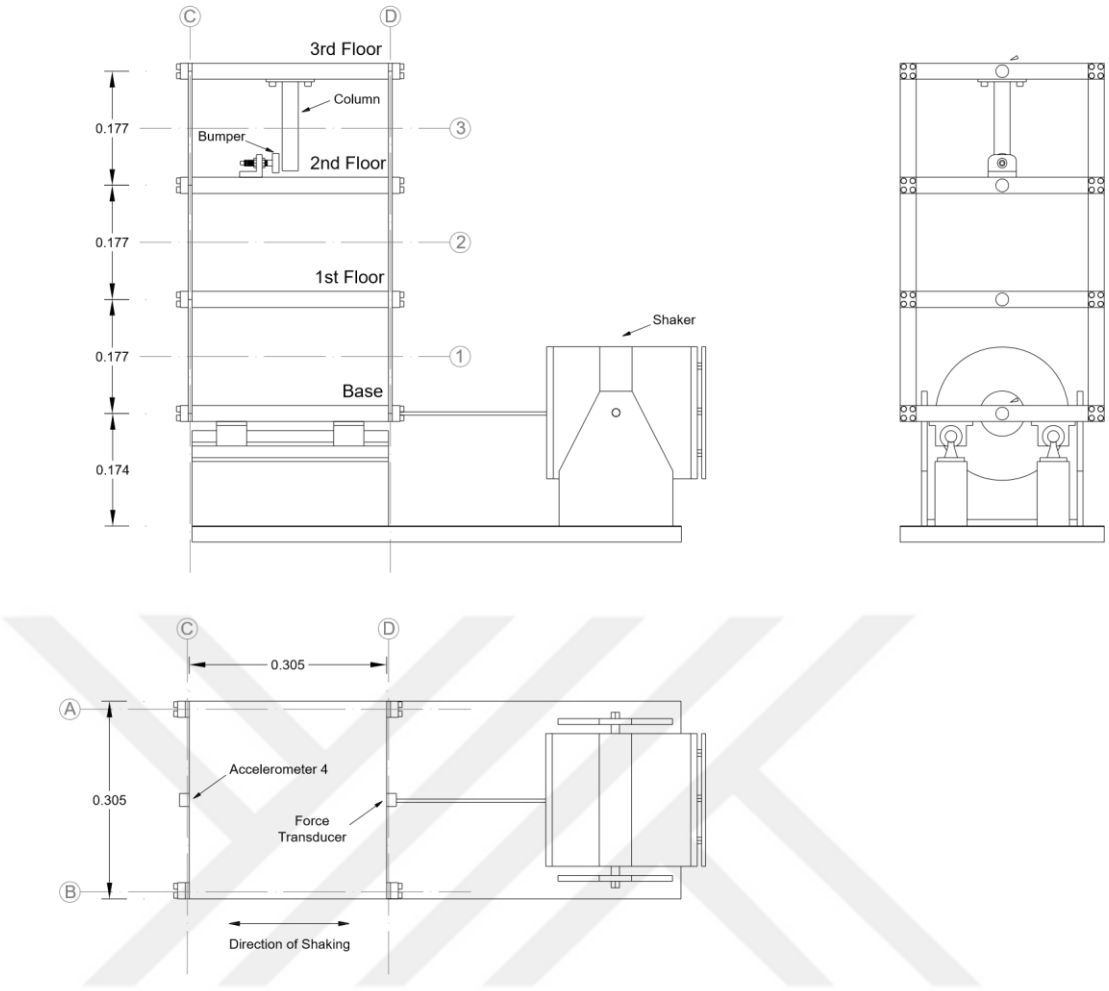

Figure 4.2: Basic Dimensions of the Three-Story Structure (unit: cm).

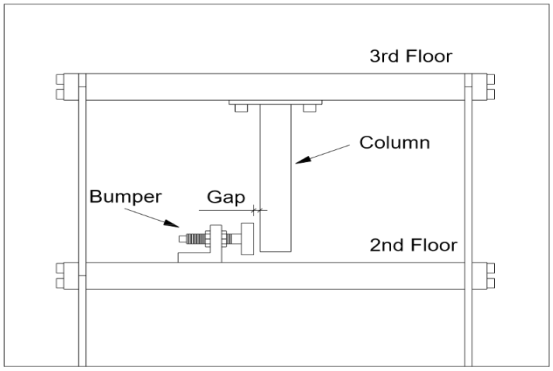

Figure 4.3: Structural Details Employed in order to Add Nonlinearity.

4.2 Data Acquisition

Various input and response time-history data from different excitations were collected in an effort to illustrate the various types of features that may be used in structural dynamics validation. electrodynamic shaker provided an excitation to the base level alongside the central line of the structure. The structure and the shaker were both mounted on a common base plate and the entire system rested on the rigid foam. This foam was designed to eliminate undesired sources of excitement from being absorbed into the structure's base floor. The input signals were random. The force transducer (Channel #1) in (Figure 4.2) with a nominal sensitivity value equal to 2.2mV/N. On the edge of the stinger, four accelerometers (from channel # 2 to channel # 5) in (Figure 4.2) with a nominal sensitivity of 1000 mV / g were mounted to the centreline of each level on the side opposite to the excitation site to measure the input force from the shaker to the structure to determine the structure's answer. Dynamic data collection system was not used to collect the data. The output channel of this assembly, the one that provides the shaker with the drive signal, was attached to a power amplifier which does the driving of the shaker.

For random excitation, signals from an analogy sensor have been distorted with 1024-time domain data points sampled at 322.58 Hz. The mentioned sampling parameters yield data windows that are 3.17s in time. A random band-limited excitation between 20-150 Hz was used as an input signal to avoid rigid body structure modes below 20 Hz. One degree of excitation; 2.6V RMS.

For this excitation type, data were acquired both from the linear and the nonlinear systems recorded for a set of variable structural state condition as presented in (Tables 4.1) with more information that describe different state. Notice that 5 time-histories were acquired for each States, and each time-history dataset consists of data from the five sensors (Channel #1 to Channel #5) in (Figure 4.2).

	State condition	Data samples (dataxxx)
State#01	Mass on the 1st floor	11 to 20
State#02	Mass at the base	21 to 30
State#08	Gap=0.13mm	160 to 169
State#09	Gap=0.10mm	170 to 179
State#10	Gap=0.05mm	180 to 189
State#11	Gap=0.15mm	190 to 199
State#12	Gap=0.20mm	200 to 209
State#13	Baseline condition	210 to 219
State#14	Gap=0.20mm + mass on the 1st floor	220 to 229
State#15	Gap=0.10mm + mass on the 1st floor	230 to 239
State#16	Gap=0.20mm + mass at the base	240 to 249
State#17	Column: 1BD – 50% stiffness reduction	251 to 260
State#18	Column: 1AD + 1BD – 50% stiffness reduction	261 to 270
State#21	Column: 3BD – 50% stiffness reduction	291 to 300
State#22	Column: 3AD + 3BD – 50% stiffness reduction	302 to 311
State#23	Column: 2AD + 2BD – 50% stiffness reduction	312 to 321
State#24	Column: 2BD – 50% stiffness reduction	322 to 331

Table 4.1: Observation File Labels for Structural State Conditions.

State#17 is describe as stiffness reduction in column 1BD, which mean that there was an 50% stiffness reduction in the column located between the base and the first floor at the intersection of plane B and D.

State#22 is describe the stiffness reduction in column 3AD+3BD, which man that there was an 50% stiffness reduction in columns located between the second and third floor at the intersection of planes A, D and B, D.

The results for structural conditions analysis #13 (baseline condition) It will be compared with the results of the analysis of the case of structural condition #08 (Gap=0.13mm) and structural state condition #10 (Gap=0.05mm) to examine the inconsistency in the results and to find out how the introduction of non-linearity property in the system changes as a result of these analysis. This is to emulate the detection of non-linear corruption and location. Then the results of analyses for the structural state condition #13 (baseline condition) is to be compared to the analyses results of the structural state condition #02 (Adding 1.2 kg at base floor) to simulate changes in structures in real-life scenarios caused by changing the operation and environment conditions, a large number of sources of variance are incorporated in the test structure. This diversity involves inducing extra mass and minimising the stiffness in a number of varying locations. Finally, the results of the analysis of the structural conditions # 13 (baseline case) will be compared with the results of the analysis of the structural state #15 (gap = 0.10 mm + mass on the first floor) to learn how to enter the nonlinearity resulting from the effects with a bumper.

It should be noted that the excitation of the sinusoidal inputs applied with a certain amplitude in each experiment is the signal that is generated by a computer that was used to control the output of the vibrator force. On the other hand, empirical data shows that the power that is measured using the transducer is not merely different from the amplitude of the sinusoidal due to scaling effects etc., but also incorporates the harmonics due to the inherent non-linear nature of the shaker dynamics. Thus, in this study, when the proposed technique for experimental data analysis was applied, the frequency range to excite the input strength that is actually used in the analysis included not only the frequency of observations but also their frequency.

4.3 Time Series Used in the Test

Time series analysis represents the issue where the that data points obtained over a period of time can have an internal structure, like autocorrelation, pattern, or seasonal variability. comparisons of the experimental data are performed by overlaying the response time-histories. However, it should be noted that the time- histories are high-dimensional features resulting in comparisons that are somewhat subjective and qualitative. However, these comparisons still provide some assessment of the numerical models' validity.

4.3.1 Linear system

(Figure 4.4) to (Figure 4.6) show overlays of experimental responses from the linear system corresponding to the different conditions. All time-histories represent accelerations from Channel #5 (3rd floor).

When examining the result from the random excitation of (#01, #13, #23) and to show an overview of the appearance of the row data, it is obvious that the amplitude of date is comparatively constant, depending on the visual examination. Since the gate to the shaker is defined as a random signal of normal distribution, it can be assumed that time dates are distributed from the baseline and additional conditions that may not have been normally damaged. This assumption is based on the known and expected result of random vibrations that will be shown by the linear system that undergoes a randomly distributed random response.

4.3.2 Non-linear system

(Figure 4.7) to (Figure 4.10) show the overlays of time-series from the nonlinear system with the bumper mechanism. All of them are the time-series from Channel #5 (3rd floor).

When we examine the result of random excitation of (#13, #08, #10, #15) Simulated damage due to non-linearity due to shock with the bumper. The suspended column hits the bumper when the structure is excited base floor. The degree of non-linearity depends on the strength of the oscillation and also the distance from the shaft to the bumper. As mentioned previously, this damage source is designed in order to simulate the fatigue cracks that may open and close when dynamic loading takes place.

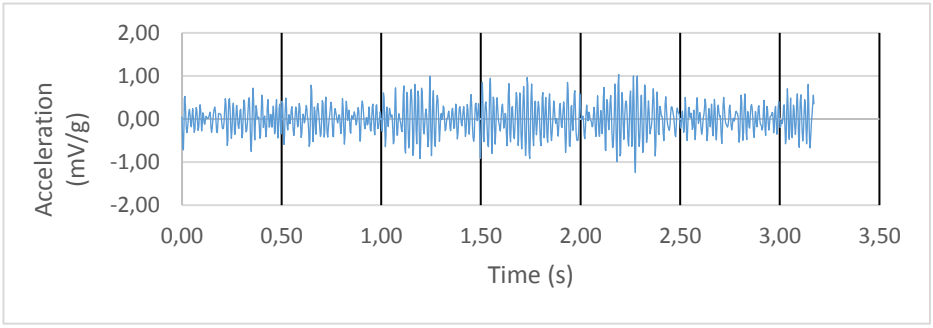

Figure 4.4: Time Series of State #01, Ch5 (3rd floor).

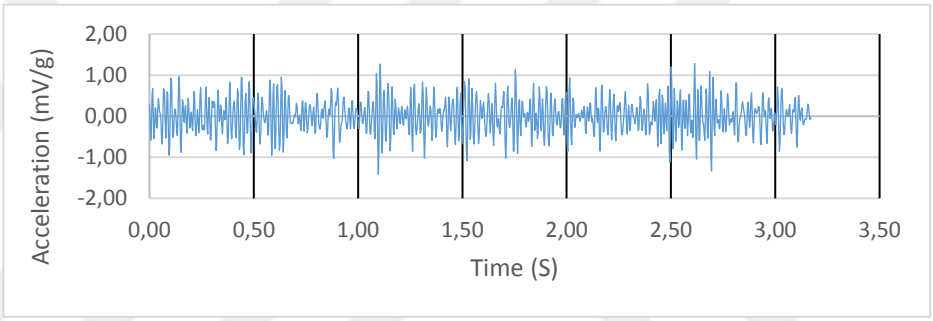

Figure 4.5: Time Series of State #13, Ch5 (3rd floor).

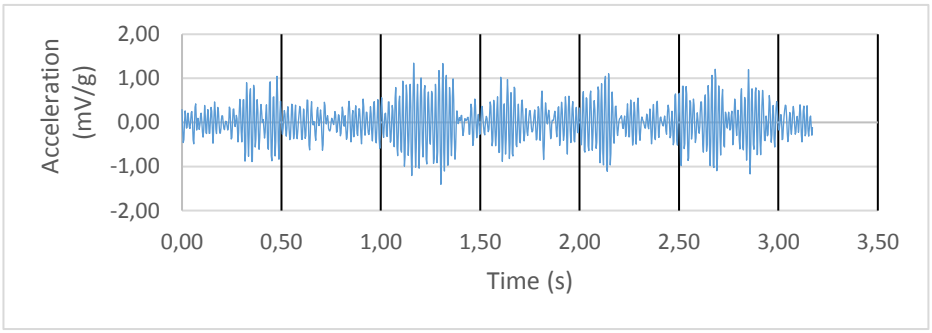

Figure 4.6: Time Series of State #23, Ch5 (3rd floor).

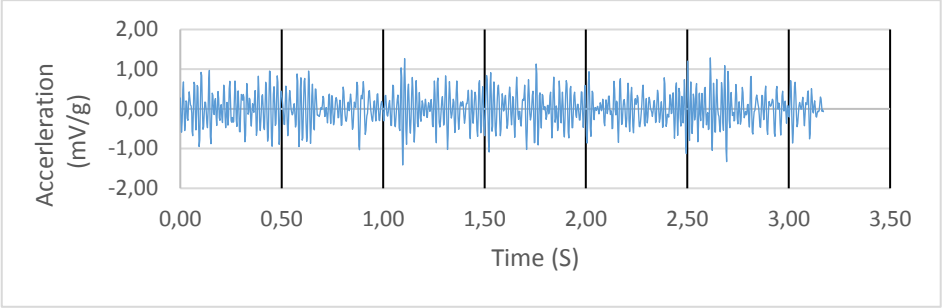

Figure 4.7: Time Series of State #13, Ch5 (3rd floor).

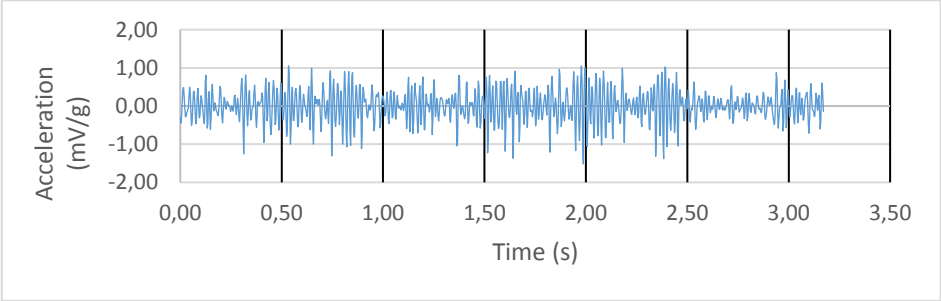

Figure 4.8: Time Series of State #08, Ch5 (3rd floor).

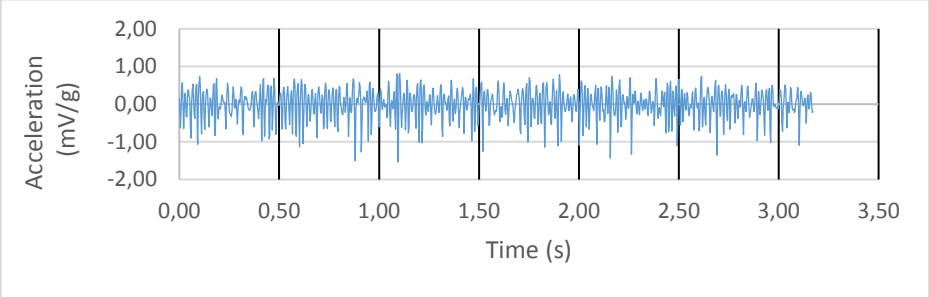

Figure 4.9: Time Series of State #10, Ch5 (3rd floor).

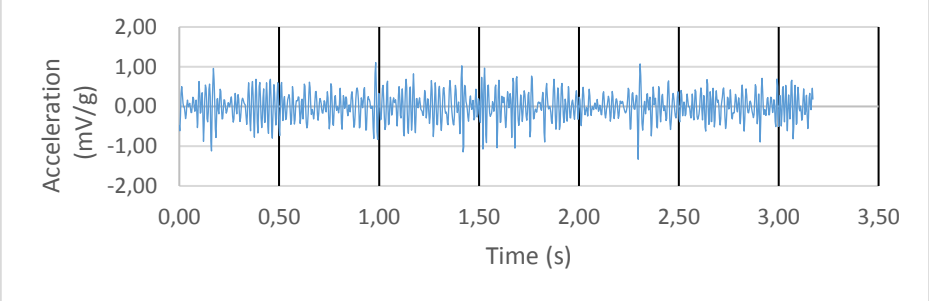

Figure 4.10: Time Series of State #15, Ch5 (3rd floor).

4.4 Frequency – Time Analysis

This section studies the time frequency amplitude representations of the considered signals in an attempt to spot the character of the vibratory movement and damage. the most useful aspect of this illustration is to trace the development of the frequency parts of the signal over a period of time.

For a static system, the frequency part shouldn't modification over time. Nonetheless, some nonlinearities introduced into the structure by a bumper may end up in a very nonstationary system. Thus, if a damage exhibits itself as a nonlinearity in the system, the signals from a damaged part will be time-variant. As a result, the frequency content could modification with relevancy time in a very way that may be correlate with damage.

The graph shows the baseline condition which can be defined as the reference structural state and is labelled (State #13). Bumper and suspended columns are incorporated in the baseline condition, although the distance between them are preserved in such a way that there are no serious impacts during the excitement. An experimental baseline distribution is created by acquiring data set under the same linear condition of test-bed three story structure. The band-limited with frequency range of 20-80 Hz for channel 5 (Third floor) and amplitude of 0.11 at frequency 55.27 Hz.

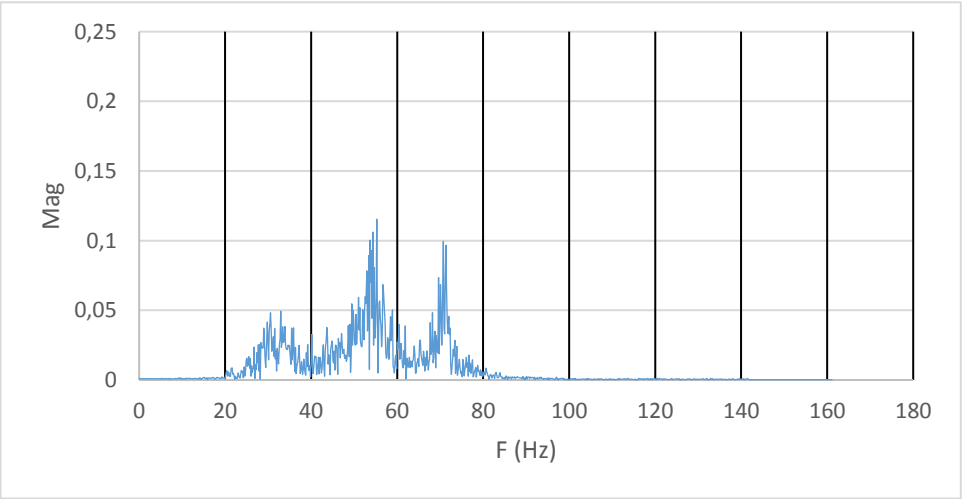

Figure 4.11: Fast Fourier Transform Spectra Analysis of State #13, ch5.

This graph includes the state with simulated operation and environment condition changes, test was carried out with different mass-loading (state # 1-2). The mass changes that have resulted from adding 1.2kg that is approximately 19% of the total mass of each floor to the base floor (State #02) and first floor (State #01). the peak amplitude of 0.096 at frequency 55.27 Hz for State #01 and 0.136 at frequency 51.968 Hz for State #02.

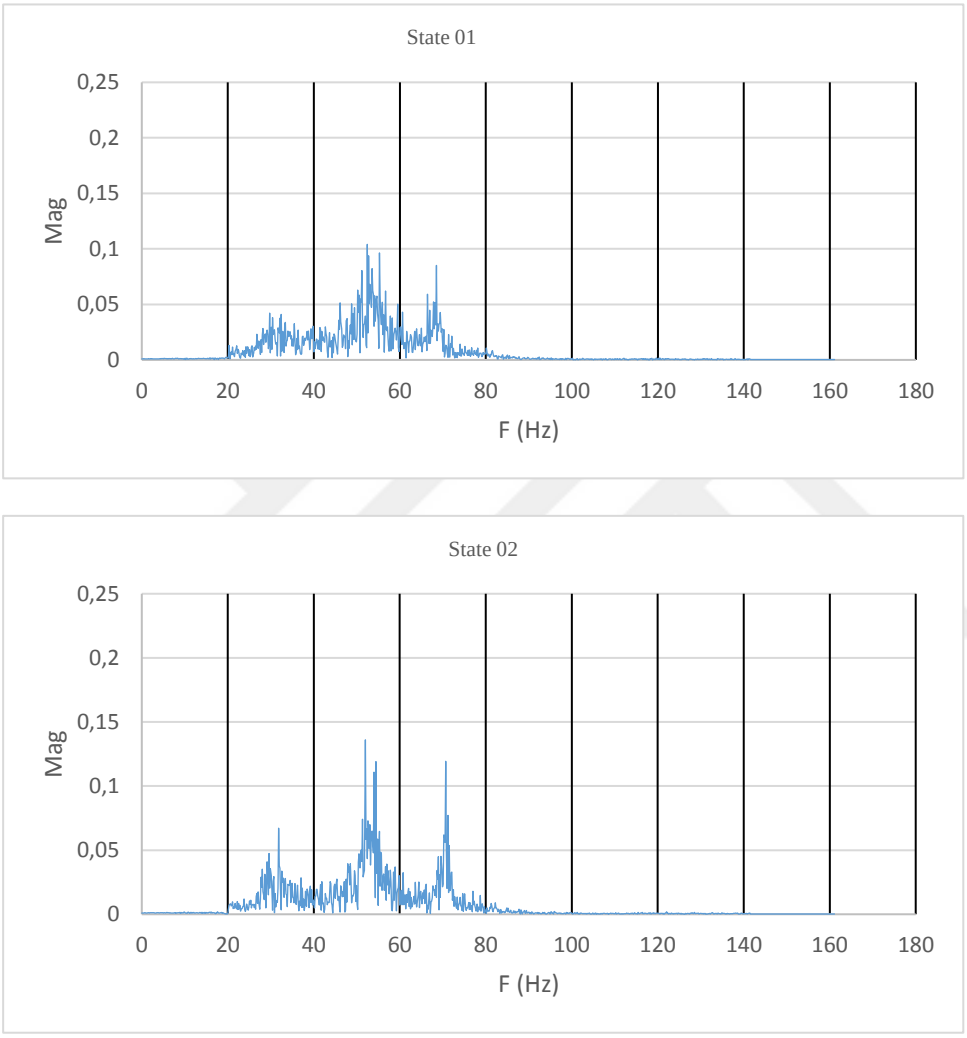

Figure 4.12: Fast Fourier Transform Spectra Analysis of (a) State #01, ch5; (b) State #02, ch5.

This graph includes the state with simulated operation and environment condition changes, test was carried out with different stiffness reduction (state # 17, #18, #21-#24). The stiffness reduction of (State #23) in columns 2AD+2BD, which mean that there was an 50% reduction in stiffness in the columns that are between the 1st and 2nd floor at the intersection line of planes A, D and B, D. the peak amplitude of 0.202 at frequency 54.803 Hz for Channel 5 (Third floor).

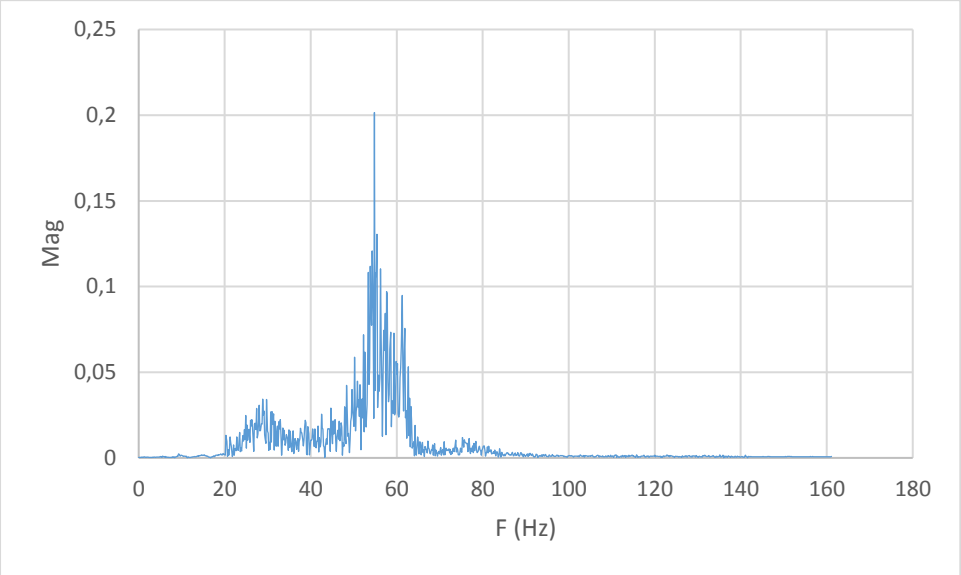

Figure 4.13: Fast Fourier Transform Spectra Analysis of State #23, Ch 5.

From Figures (4.11), (4.12), can observe that:

a) there is a slight difference between the baseline condition (State 13) and the base mass of 1.2 Kg (State 02), which shows that the addition of 1.2 Kg to the base floor has a very small effect on the dynamic response (contributes little to the dynamic response).
b) The cases with adding mass at base floor (State 01), it observed that decreases from baseline condition (State 13) to the base floor (State 02) and first floor (State 01) as the mass added into bases, and decreasing steadily as the mass moves from the base floor to the first floor.

From Figures (4.11), (4.13), we can observe that:

a) Only has one peak when 50% stiffness reduction in columns 2AD+2BD (State 23) and two peaks for baseline condition (State 13).
b) With respect to the effect of the reduction of stiffness, the frequency changes at the peaks differ from the baseline state (State 13) to the stiffness reduction (State 23).
c) For the cases of stiffness reduction, one can observed that FFT doesn't hold the same rule; It will be difficult to draw a conclusion for the detection of damage, or it will be difficult to find a clear rule for predicting damage.

These graphs were simulated by the introduction of nonlinearities into the studied structure. A suspended column and a bumper were used with variable gaps in between them. The space between bumper and suspended column was 0.13mm (State #08) and 0.05mm (State #10). the amplitude of 0.124 at frequency 55.59 Hz for State #08 and 0.096 at frequency 58.9 Hz for State #10.

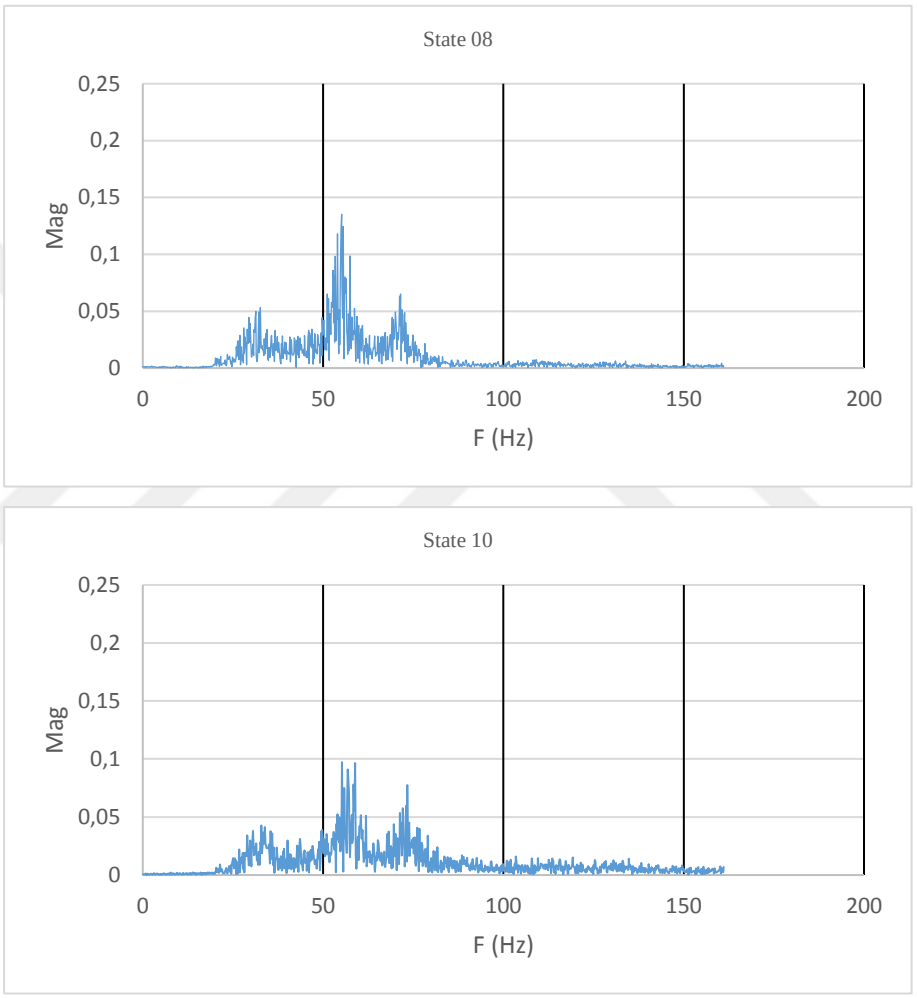

Figure 4.14: Fast Fourier Transform Spectra Analysis of (a) State #08, ch5; (b) State #10, ch5.

These graphs used to detect damage when the structure has undergone structural changes caused by operational and environmental effects. For this purpose, State #14 (Gap =0.20mm +mass on the 1st floor) and State #15 (Gap=0.10mm + mass on the 1sf floor). the amplitude of 0.105 at frequency 52.75 Hz for State #14 and 0.075 at frequency 55.59 Hz for State #15.

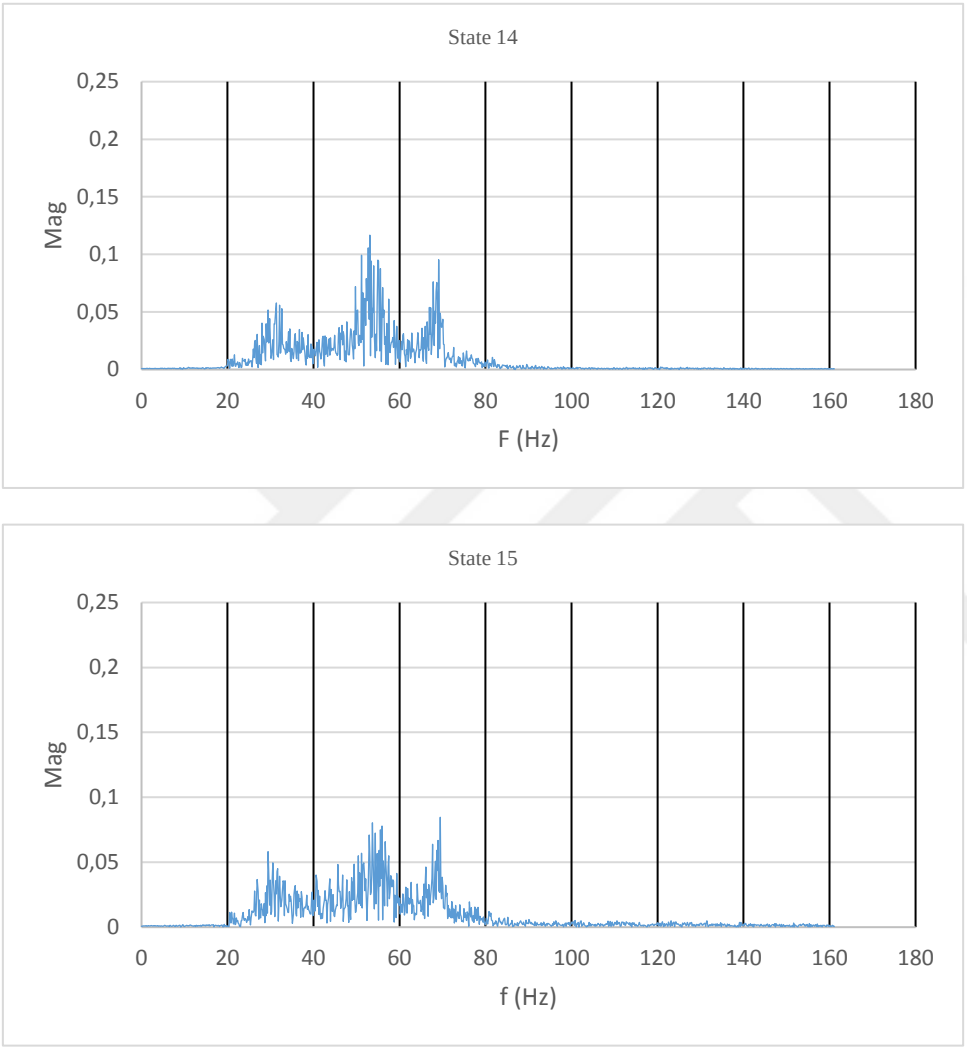

Figure 4.15: Fast Fourier Transform Spectra Analysis of (a) State #14, ch5; (b) State #15, ch5.

5. CONCLUSION AND RESULT

Dynamic behaviour occurs for all winds and earthquakes in buildings. But planning for wind and earthquake movements is completely different. However, in the design of the earthquake, structure is exposed to random ground movement at its foundation, causing the forces of inertia within the building which, in effect, raise pressure; This can be a displacement-type load. The demand for building is that the displacement (i.e. the horizontal axis) of the displacement-type loading is due to earthquake vibration.

Earthquake shaking allows building to be able to withstand relative displacement inside it because of the forced displacement at its foundation, the particular displacement obligatory below the building isn't as exactly understood. Seismic vibration is most extreme, as it causes displacement under houses, which varies in time. This, in turn, requires a side deformation of the structure between its base and its highest elevations. The higher is the seismic region, and the larger is the intensity of this imposed relative distortion. Hence, a big challenge is to meet the double demand - the structure must have capacity to withstand this forced deformation with damage under low-intensity vibration and without collapsing under high-intensity vibration. The building must have a wide capacity for inflexible deformation and must have energy, in all its members, to withstand the forces and moments that cause it.

In the experience of our own simulation, the use of the structure of a component three-storey building as a location detector test is damaged, with the presence of Shaker provides electro-magnetic excitation in the main floor of the structure. Channel 1 (transducer) used to measure the input strength of the vibrator, and channel 2-5 (4 accelerometers) are connected to the centre of each floor on the side opposite the excitation source used to measure the response from each floor.

Structure condition is divided into four groups:

1. Baseline condition.
2. The baseline condition when the structure is subject to changes in adding mass and stiffness reduction due to operational and environmental impacts
3. The State of condition with non-linearity imposed by the bumper.
4. The state of condition with non-linearity and environmental and operational impacts.

FFT used to measure the frequency quality of signal sections over time. FFT provides information about frequency content as well as about the evolution of frequency content over a period of time. Considering a specific sampling rate, the FFT frequency accuracy is calculated by the window length or period. Remember that the quality of the signal frequency from the stationary device does not change over time. The Fourier Analysis command is used in excel to measure FFT and imagine how frequency components change over time.

In Fourier analysis, frequency information can be extracted only for the entire duration of the f(t) signal. An integral part of the Fourier transform equation runs from approximately ∞ to $+\infty$ causing the information you provide in the frequency field to appear from the average along the entire signal.

this will result in Fourier transform F (ω), but its position will be lost on the time axis. The cause of the value of F (ω) at ω is unknown and cannot be determined if it is caused by frequencies present throughout the life of f (t) or only during one or a few specific times. However, this defect is solved in wavelet analysis. Differences in frequency components may be observed over time using waves.

In this study, each time series for 8192 data point acceleration is divided into 1024 points for FFT calculation. For each segment, a Fast Fourier transform is calculated to find an estimate of the frequency variable over time for the

signal. If the chronological date used to calculate the FFT represents a fixed system, it can be anticipated that one will not notice any changes in the frequency content as a function of time.

The vibrator was used with the harmonic excitation of the signal frequency to stimulate the structure in the basement across channel 1 and the structure response can be calculated by the accelerometer 4 installed in the middle of each floor on the opposite side of the source excitation, and therefore it is not successful to calculate the torsional conditions of the structure.

When examining the result from the random provocation of states (# 01, # 13, # 23) and to show an overview of the appearance of row data, it is obvious that the amplitude of the date dates is comparatively consistent, depending on the physical examination. Since the portal to the shaker was identified as a random signal for normal distribution, one assumption is that the time dates are distributed from the baseline and other conditions that are not normally damaged. It is clear that this assumption depends on the commonly known result of the random vibrations that a linear system that undergoes a randomly distributed naturally-inserted random response will show.

To simulate the changes in real-world structures caused by a number of operational and environmental conditions, many sources of variance are incorporated in the test structure. This variation includes the addition of mass and reduction of hardness in several variable locations as in state #01 adding a mass of 1.2 kg to the first floor, and state #23 describes a decrease in stiffness in column 2AD + 2BD, which indicates a 50% decrease in stiffness in columns between the first and second floors at The intersection of planes A, D, B, and D. The state with the added mass leads to a decrease in frequency, the state of reducing stiffness increases the normal period due to the increased state of damage.

The simulated damage was introduced by the nonlinearity caused by the shock with the bumper. The suspended column hits the bumper at a time when the chassis is excited at the base. The level and amplitude of the nonlinearity property depends on the amount of the oscillation and the size of the gap between the shaft and the bumper. The purpose of this damage

source is to simulate the fatigue cracks that usually open and close during dynamic loading.

The mass of the *i* the story is designated *mi* (*i* = 1,..,3), and the columns are coupled with the stiffness *ki* (*i* = 1,..,3) and the damping coefficients *ci* (*i* = 1,..,3). Notices that the base floor mass *m1* that move on the rails. The spring and damper with stiffness and damping values *k1* and *c1* are designed to show friction between the rails and bottom floor of the structure. The numerical values of *mi* is determined by the actual measured mass of the various structural elements. The stiffness *k2, and k3* It is determined as the summation of bending stiffness of four columns with rotation at either end of the column restrained; determined on the basis of *Euler-Bernoulli beam-theory (12EI/L3)*, where *I* is the cross-sectional area the moment of inertia, *L* is the distance between-floors, and *E* is the nominal Young's aluminium Module (65GPa). For stiffness *k1*, a comparatively low value is given compared to other stiffness because friction between rails and structure may be minimal in this system.

In the case of States (#08- #12), the nonlinear impact between the 2nd floor and the 3rd floor is defined as a bilinear model. During the time when the bumper on the 2nd floor contacts the suspended column on the 3rd floor, the bending stiffness of the suspended column is applied to the stiffness of the *k3* column For this model, the relationship between the relative displacement X = x3 – x2 and the internal force on the 2nd or 3rd floors was defined by a nonlinear load-displacement relationship. The stiffness between the 2nd floor and 3rd floor becomes higher when the bumper hits suspended column; however, the impacts induce energy dissipation.

The spectrogram of State 13 (The baseline condition), The state 12 (Gap =0.20 mm) and the state 10 (Gap =0.05mm) show that:

1. All Cases show a large energy content around the resonant frequency components of the three specifics, at 32, 55, and 71 Hz (for the baseline condition). Note first frequency ingredient is less than 20 Hz. the 1st mode of the test bed structure is the rigid body mode associated with the sliding system on the rails; thus, the tests are only seen for the 2nd, 3rd and 4th modes

2. The second component of the resonance frequency (32 Hz) It has less energy content of other components
3. Damaged State #10 appears to spread the energy content more uniformly across the spectrum by reducing energy to the frequency components;
4. There isn't clear evidence that the two affected States #12 and #10 derive from a non-stationary system; However, in the case of State #10, the damage tends to gradually increase natural frequencies over time for the other two countries.

While, in theory, the stiffness of the structure will change during the measurement due to the effects between the bumper and the suspended base, the spectrum patterns do not exhibit this effect. There are two reasons for explaining this result:

i. In the case of the low degree of damage (State 12), the effects occur fairly frequently in a timely manner and are not necessary to adjust the frequency ingredient for a specified period of time. However, high level of damage (state 10), large number of effects makes the structure more solid, but due to the occurrence of many effects during a given time period, its effects tend to be measured in the spectral estimation process, and these effects are similar in every window; Therefore, the system still has fixed properties;
ii. The trade-off between frequency accuracy and the length of the Fourier transform window restricts detection of changes due to short-frequency HF components; The lower the window length at time, the weaker the frequency accuracy. Remember that short-term windows allow good time resolution but poor frequency accuracy. On the other hand, older windows require good frequency accuracy but bad time accuracy.

The State concerned is divided into two categories to demonstrate the effect on the parameters of the organizational and environmental impacts. The numbers in APPEANDIX (A) showing increasing in the degree of nonlinearity in damaged cases appears to the amplitude of the

parameters. To further explain these changes, this figure shows the scale of all situations in Channel 5. One can generally see the relationship between capacitance and the non-linear level of damaged condition conditions without simulating operational and environmental changes (states # 08 - # 12), however, capacitance states affected by these differences (cases # 15-17) have nothing to do with the degree of deformation. These results indicate that operation and environment differences can bring about structural response changes and mask damage-related responses. This fact makes the distinction between the affected countries a challenge, with operational and environmental differences from all unaffected countries.

One can note that in general the differences for undamaged condition conditions decrease (states # 01,02,17,18,21- # 24) and increase for affected countries with no changes in mass or hardness (states # 08- # 12).

in conclusion, the FFT study indicates that there are no significant improvements in the frequency ingredient for the lowest vulnerability (State #12). However, some small signs of a temporal quality of the signal frequency quality of the affected state corresponding to most of the effects (State # 10) can be seen, but it will be difficult to establish a damage estimate for these subtle adjustments. Remember that Fourier transforms reflect the average signal characteristics within a given range, and these mean properties remain constant throughout the date of time.

REFERENCES

Afrouz, S.G., Razavi, M.R., Pourkand, A., and Wilson, C.M. (2019) Dynamic Placement of an Aluminium Frame Using Close Range Photogrammetry. *MDPI building journals*, Vol. 9, No. 176, doi.10.3390/building9080176.

Ahmad, A., Mashhuri, A.M. (2008) Development of Camera Calibration Software using Bundle Adjustment Method. PH. D Thesis, University Technology of Malaysia, Faculty of Geoinformation Science and Engineering: Johor, Malaysia.

Anonym. (2002) Structural Deformation Surveying (EM1110-2-1009). US Army of Engineers, Washington, DC 20314-1000.

Antova, G. (2015) Terrestrial Laser Scanning for Dam Deformation Monitoring- Case study (7885). *FIG Congress from the Wisdom of the Ages to the Challenges of the Modern World*, Sofia, Bulgaria, 17-21 May 2015.

Avsar, Ö., Akca, D., and Altan, O. (2014) Photogrammetric Deformation Monitoring of The Second Bosphorus Bridge in Istanbul. *The International Archives of the Photogrammetry, Remote Sensing and Spatial Information Sciences,* Volume XL-5-71-2014, ISPRS Technical Commission V Symposium, 23 – 25 June 2014, Riva del Garda, Italy.

Aziz, W., Nordin, Z., Amin, Z. M., Yahya, M.H., and Kok, S.K. (2008) The Current and The Future Trends on Structural Health Monitoring Scheme in Malaysia. *2nd Engineering Conference on Sustainable Engineering, Infrastructures Development & Management,* Kuching, Sarawak, Malaysia, December 18 -19, 2008.

Ding, X., Qin, H. (2000) Geotechnical Instruments in Structural Monitoring, *journal of Geospatial Engineering*, 2(1):45-56.

Erol, B (2010) Evaluation of High- Precision Sensors in Structural Monitoring. *MDPI Sensors Journals* 2010, 10(12), 10803-10827.

Erol, S., Erol, B., and Ayan, T. (2004) General Review of Deformation Monitoring Techniques and a Case Study: Analysis Deformation Using GPS / Levelling. *XXth ISPRS Congress*.12-23, 2004.

Farrar, C.R., Doebling, S.W., and Nix, D.A. (2001) Vibration-Based Structural Damage Identification. *Philosophical Transactions of the Royal Society* 359, 131-149.

Gordon, S., Lichti, D., Stewart, M., and Franke, J. (2003) Structural Deformation Measurement Using Terrestrial Scanners. *Proceedings, 11th FIG Symposium on Deformation Measurements*, Santorini, Greece, 2003. GPO Box U1987, PERTH WA 6845 Australia.

Ibanez, W., and Poleszuk, G. (2018) Experience of Using Total Station and GNSS Technologies for Tall Building Construction Monitoring. *International Congress and Exhibition "Sustainable Civil Infrastructures: Innovative Infrastructure Geotechnology"* GeoMEast 2017: Facing the Challenges in Structural Engineering, pp 471-486.

Jatmiko, J., and Psimoulis, P. (2017) Deformation Monitoring of Steel Structures Using 3D Terrestrial Laser Scanner (TLS). *Digital Proceeding of the 24th EG-ICE International Workshop on Intelligent Computing In Engineering*, July 2017, pp 168-177.

Jo, C.H., Sohn, G.H., and Lim, M.Y. (2020). A Lidar Point Cloud Data-Based Method for Evaluating Strain on a Curved Steel Plate Subjected to Lateral Presuure, *MDPI sensor journal*, Vol. 20, Issue 3, 721. 28 January 2020.

Kok, K. (2005). High Rise Building Movement Monitoring using RTK-GPS (Case Study: Menara Sarawak Enterprise). Masters master, university technology of Malaysia, ID code: 4370

Newland, D.E., Madabhushi, S.P. and Teymur, B. (2001) Application of Wavelet Theory in the Analysis of Earthquakes Motions Recorded During the Kocaeli Earthquakes, Turkey 1999. *Fourth International conference on Recent Advances in Geotechnical Earthquakes*, Engineering and soil Dynamics, Missouri University of Science and Technology, 28 March 2001.

Roberts, G. W., Dodson, A., and Meng, X. and Cossor, E. (2004) High Frequency Deflection Monitoring of Bridges by GPS. *Journal of Global Positioning Systems* (2004) Vol. 3, No. 1-2: 226-231, December 2004.

Sohn, H., and Farrar, C. R. (2004) Wavelet-Based Active Sensing for Delamination Detection in Composite Structure. *IOP science journal*. Smart material and structure, Vol.13, No 1, December 2003.

Worden, K., and Farrar, C.R. (2007). Non-linear System Identification for Damage Detection, LA-14353-MS, November 2007, Los Alamos National Laboratory, DE-AC52-06NA25396.

Worden, K., Sohn, H., and Farrar, C.R. (2002). Novelty Detection in a Changing Environment, *journal of sound and vibrations*, Vol. 258, Issue 4 page 741-761, 5 December 2002.

APPENDICES

APPENDIX A: Figures

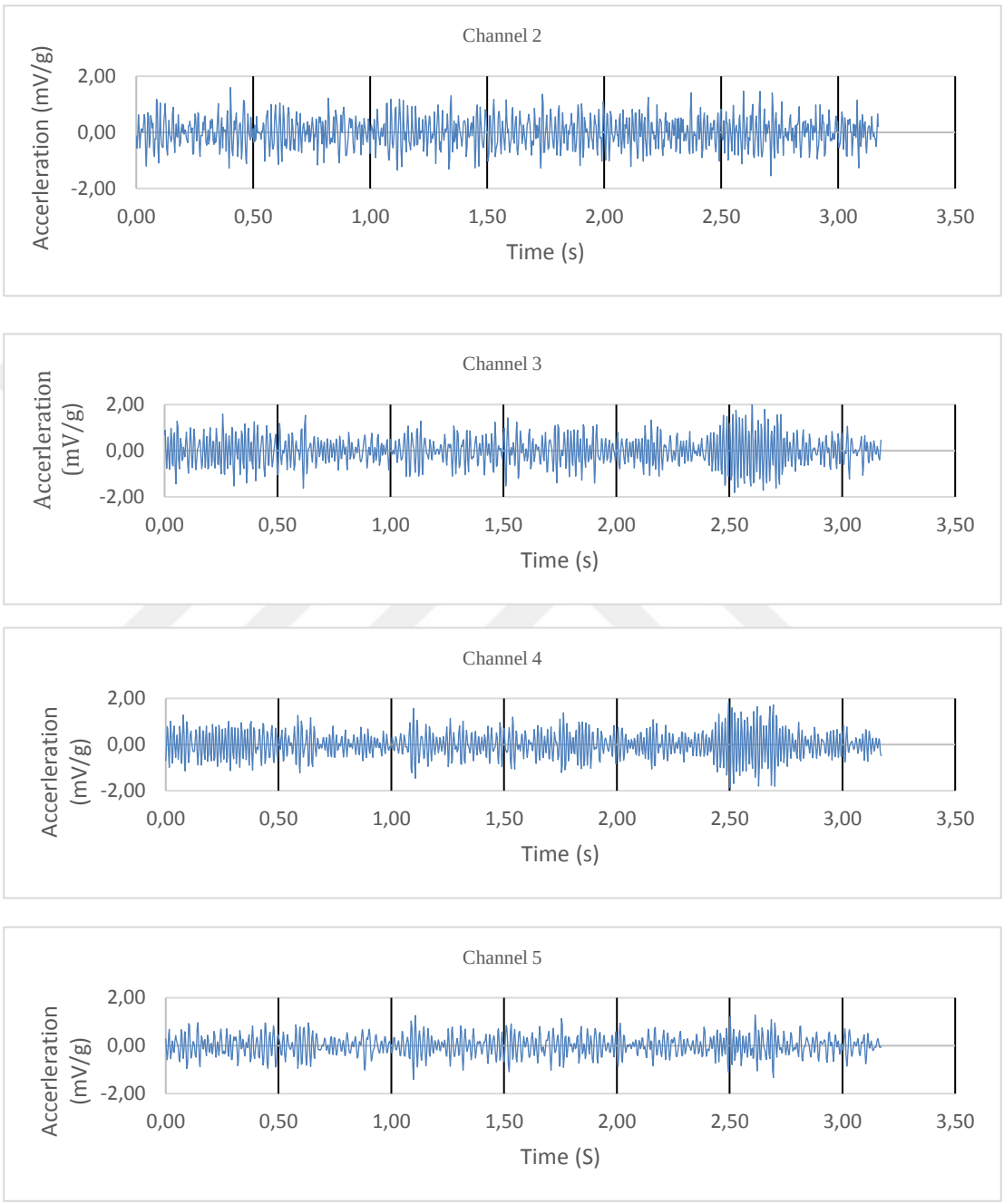

Figure A.1: Acceleration-Time Series of State #13.

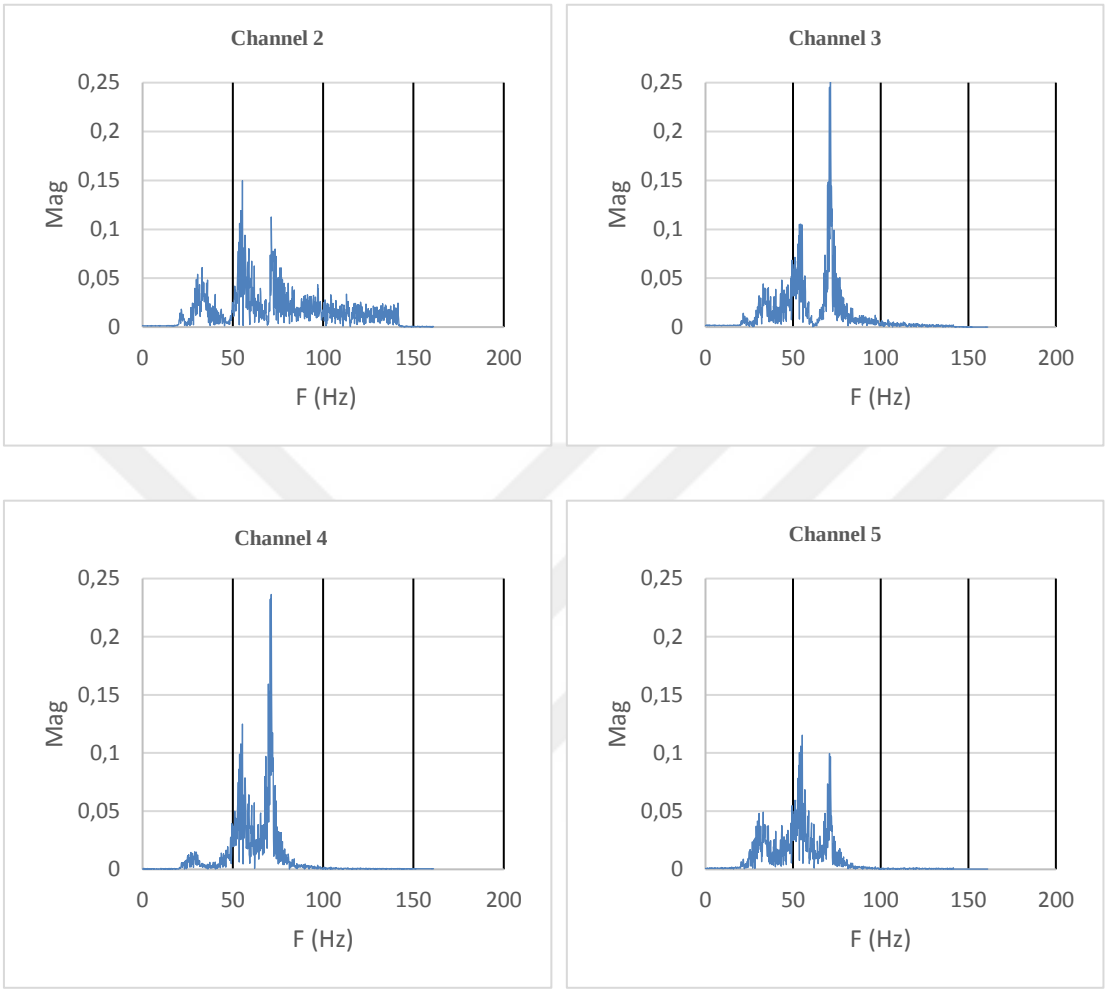

Figure A.2: Fast Fourier Transform Analysis of State #13.

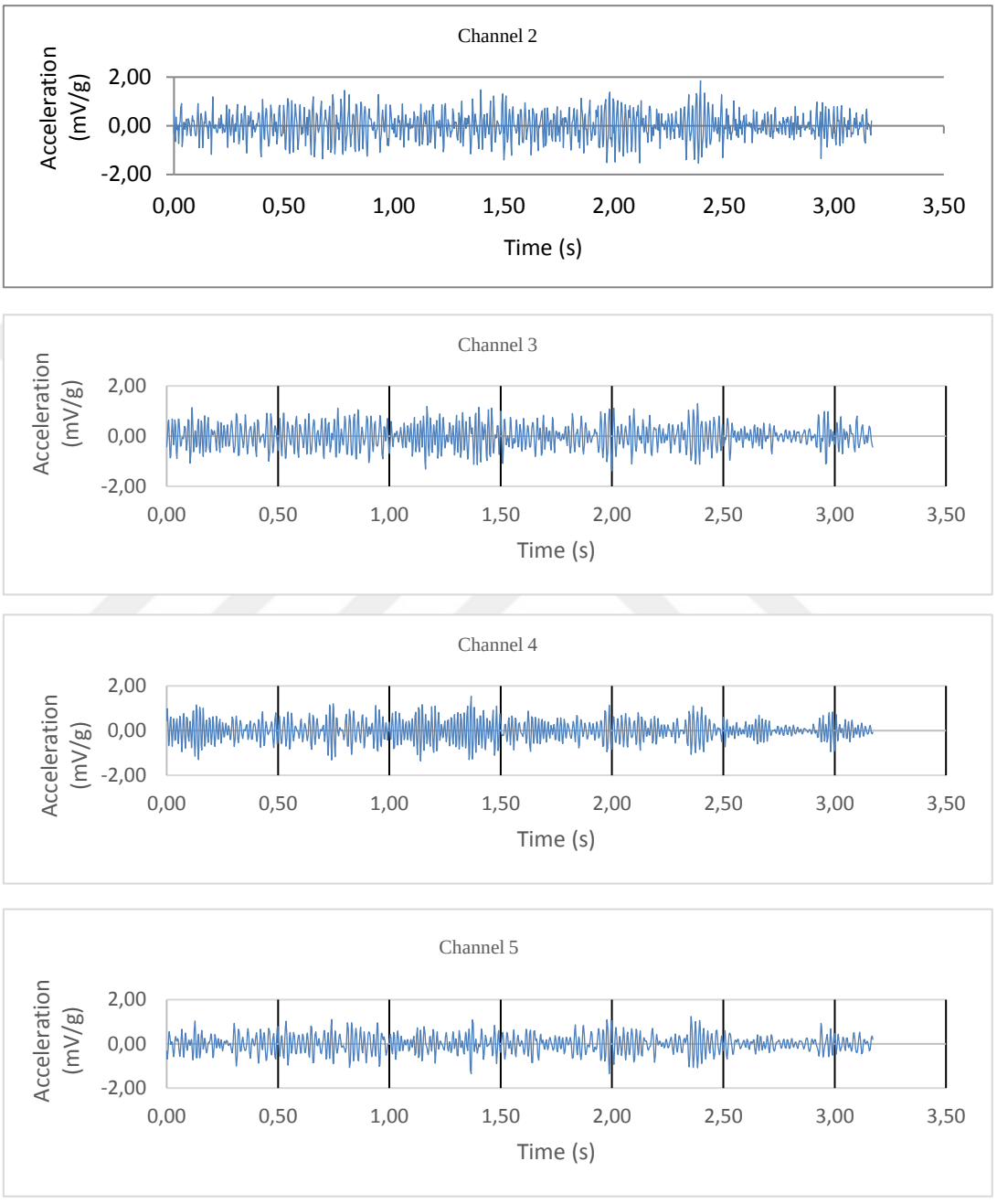

Figure A.3: Acceleration-Time Series of State #14.

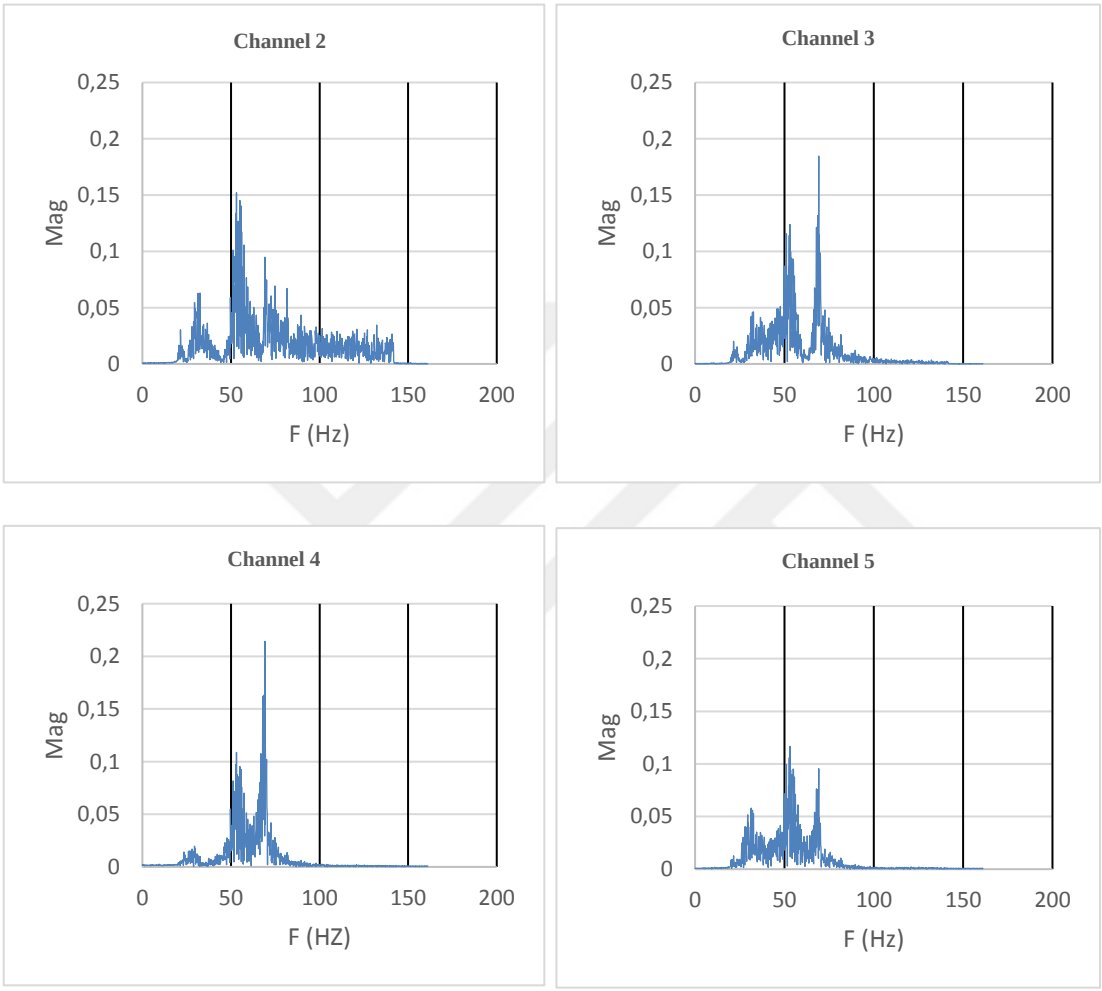

Figure A.4: Fast Fourier Transform Analysis of State #14.

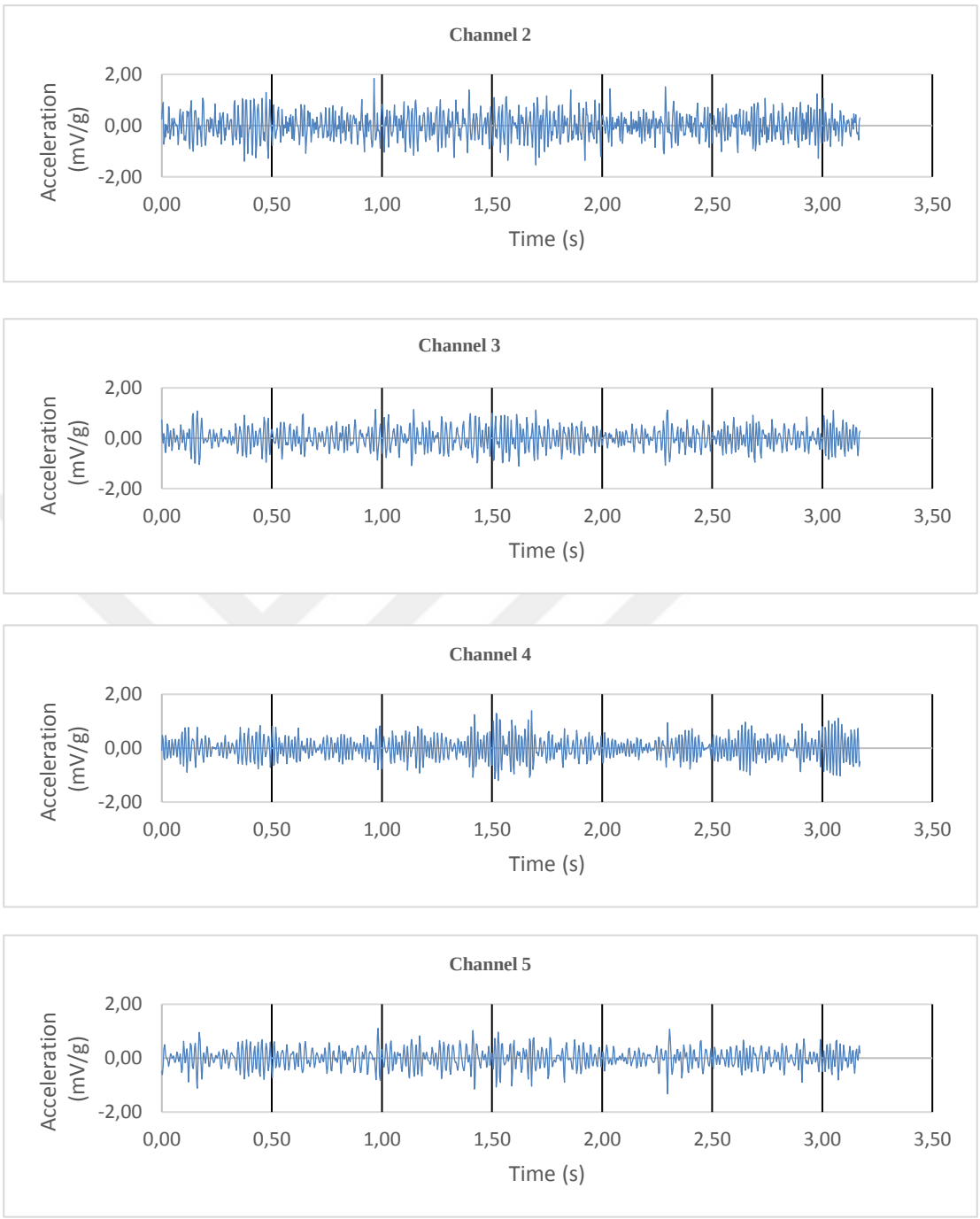

Figure A.5: Acceleration-Time Series of State #15.

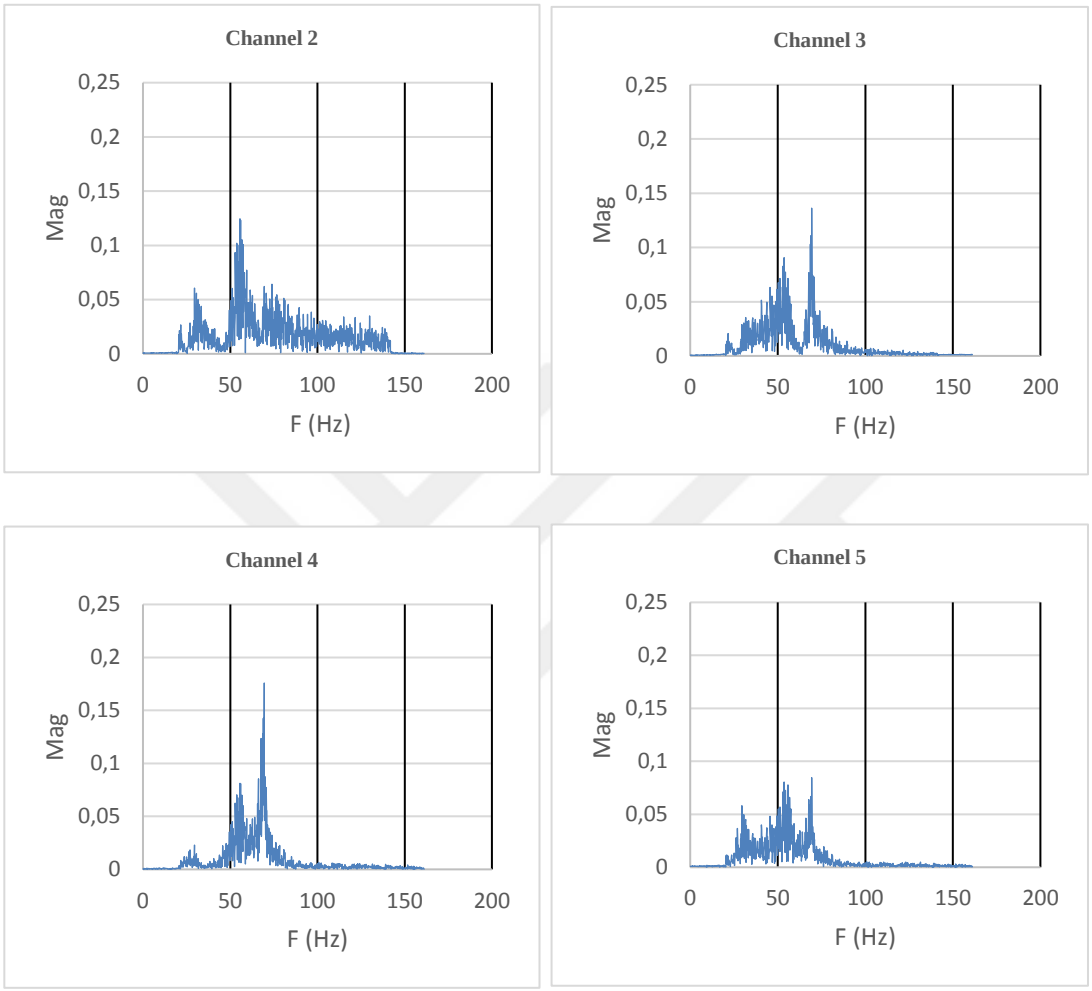

Figure A.6: Fast Fourier Transform Analysis of State #15.

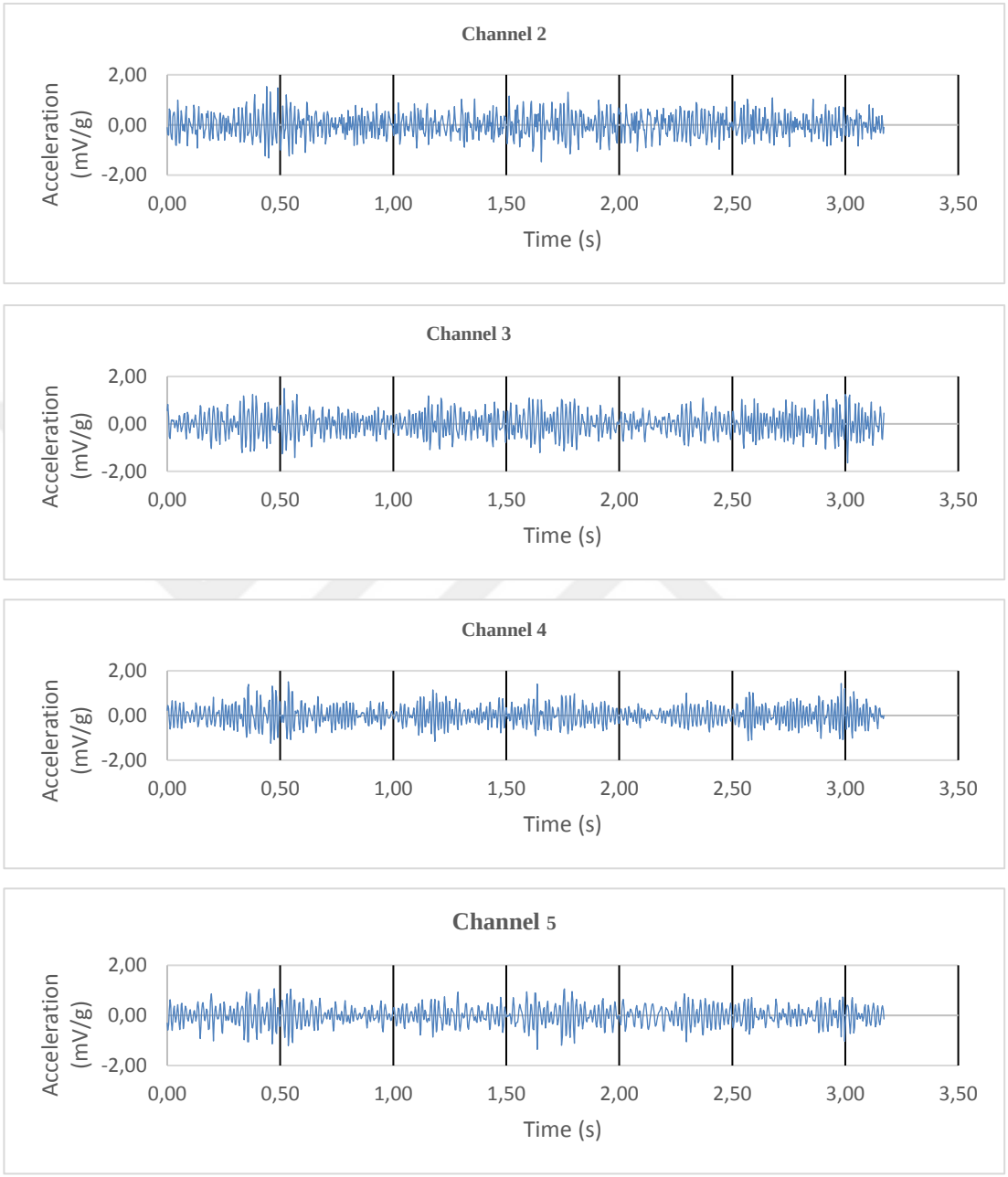

Figure A.7: Acceleration-Time Series Analysis of State #16.

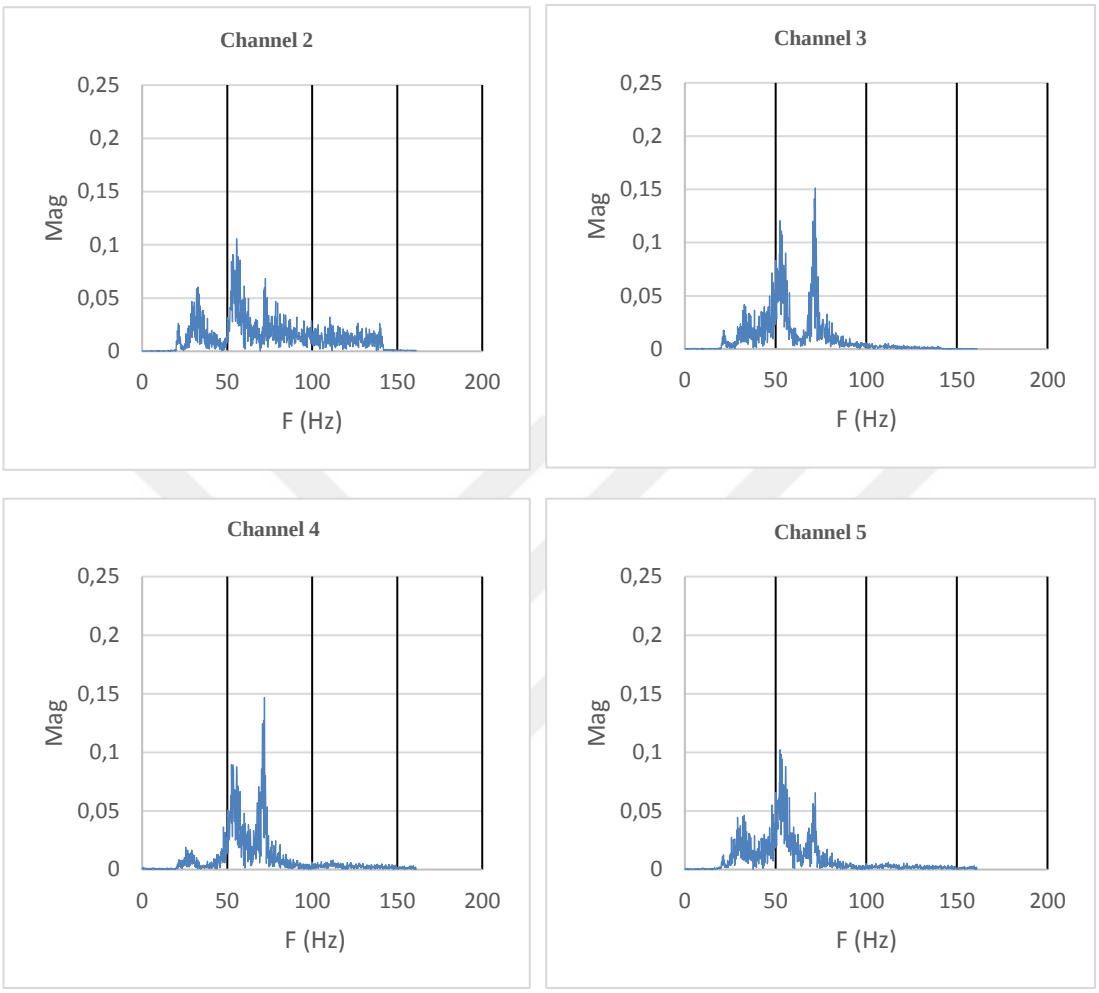

Figure A.8: Fast Fourier Transform Analysis of State #16.

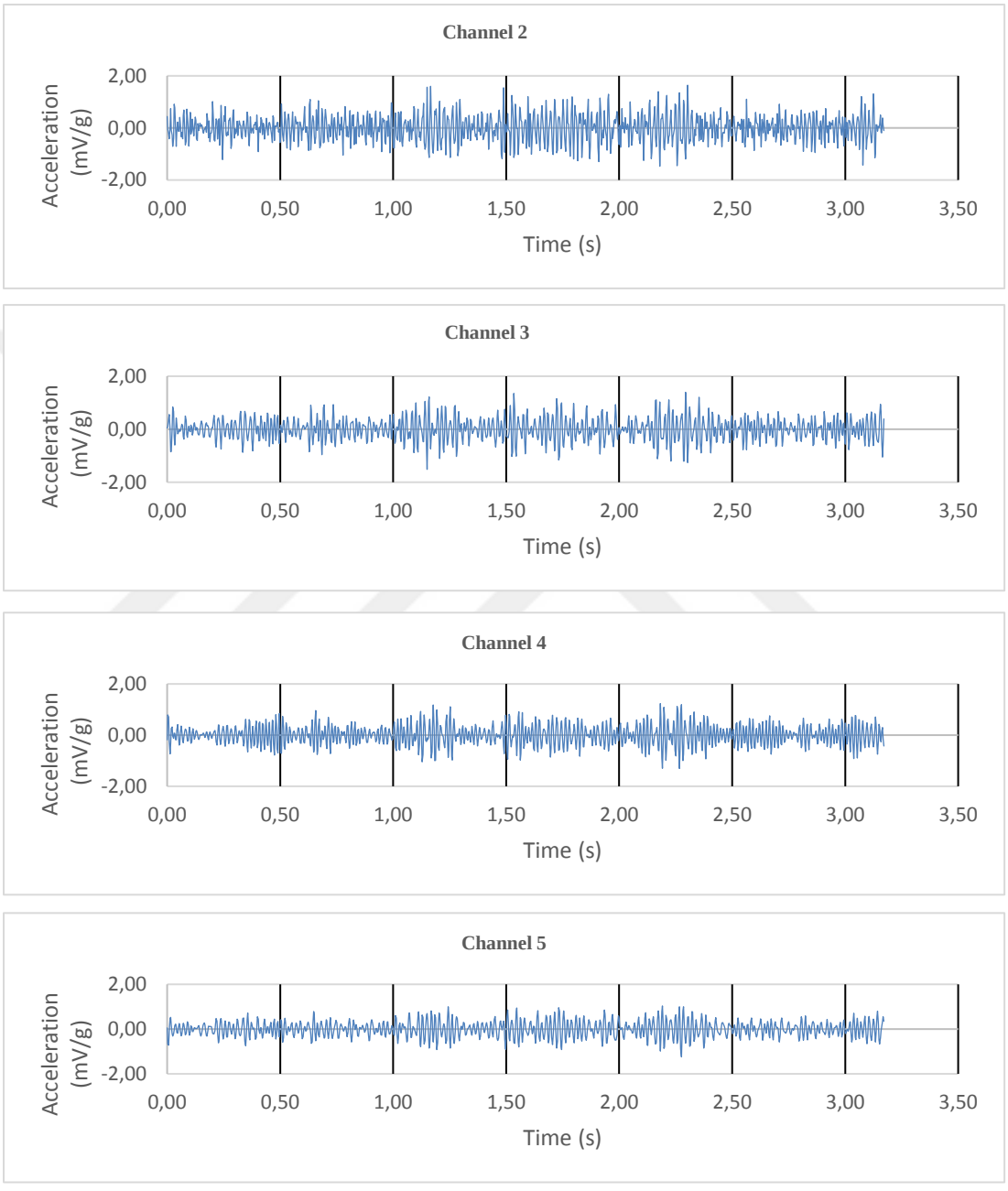

Figure A.9: Acceleration-Time Series Analysis of State #01.

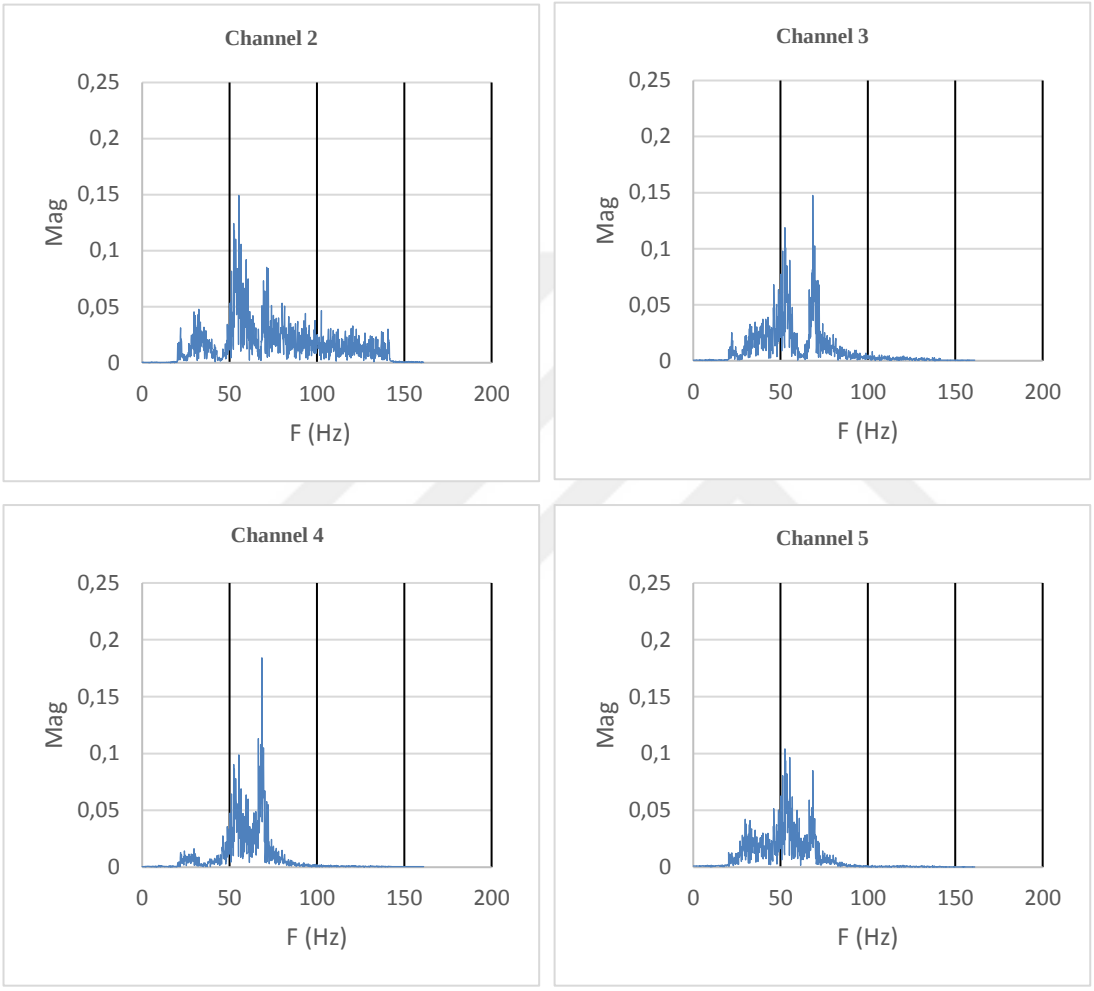

Figure A.10: Fast Fourier Transform Analysis of State #01.

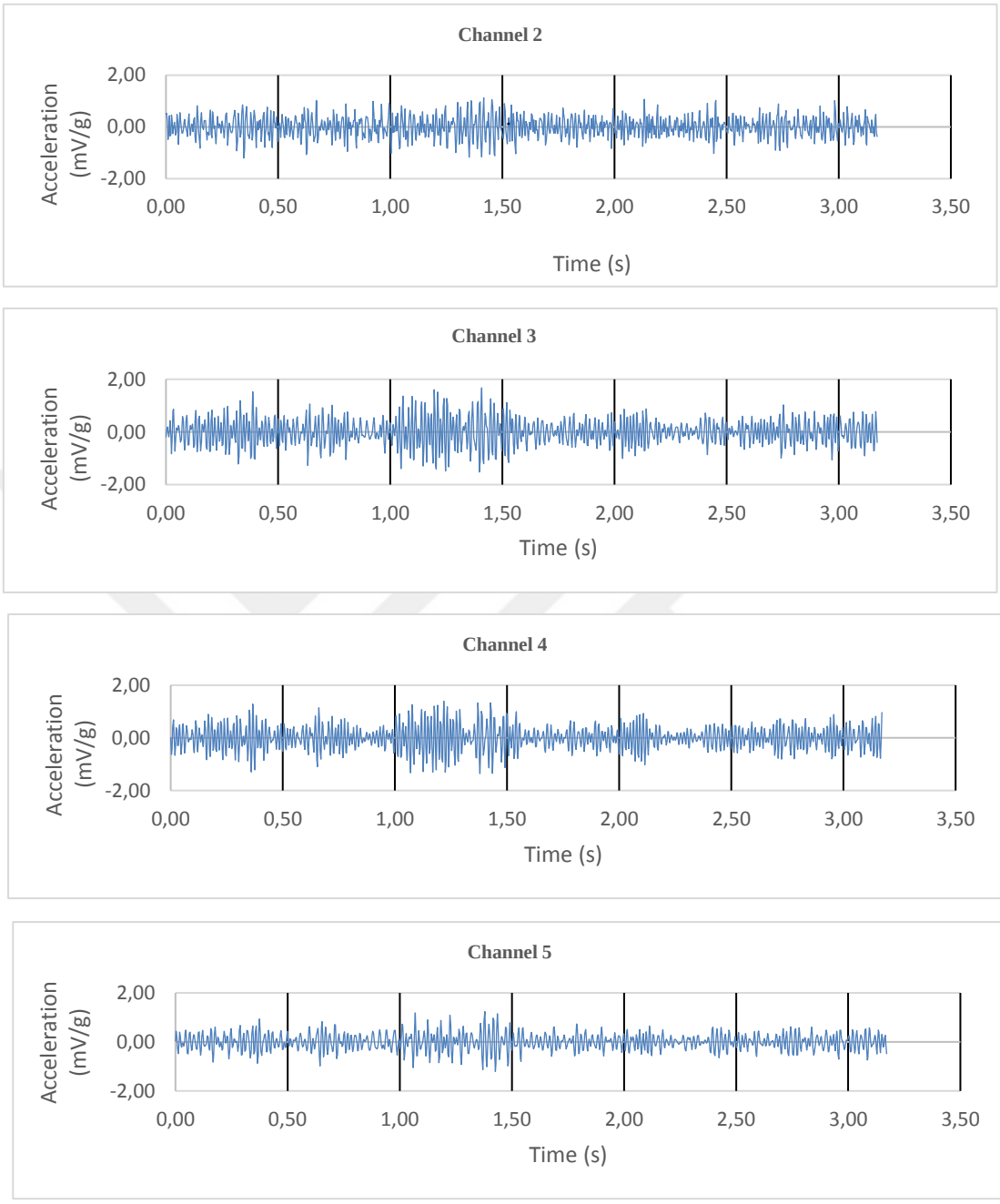

Figure A.11: Acceleration-Time Series Analysis of State #02.

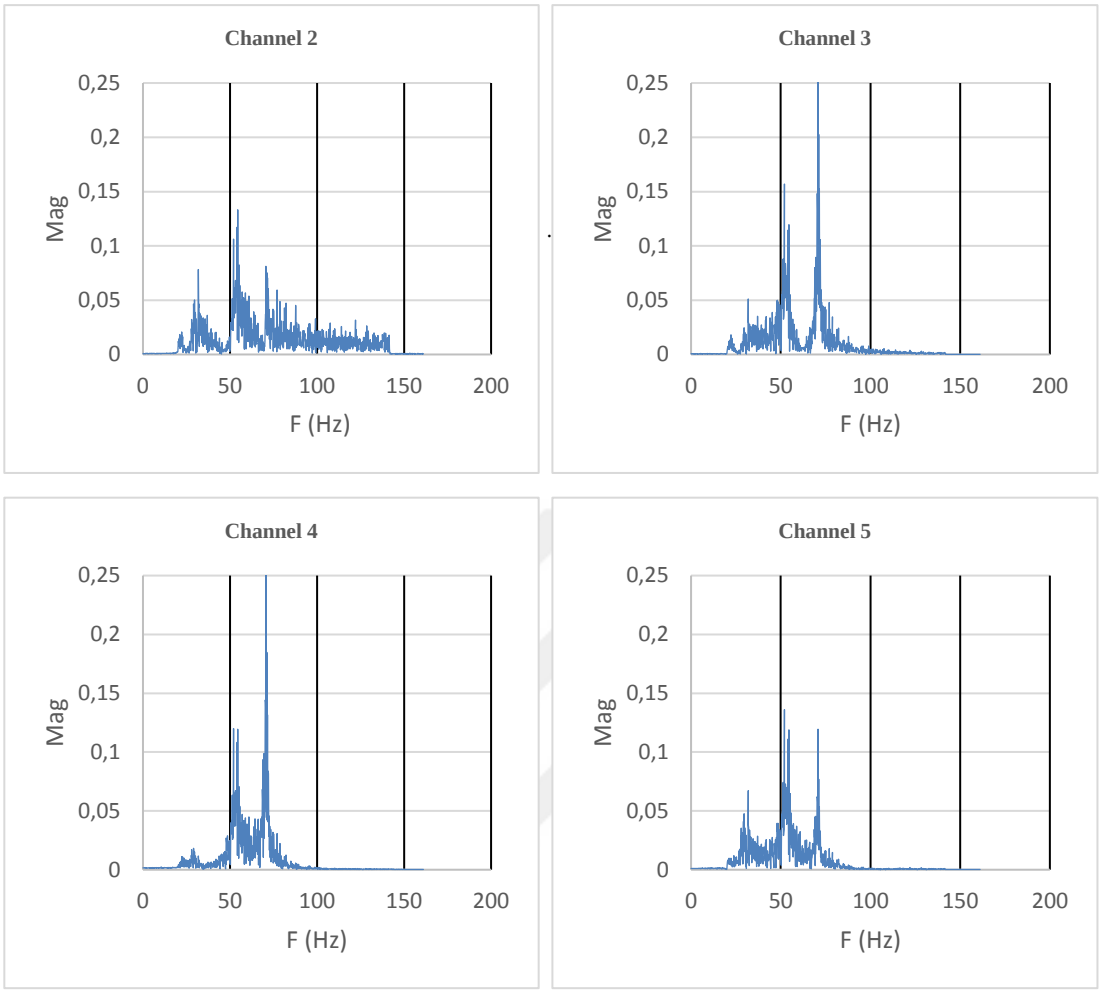

Figure A.12: Fast Fourier Transform Analysis of State #02.

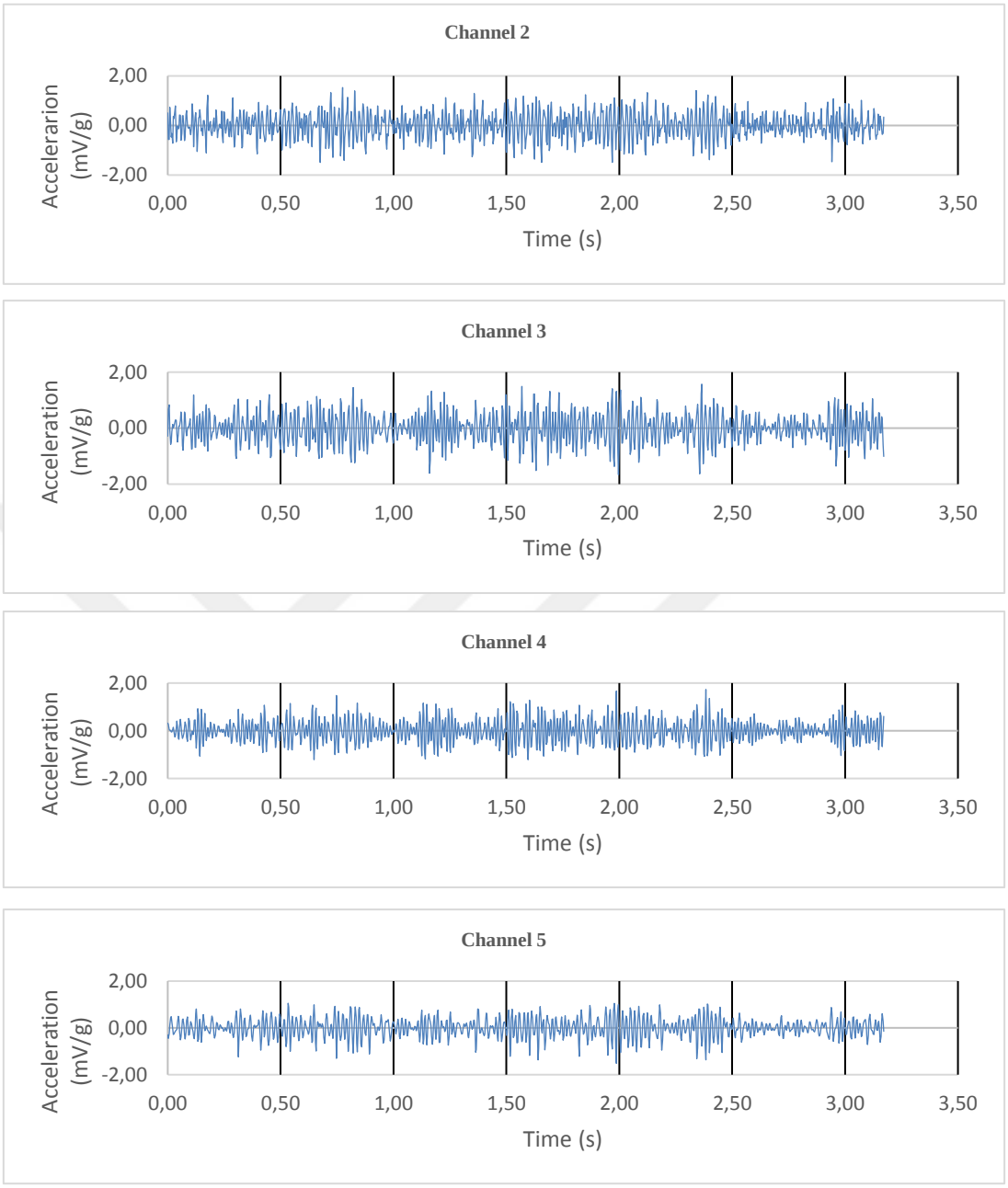

Figure A.13: Acceleration-Time Series Analysis of State #08.

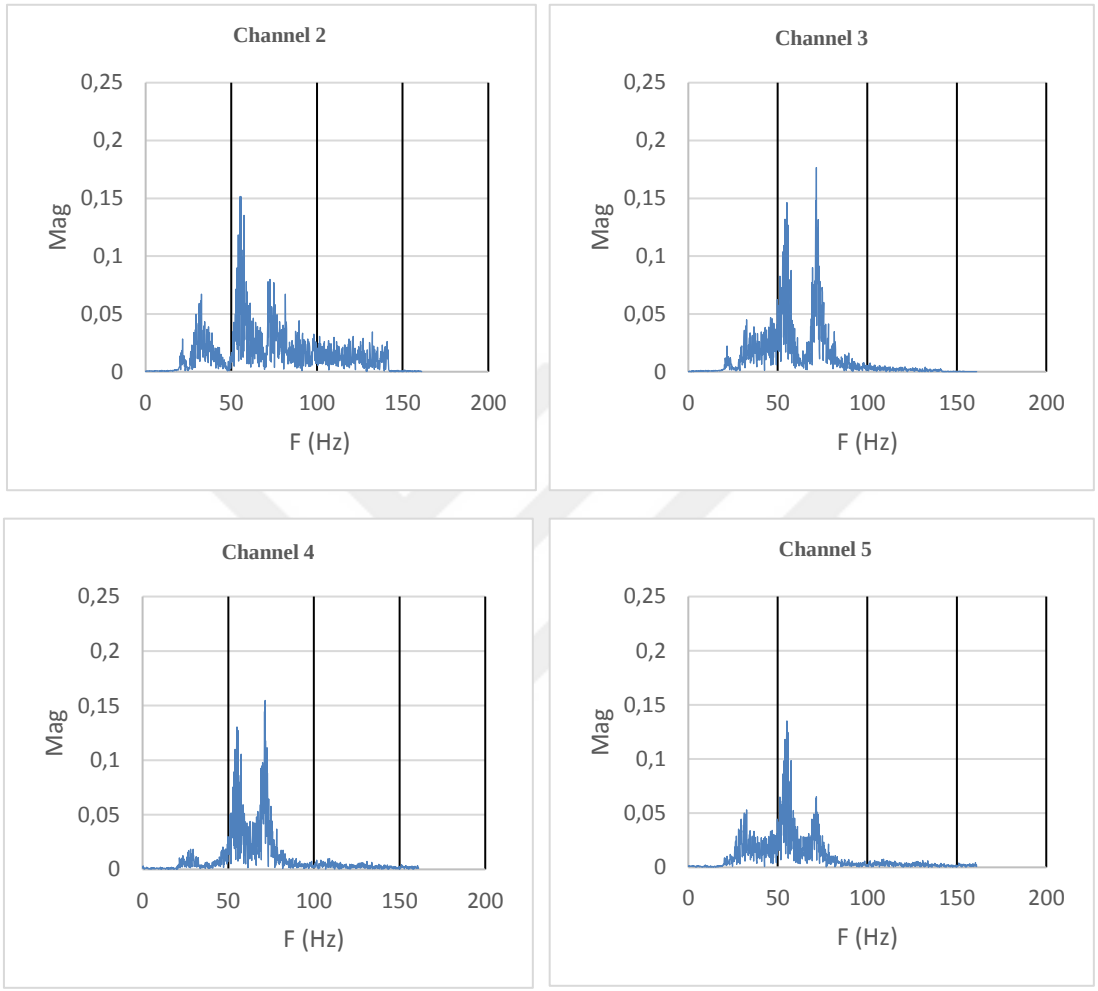

Figure A.14: Fast Fourier Transform Analysis of State #08.

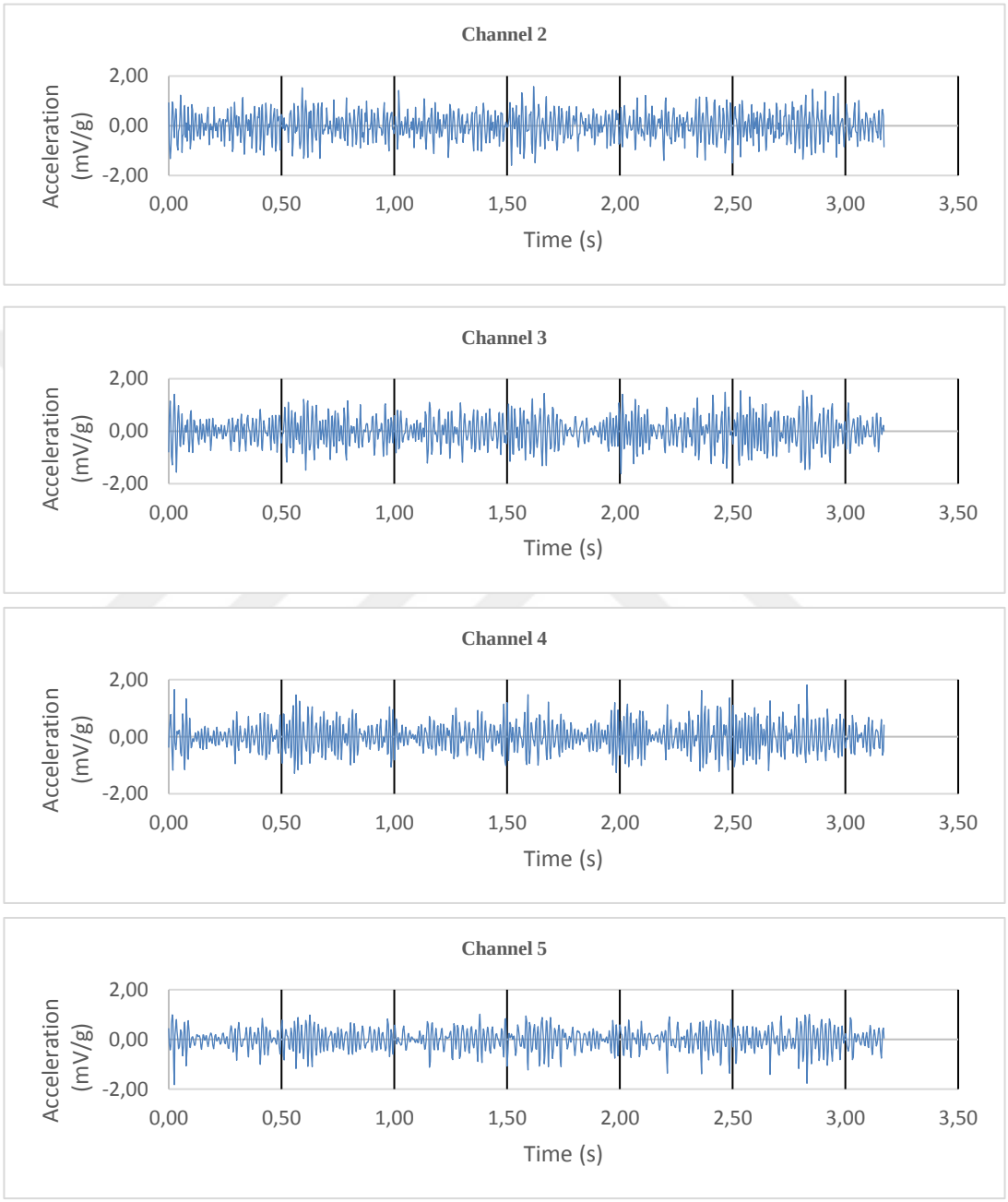

Figure A.15: Acceleration-Time Series Analysis of State #09.

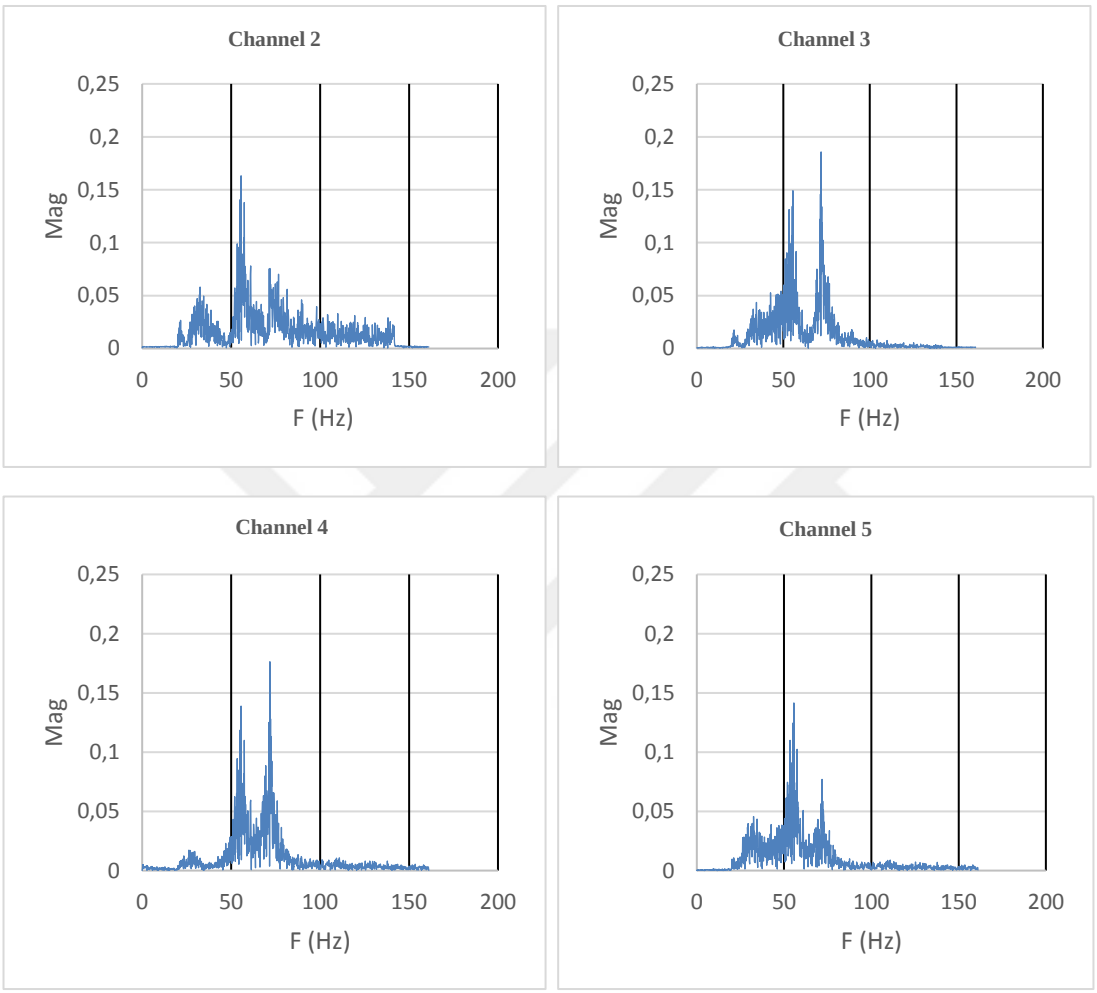

Figure A.16: Fast Fourier Transform Analysis of State #09.

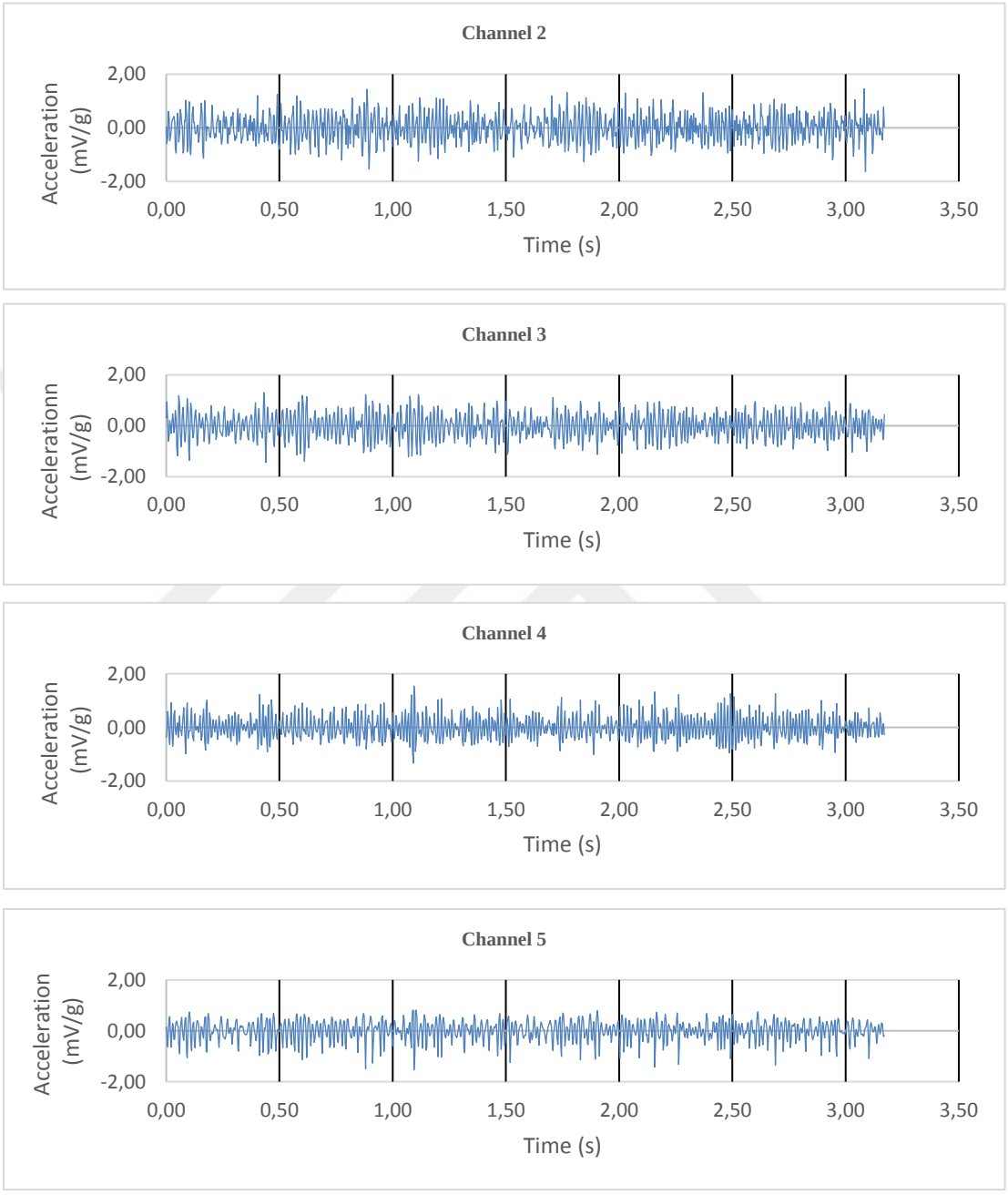

Figure A.17: Acceleration-Time Series Analysis of State #10.

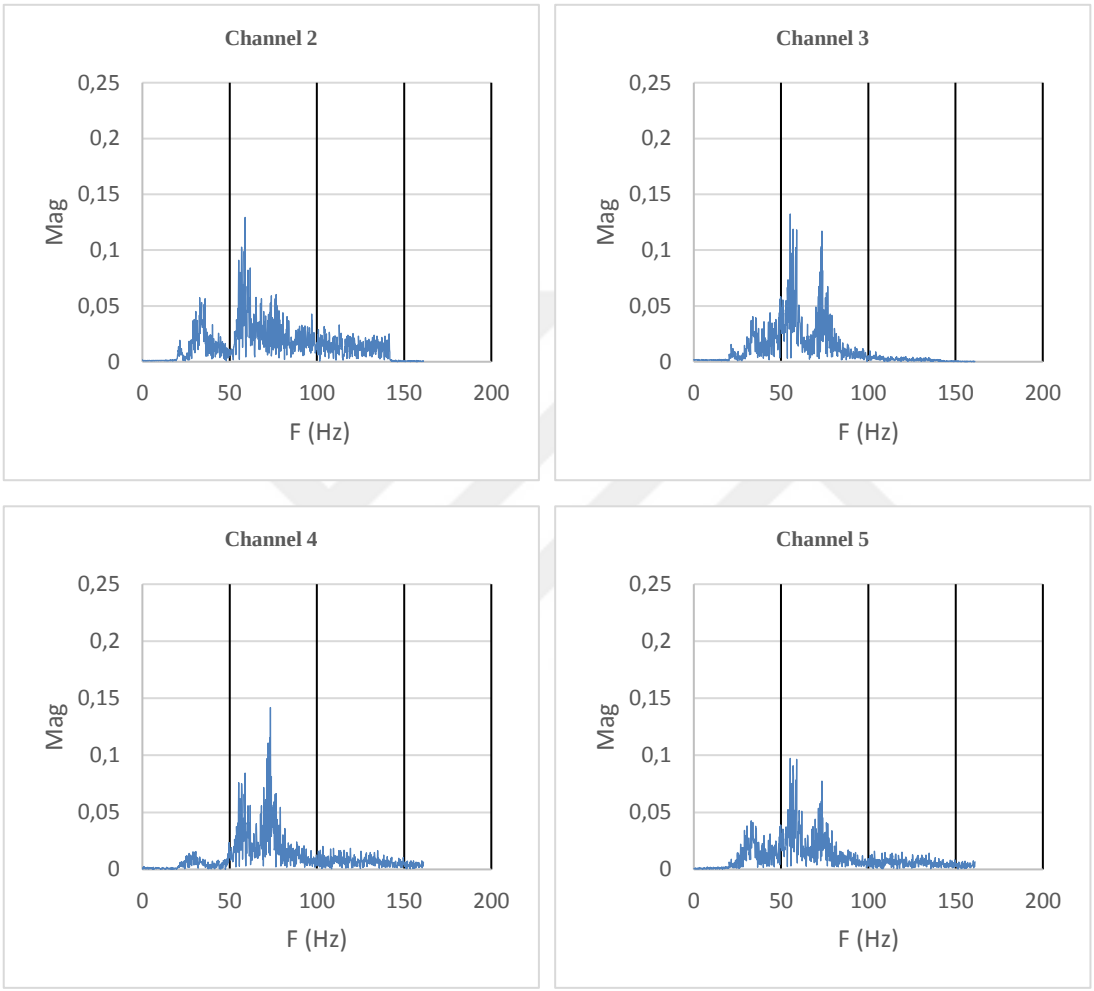

Figure A.18: Fast Fourier Transform Analysis of State #10.

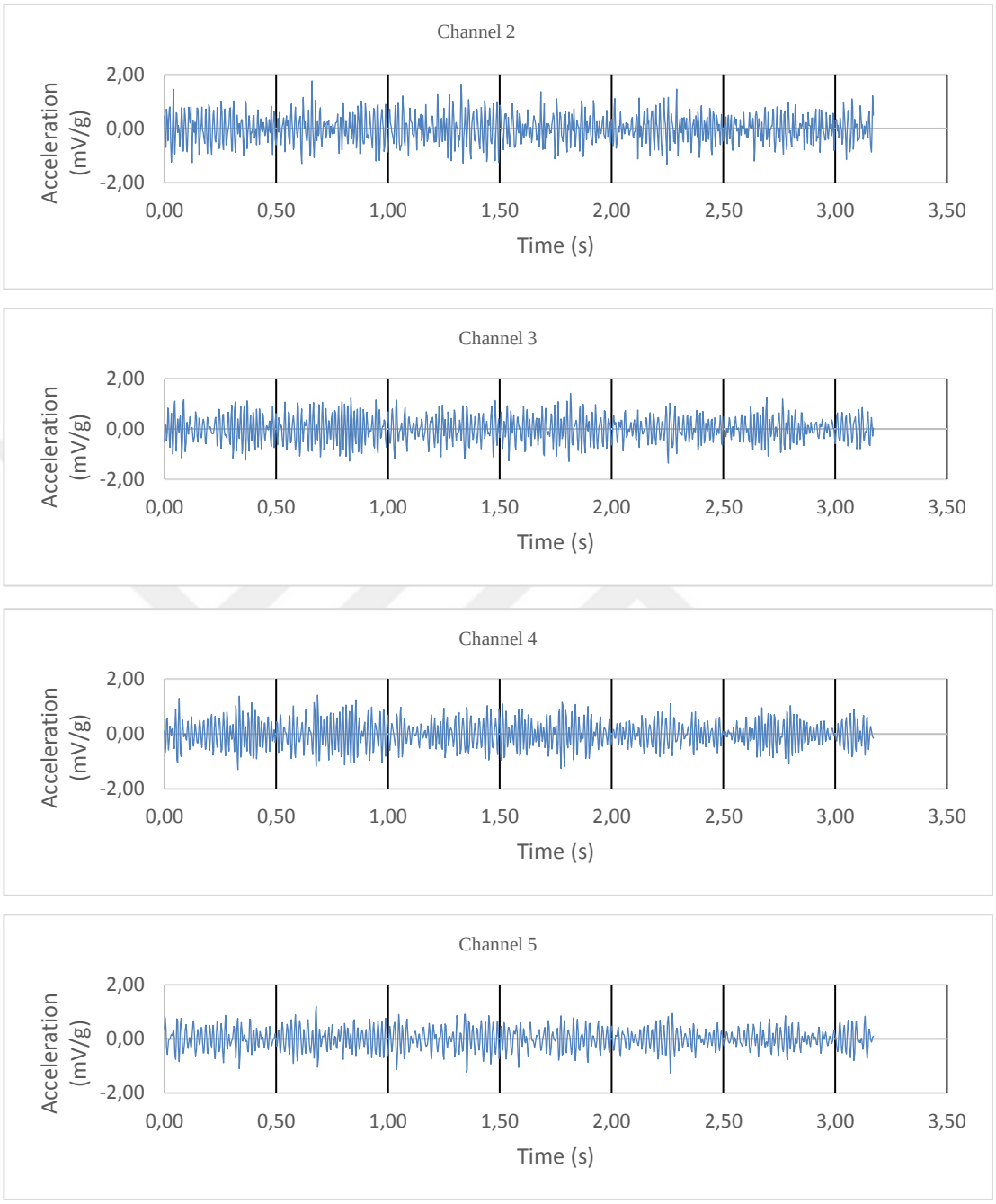

Figure A.19: Acceleration-Time Series Analysis of State #11.

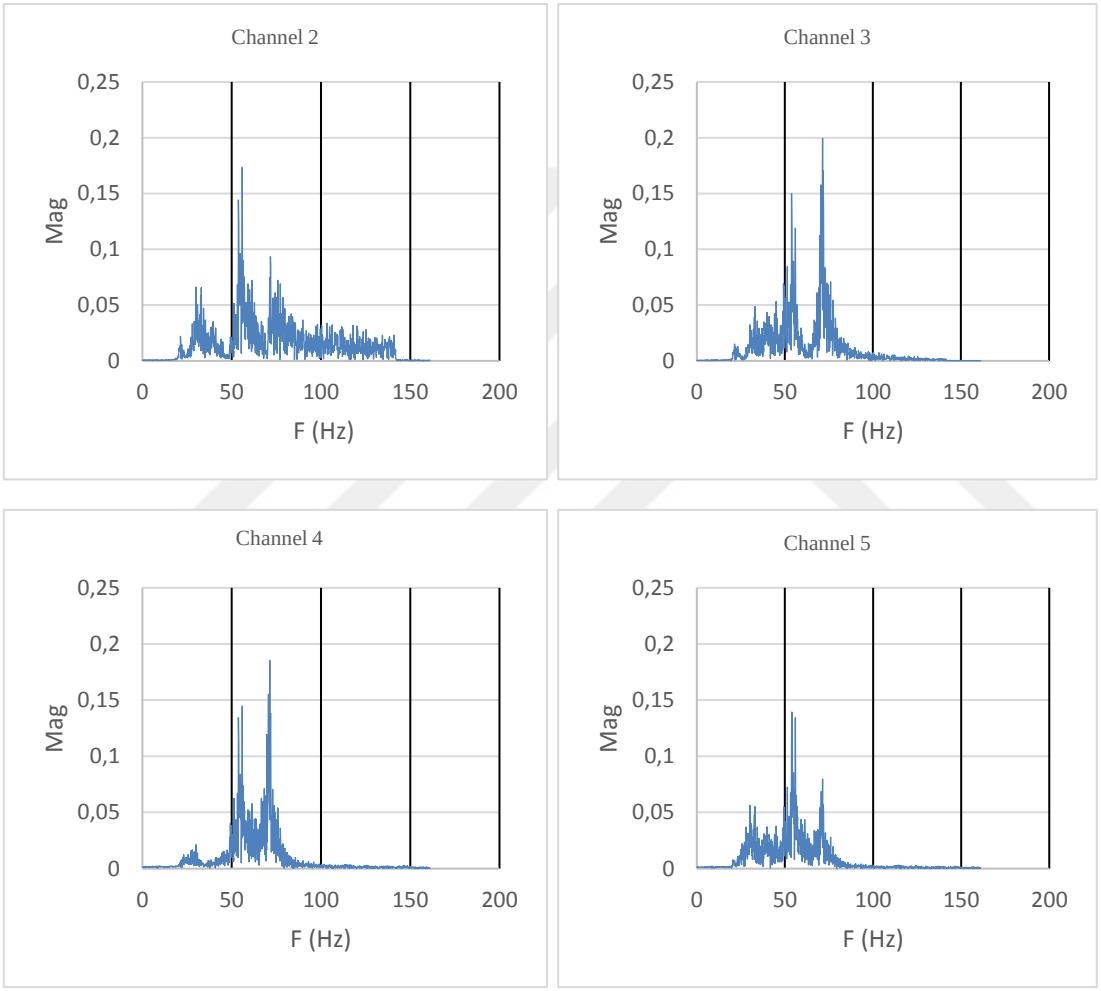

Figure A.20: Fast Fourier Transform Analysis of State #11.

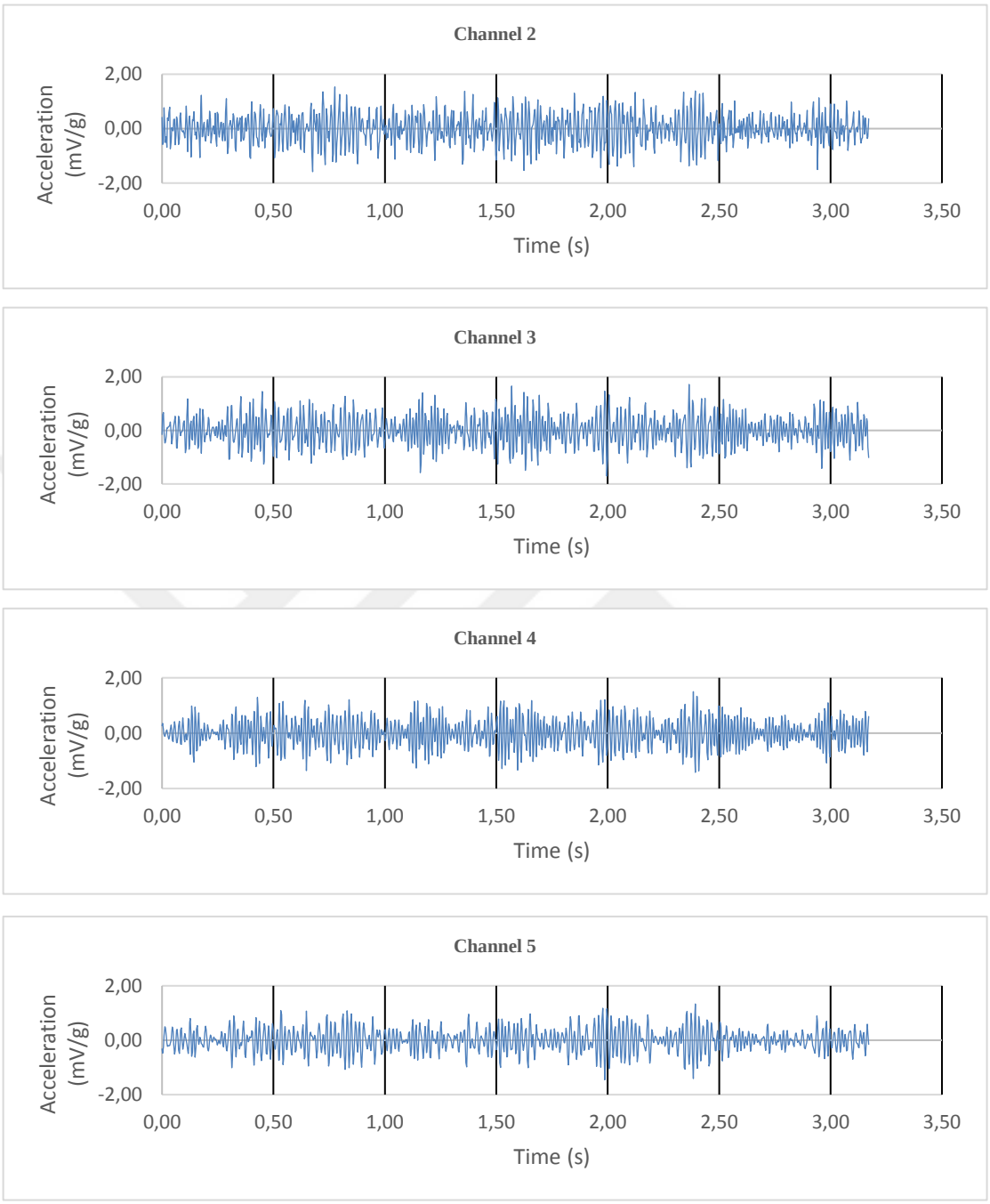

Figure A.21: Acceleration-Time Series Analysis of State #12.

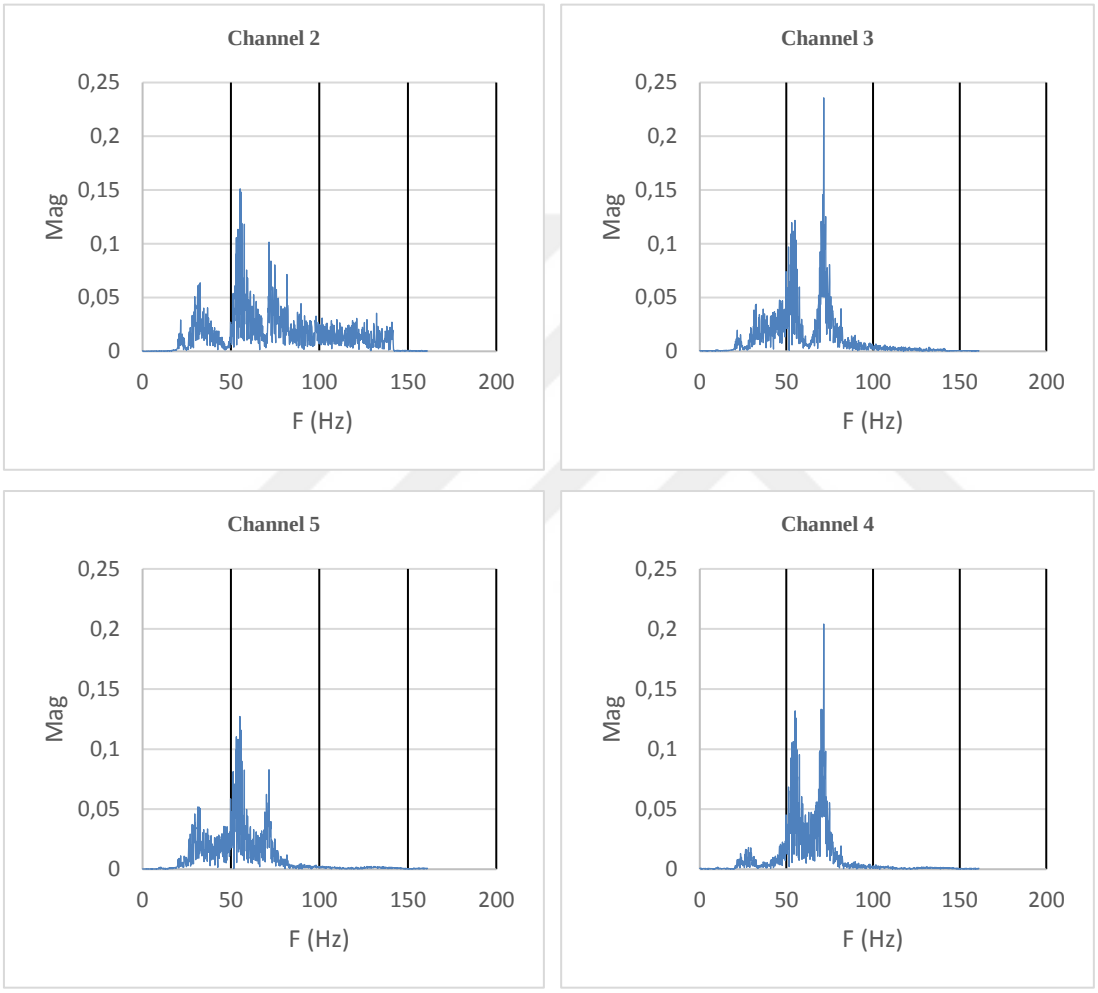

Figure A.22: Fast Fourier Transform Analysis of State #12.

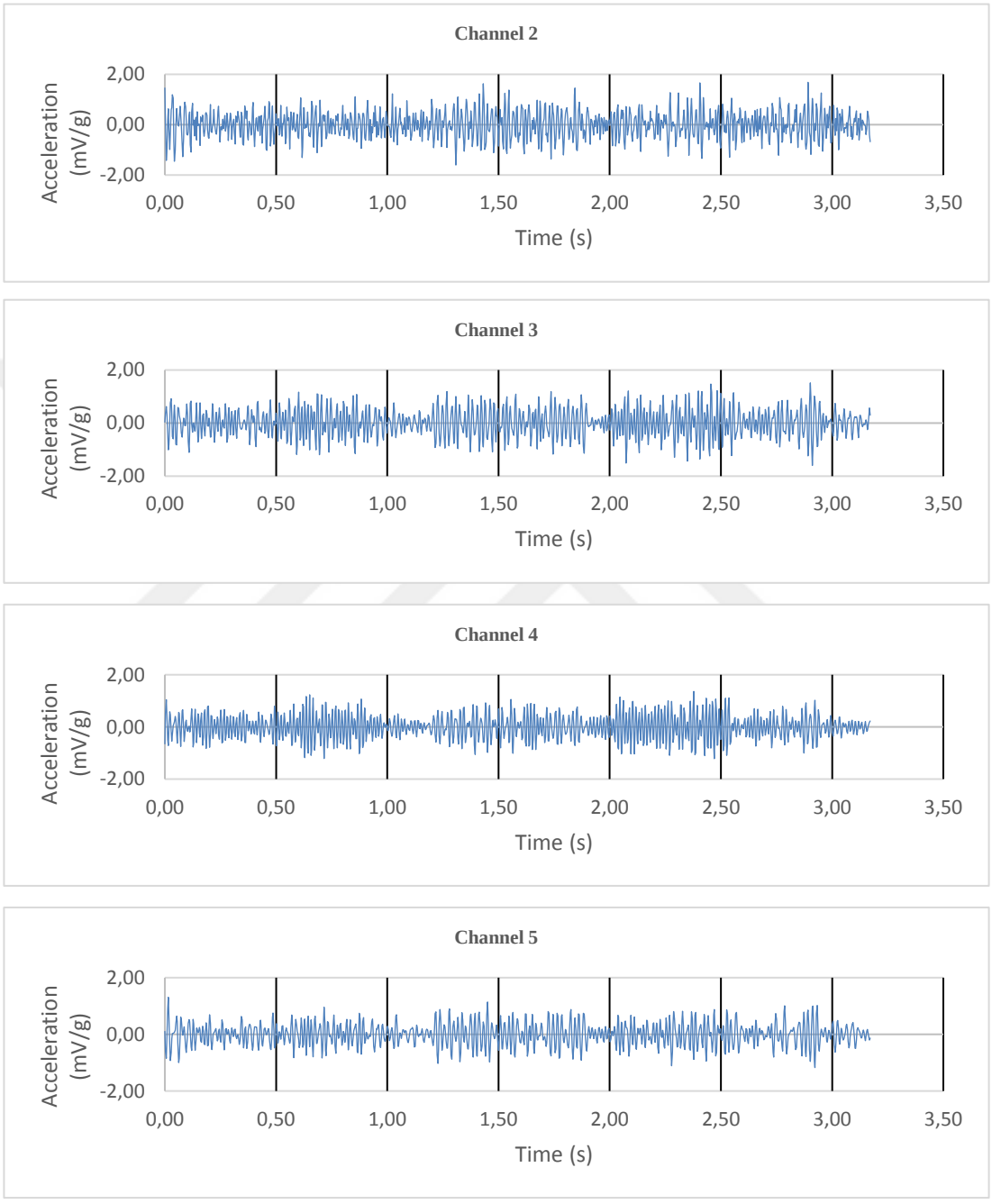

Figure A.23: Acceleration-Time Series Analysis of State #17.

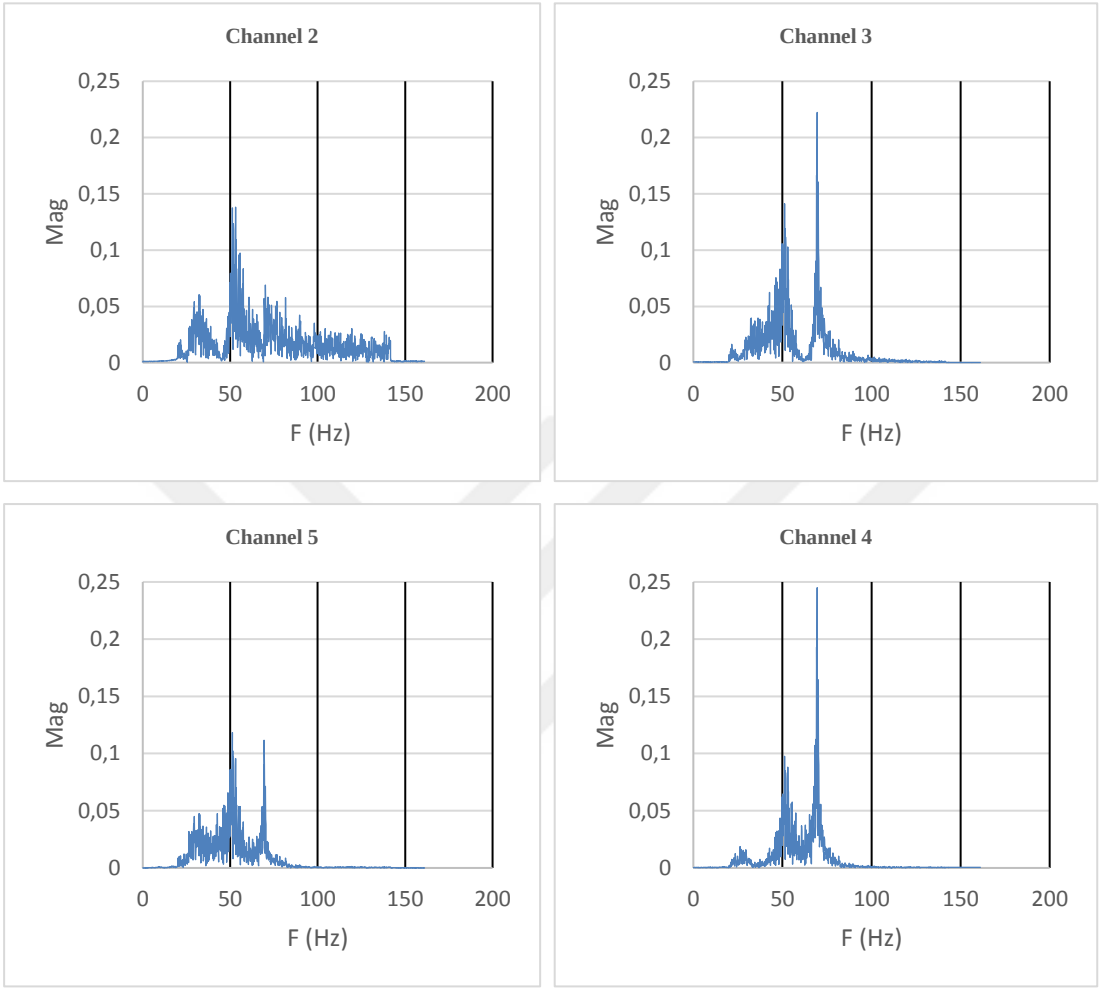

Figure A.24: Fast Fourier Transform Analysis of State #17.

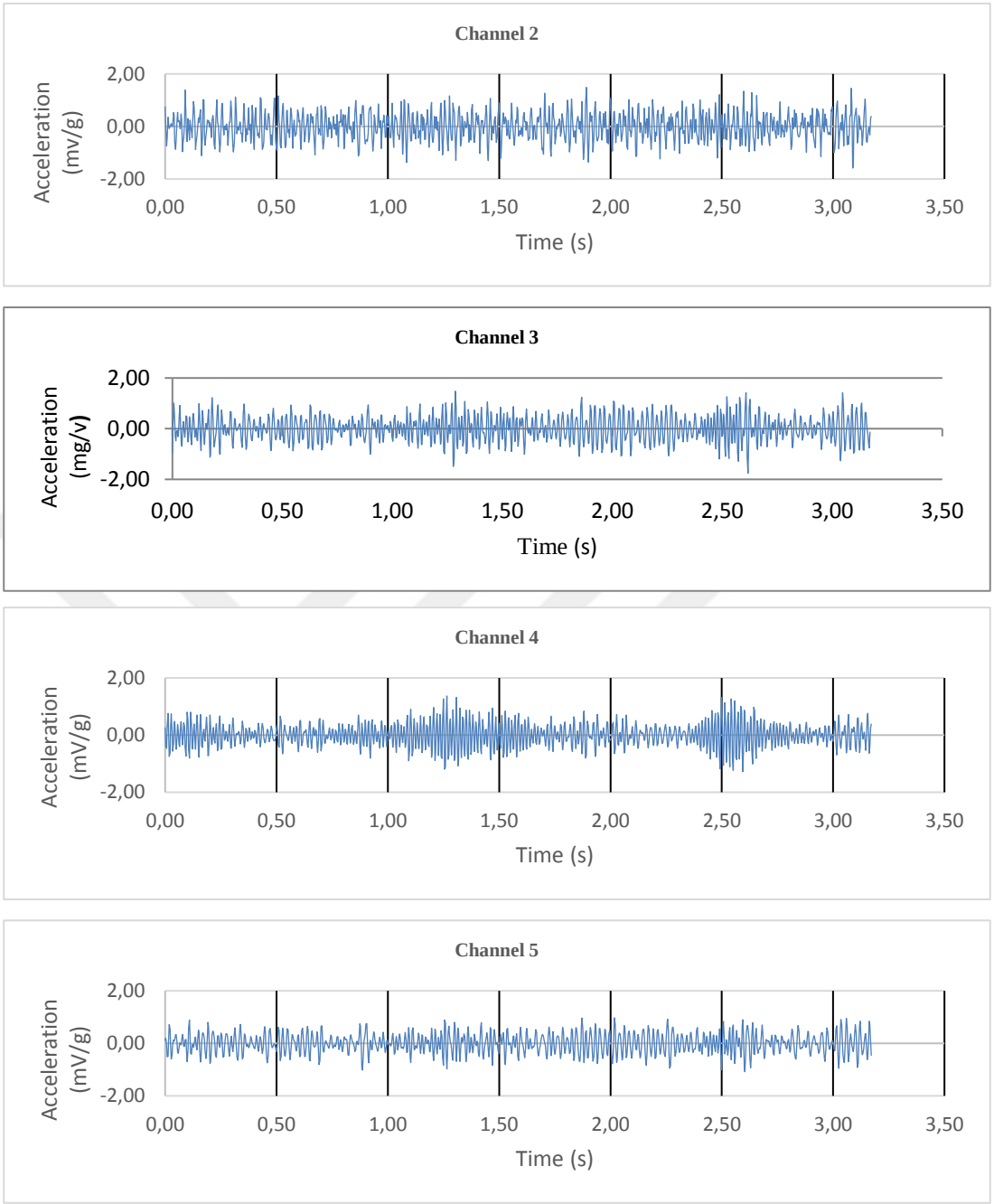

Figure A.25: Acceleration-Time Series Analysis of State #18.

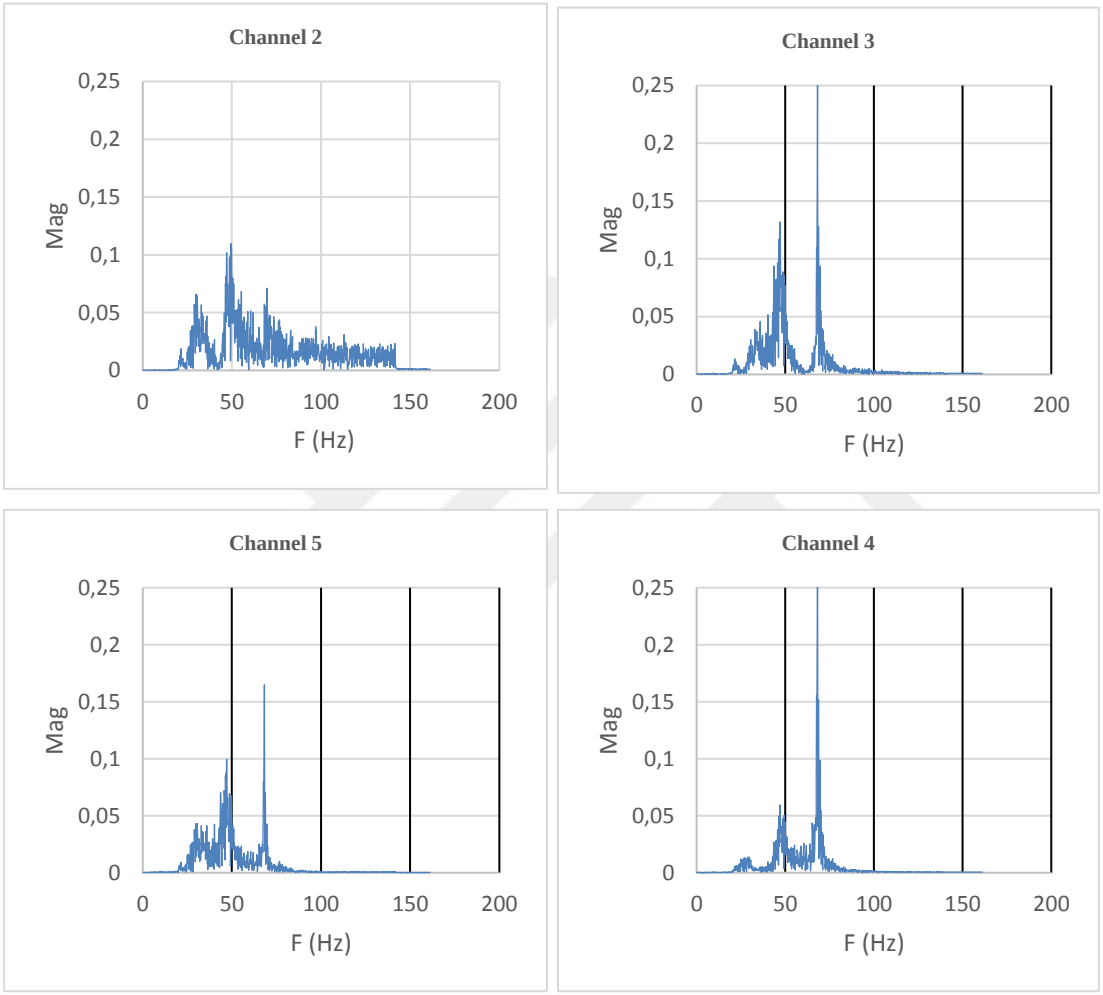

Figure A.26: Fast Fourier Transform Analysis of State #18.

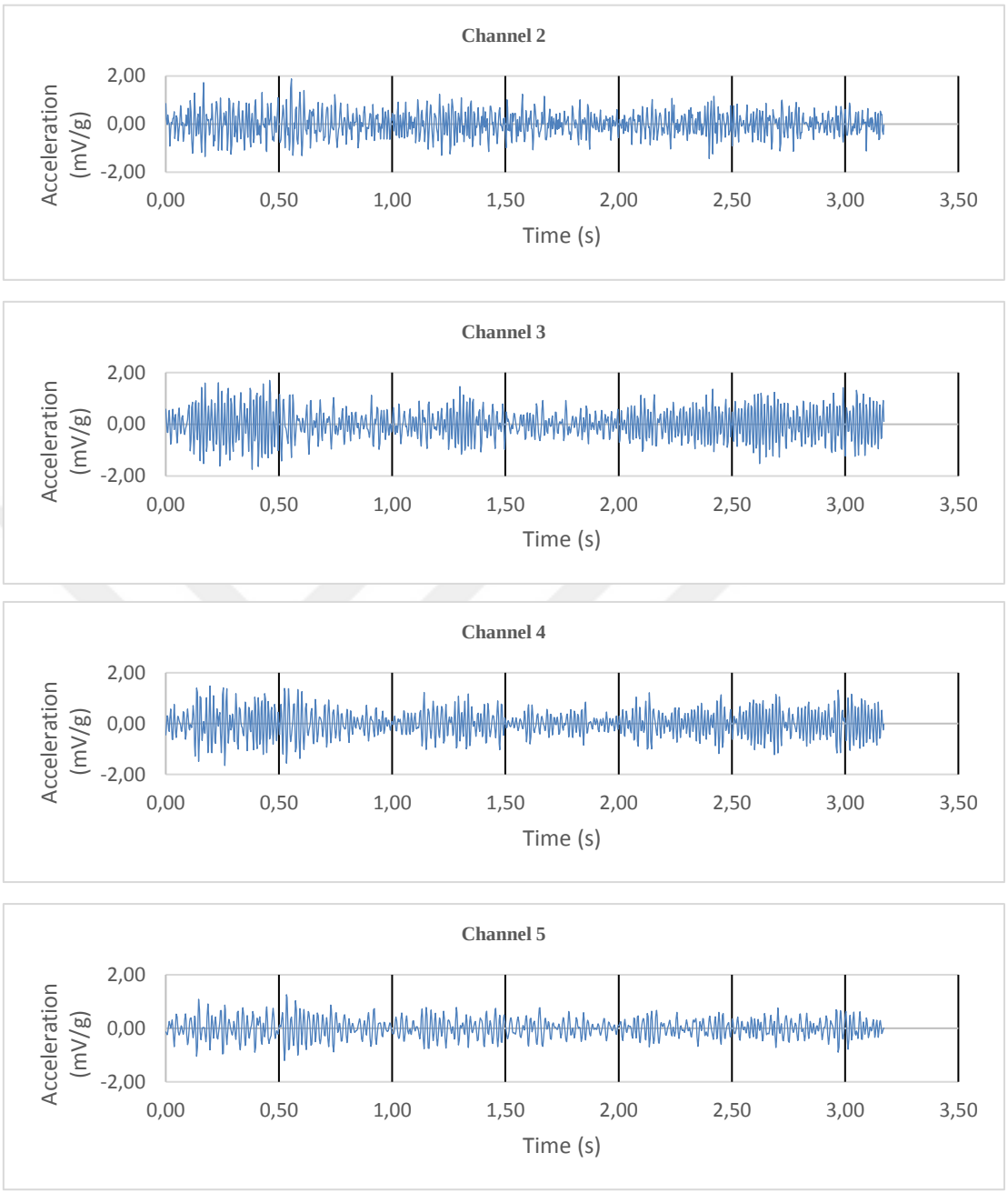

Figure A.27: Acceleration-Time Series Analysis of State #21.

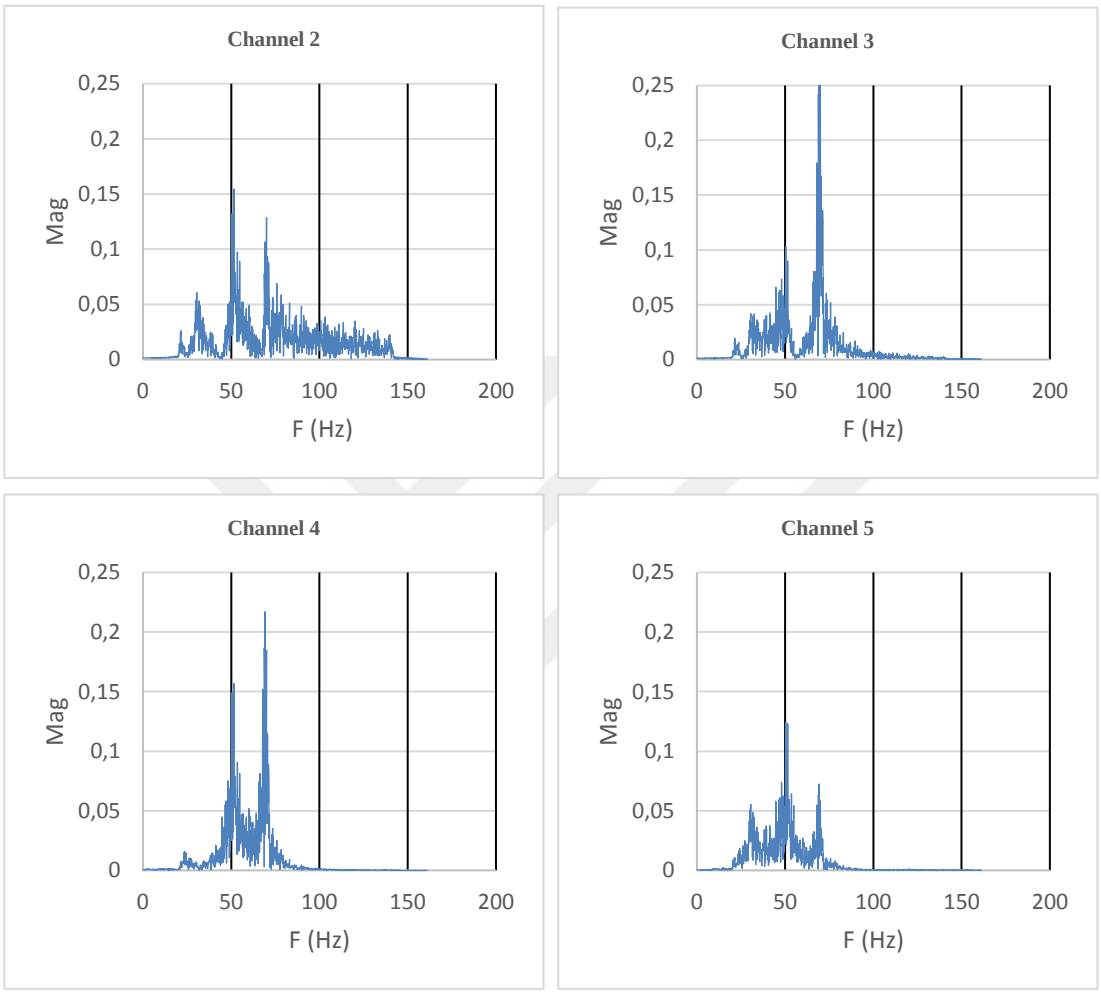

Figure A.27: Fast Fourier Transform Analysis of State #21.

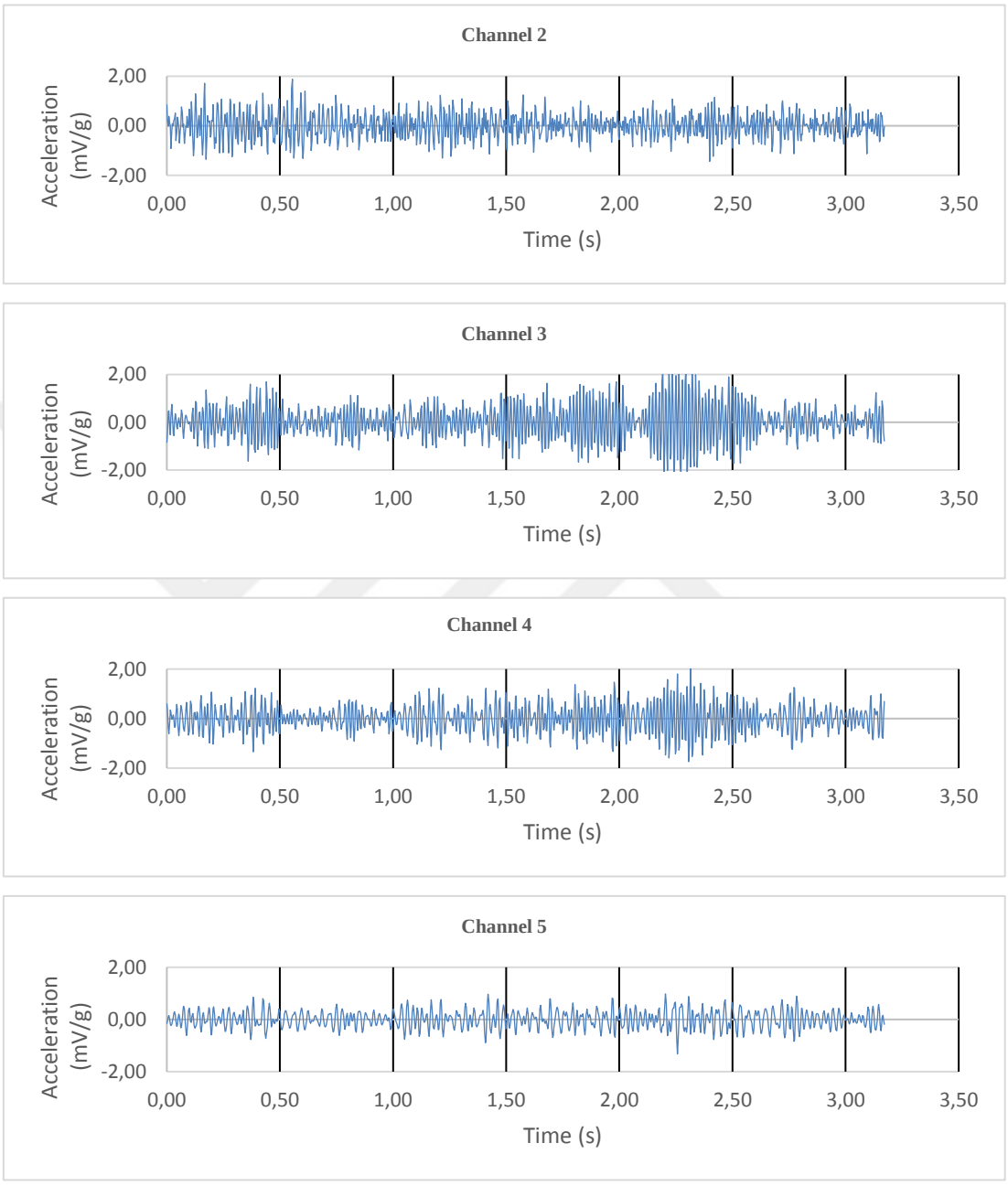

Figure A.29: Acceleration-Time Series Analysis of State #22.

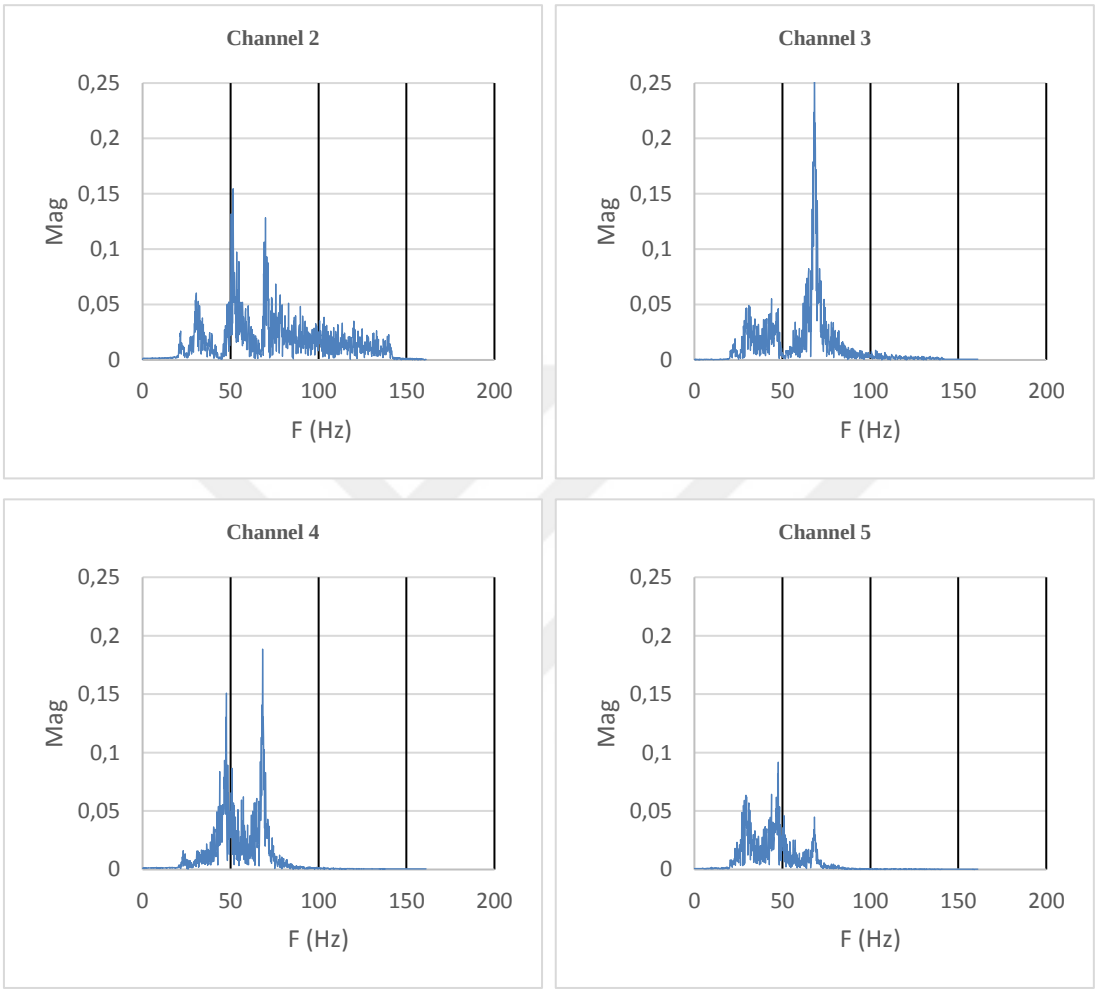

Figure A.30: Fast Fourier Transform Analysis of State #22.

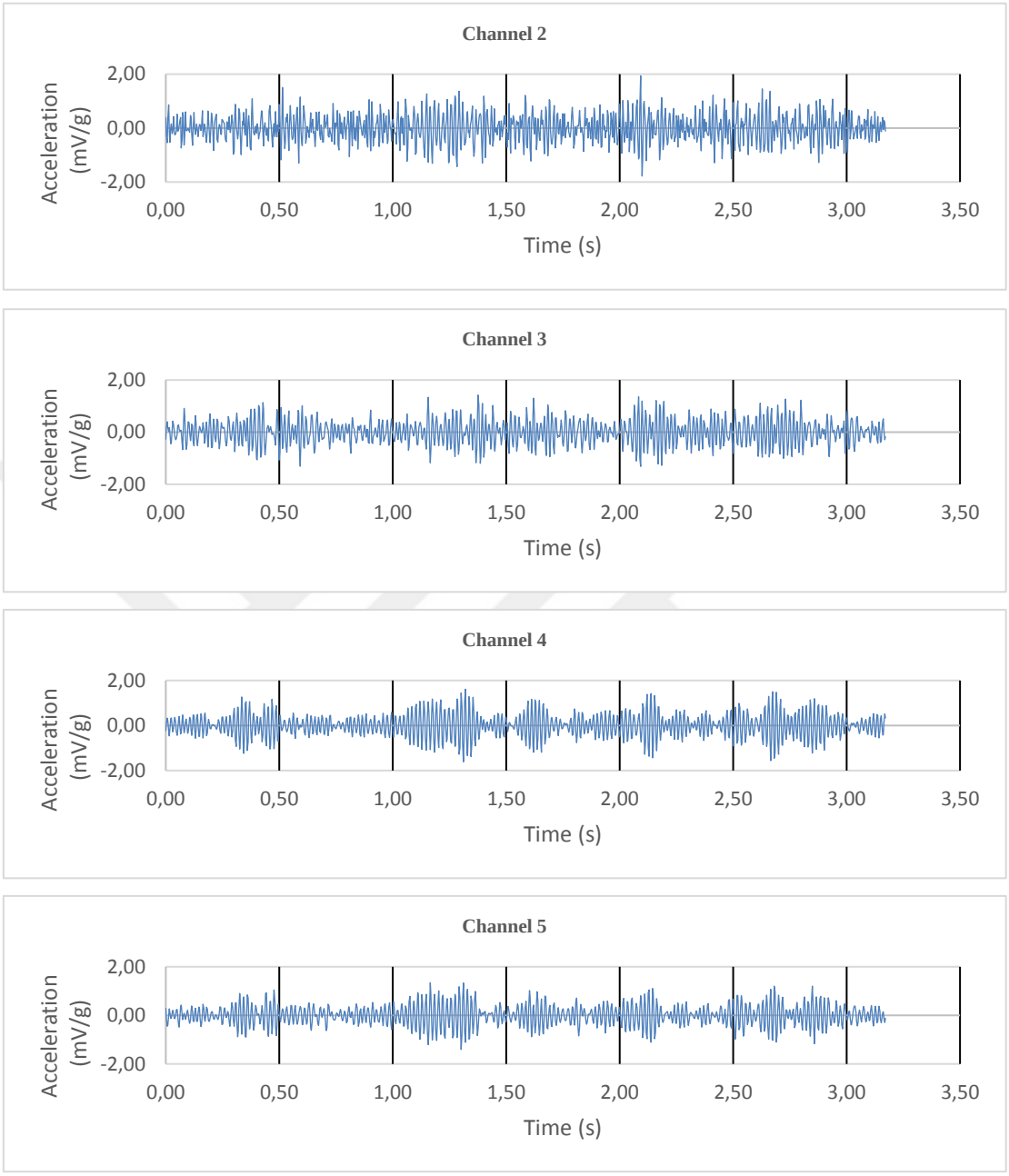

Figure A.31: Acceleration-Time Series Analysis of State #23.

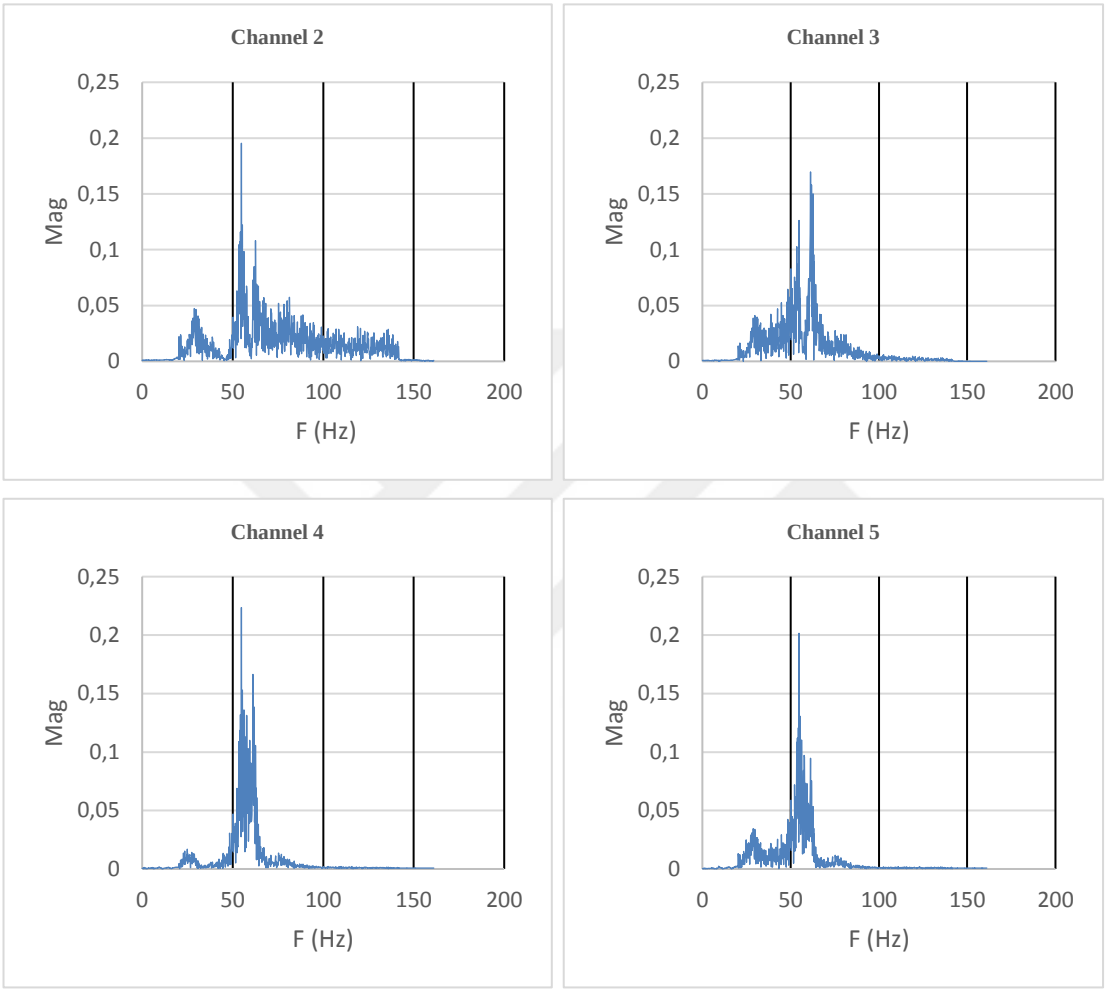

Figure A.32: Fast Fourier Transform Analysis of State #23.

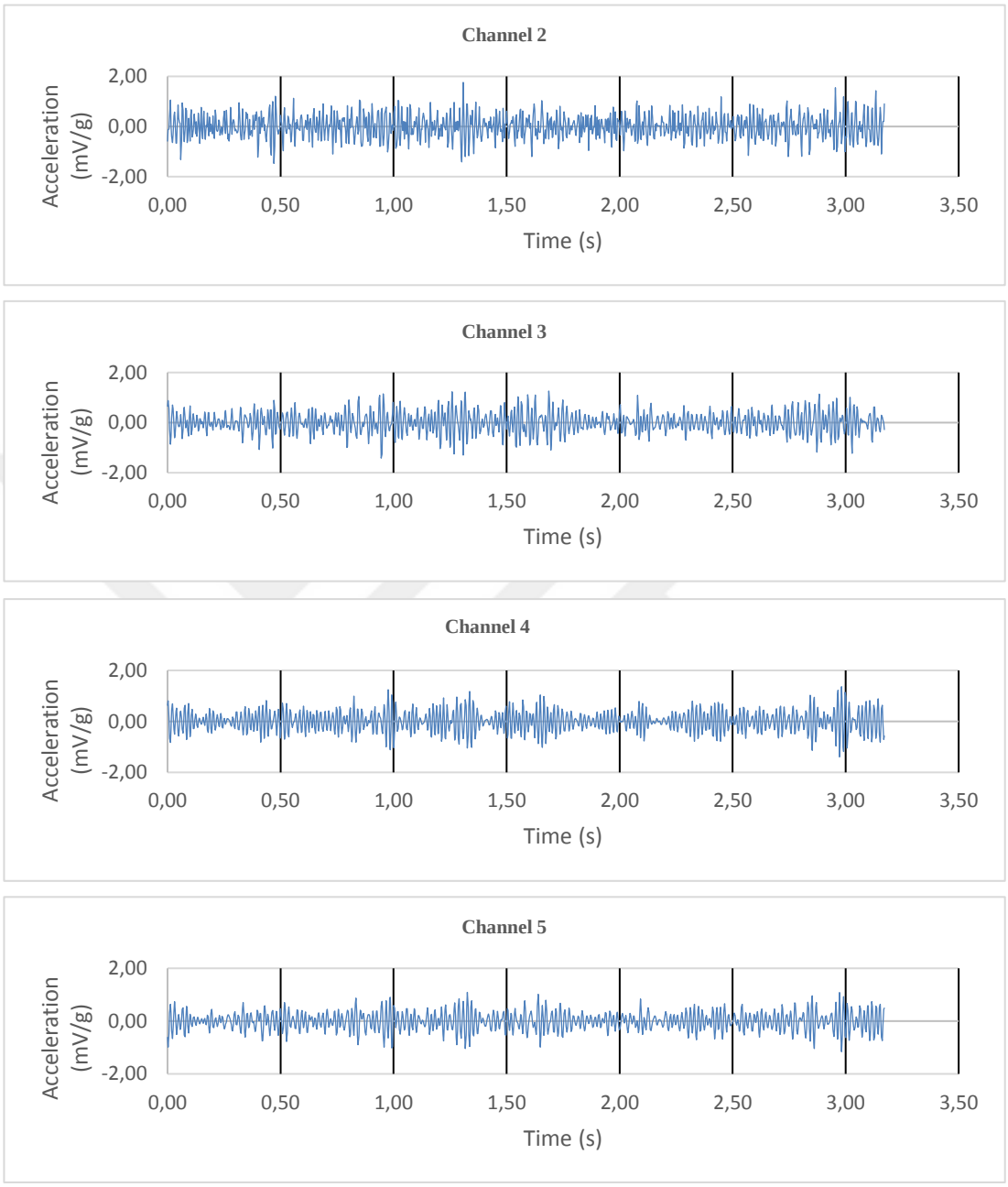

Figure A.33: Acceleration-Time Series Analysis of State #24.

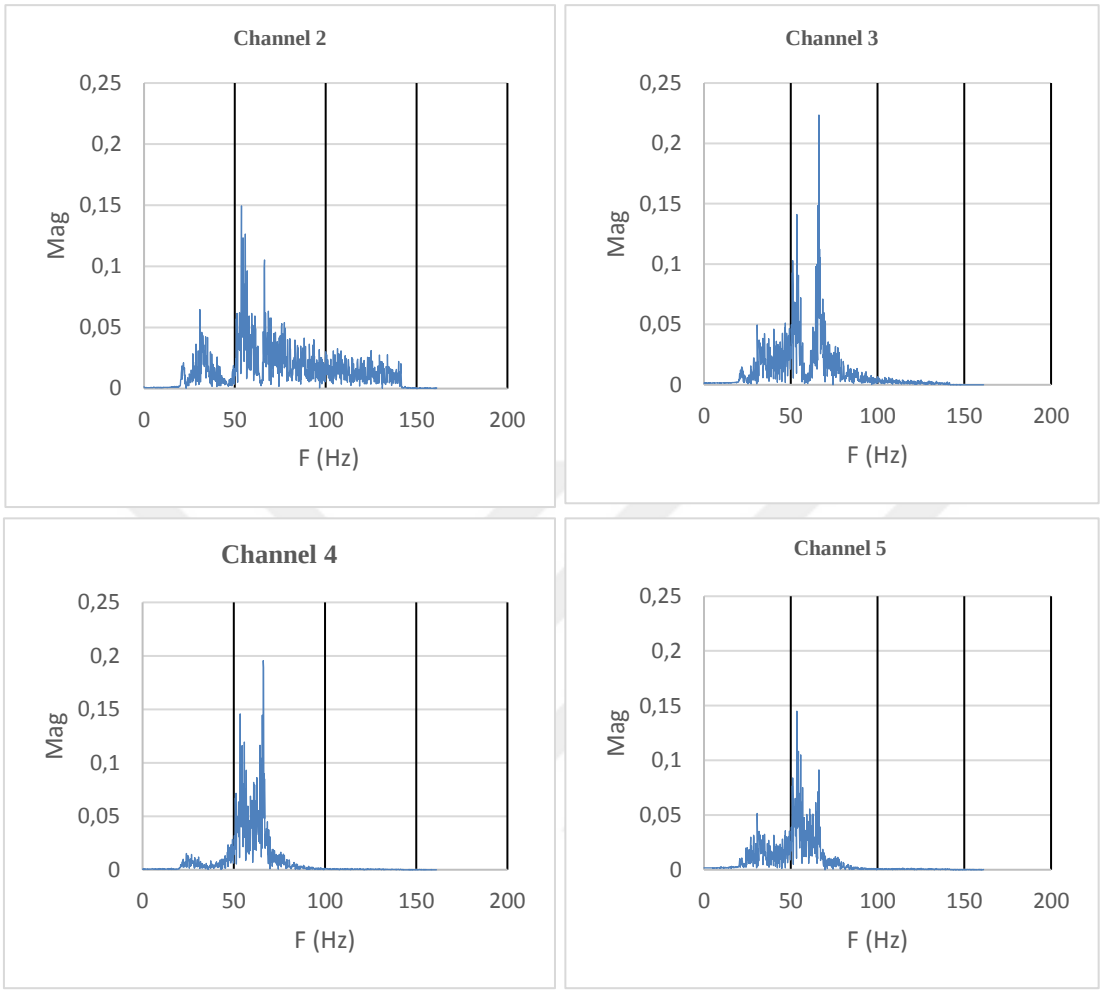

Figure A.34: Fast Fourier Transform Analysis of State #24.

CURRICULUM VITAE

Name Surname : Rihab Tawfeeq Hussein

Place and Date of Birth : 07/08/1991 Iraq, Baghdad

E-Mail : rehab.taufiq@yahoo.com

EDUCATION :

- **B.Sc.** **:** 2013, AL-NAHRAIN University, Civil Department

PROFESSIONAL EXPERIENCE AND REWARDS:

- 2013-2016 AL-NAHRAIN University at Engineering Consulting Office, Materials Laboratory.